SDC-91-00054

SDC
SOLENOIDAL DETECTOR NOTES

MONTHLY REPORT OF THE SOLENOIDAL DETECTOR COLLABORATION

July 1991

SDC 91-000-54

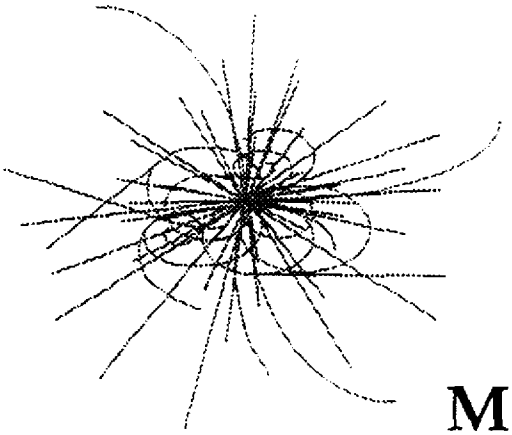

Monthly Report of the Solenoidal Detector Collaboration

July 1991

Contents

A. TECHNICAL PROGRESS 3

1. OAK RIDGE NATIONAL LABORATORY (ORNL) 3
2. UNIVERSITY OF WISCONSIN (PSL) - MUON 4
3. UNIVERSITY OF WISCONSIN (PSL) - TRIGGER 14
4. FERMILAB (FNAL) 15
5. ARGONNE NATIONAL LABORATORY (ANL) 22
6. WESTINGHOUSE SCIENCE AND TECHNOLOGY CENTER (WSTC) 26
7. UNIVERSITY OF MICHIGAN 27
8. LOS ALAMOS NATIONAL LABORATORY (LANL) 29
9. ICF – KAISER ENGINEERS (KE) 34
10. LAWRENCE BERKELEY LABORATORY (LBL) 80

B. PROGRAM COSTS 94

MONTHLY REPORT OF THE SOLENOIDAL DETECTOR COLLABORATION

JULY 1991

A. TECHNICAL PROGRESS

1. OAK RIDGE NATIONAL LABORATORY (ORNL)

The main activities for the month were revisions of the "Magnet and Central Tracker RRR and Interface Control Document," SDC Tech. Note No. SDC-91-00026, update of the cost and schedule for the scintillating fiber outer tracker, and support of updating the cost estimate for the hybrid central tracker. A meeting was held in Oak Ridge on July 22-24, 1991 which reviewed the hybrid concept and updated the cost estimate. Support was also provided regarding analysis and design for the modular straw concept and, in particular, the design of the shell for the modules.

The remainder of the time was expended in preparing for the collaboration meeting in August. A presentation will be made at LBL on the results of work by the Task Force Magnet/Tracking Configuration. The latest revision of the "Magnet and Central Tracker RRR and Interface Control Document" was distributed in preparatior for discussions and corrections at the LBL meeting. This report describes the physical requirements and resources for the Magnet and Central Detector of the SDC. This includes the Magnet, Outer Tracker, Intermediate Tracker and Silicon Tracker. The purpose of this document is to define the envelopes, interfaces and facility requirements for these components of the SDC.

2. UNIVERSITY OF WISCONSIN PHYSICAL SCIENCES LABORATORY (PSL) - MUON SYSTEM

Muon System

Work continued on refining the overall cost estimates for the muon chamber production. Work began on developing an overall factory model for this production. This factory model will help develop parts and materials requirement and flow through production facilities. A second pass was made at estimating the surface facility dimensions for muon system assembly at SSCL. The factory model and surface facility are to be consistent with the constraints of the overall SDC schedule. Cost and schedule dependencies are under investigation. Three cost reduction alternatives to the LOI were investigated. These options include rearranging the muon chamber layout and/or changing the muon system dimensions. Results of this study are tabulated and will be presented to the muon group at the August meeting. A cost estimate was prepared for chambers required to make one BW2,BW3 tower.

Muon Chamber Prototype

Sample extruded tubes for the chamber were delivered and measured. Dimensions are well within specified tolerances. A Purchase Order was released for 52 pieces at 9.5 meters to make a 32 cell prototype (Figs. 2-1 and 2-2). Samples were made with different aluminum finishing techniques in order to evaluate chamber performance. All shop drawings are ready and prototype pieces are being fabricated. An assembly station was set up and will be surveyed. Most purchased parts were received.

Preliminary Design (Coils)

The conceptual design of the Muon Barrel Toroid steel continued in July with extended lower-level details (Figs. 2-3 through 2-8). Improved drawings were made using SSC drafting and UW-PSL engineering. These drawings show block tolerances, plate tolerances, bolting details, and pin details. A parts list and fabrication operations list were also prepared. The size and number of auxiliary holes for coil mounting, chamber mounting, support interfaces, and the cryogenic feed through were specified. This new information was sent to the U.S.S.R as part of the package for cost estimating. The information was also included in the final version of the Muon Barrel Toroid Conceptual Design Report.

The emphasis of the coil work this month was on production methods. A production flow chart was developed (Fig. 2-9). The details of each operation are beginning to be filled in. A braze joint detail was designed and brazing using induction heating was investigated. Water fittings and hose were selected. Lifting fixtures for the conductor and partially completed coils were studied. A coil calculation spread sheet was completed and a new conductor size with a larger water hole was selected.

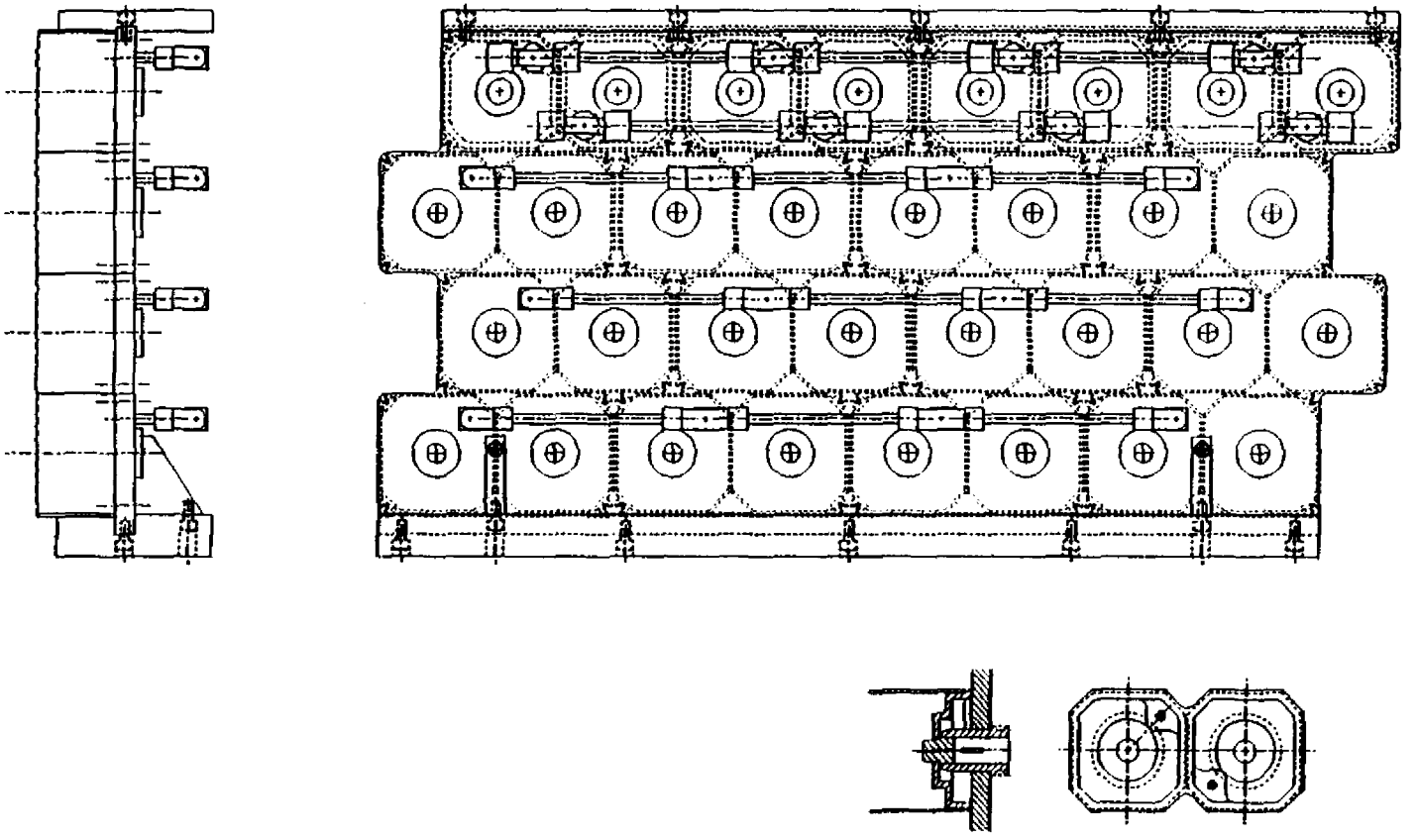

PROTOTYPE MUON CHAMBER ASSY
(PLOTTED FROM INCOMPLETE DRAWING)

Figure 2-1

PRODUCED ON 07/ AT 16:07 AMR DRAWING FILENAME R4626032E PLOTTED AT SCALE 1/1

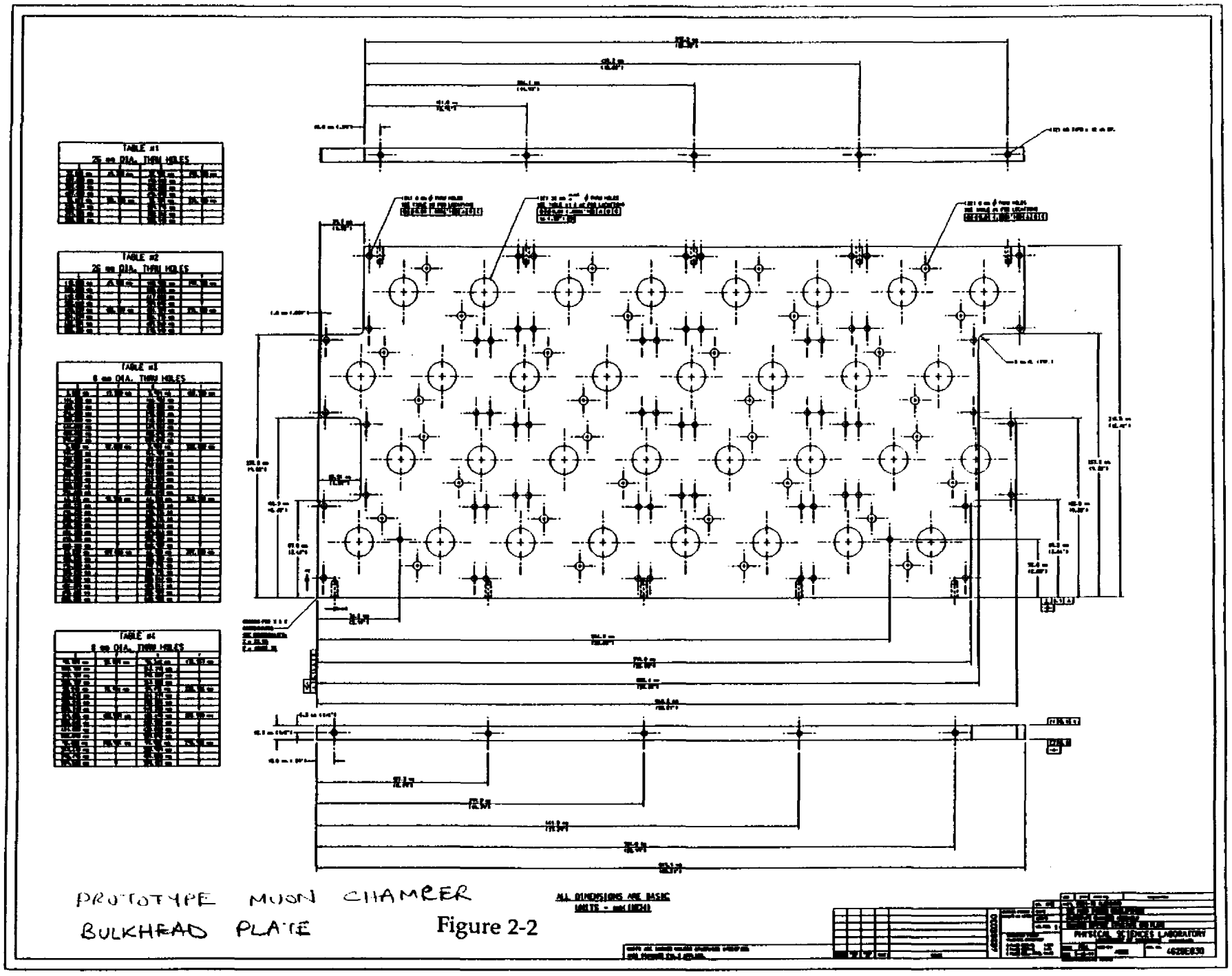

PROTOTYPE MUON CHAMBER BULKHEAD PLATE

Figure 2-2

PRODUCED BY AHR ON 07/30/91 AT 15:59

DRAWING FILENAME A4626030E PLOTTED AT SCALE 1:1

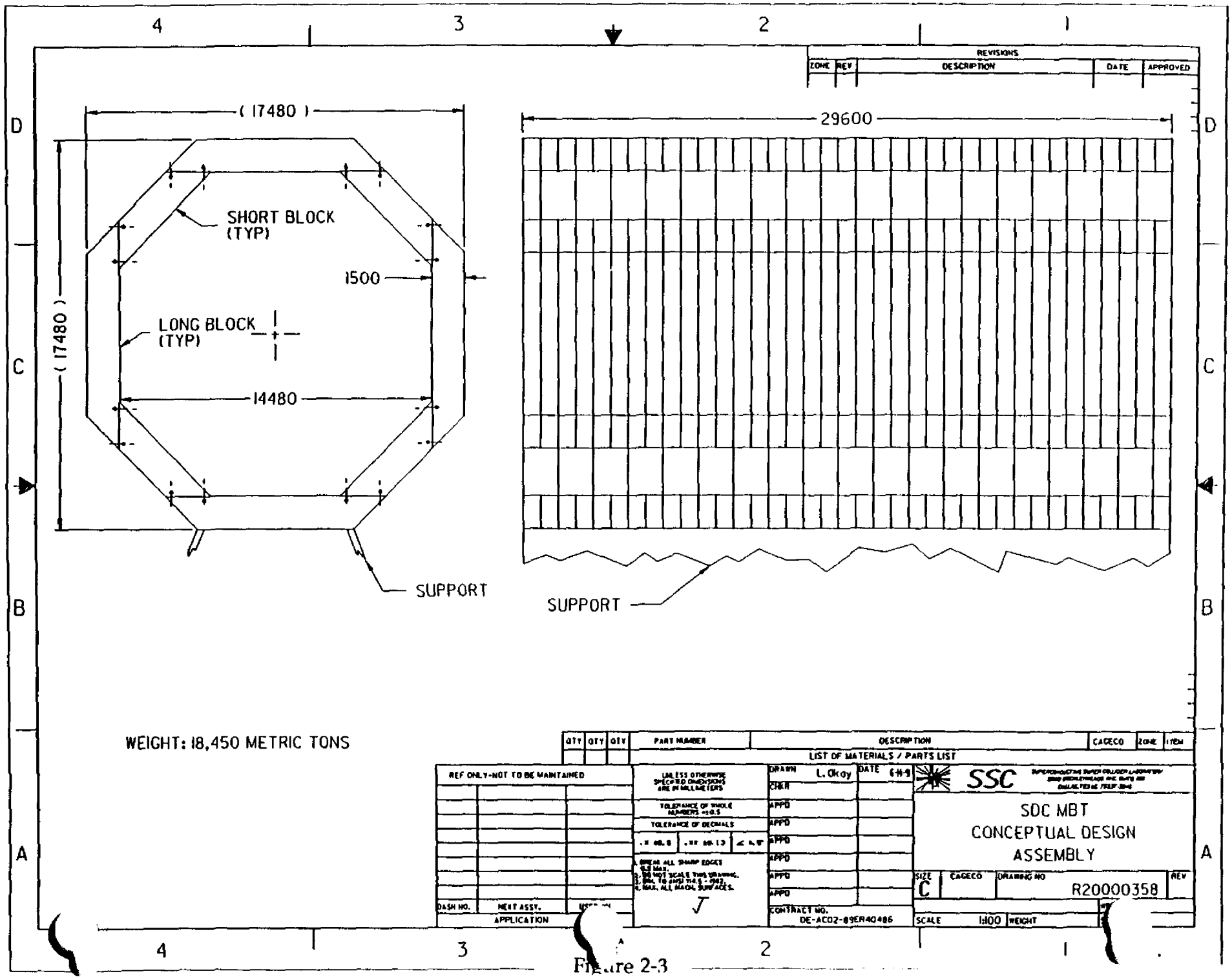
REVISIONS
ZONE
REV
DESCRIPTION
DATE
APPROVED
(17480)
SHORT BLOCK
(TYP)
1500
LONG BLOCK
(TYP)
(17480)
14480
SUPPORT
29600
SUPPORT
WEIGHT: 18,450 METRIC TONS
QTY
PART NUMBER
DESCRIPTION
CAGECO
ZONE
ITEM
LIST OF MATERIALS / PARTS LIST
REF ONLY-NOT TO BE MAINTAINED
DASH NO.
NEXT ASSY.
APPLICATION
UNLESS OTHERWISE SPECIFIED DIMENSIONS ARE IN MILLIMETERS
TOLERANCE OF WHOLE NUMBERS ±0.5
TOLERANCE OF DECIMALS
DRAWN
L. Okoy
DATE
CHKR
APPD
CONTRACT NO.
DE-AC02-89ER40486
SSC
SDC MBT
CONCEPTUAL DESIGN
ASSEMBLY
SIZE
C
CAGECO
DRAWING NO
R20000358
REV
SCALE
1:100
WEIGHT

Figure 2-3

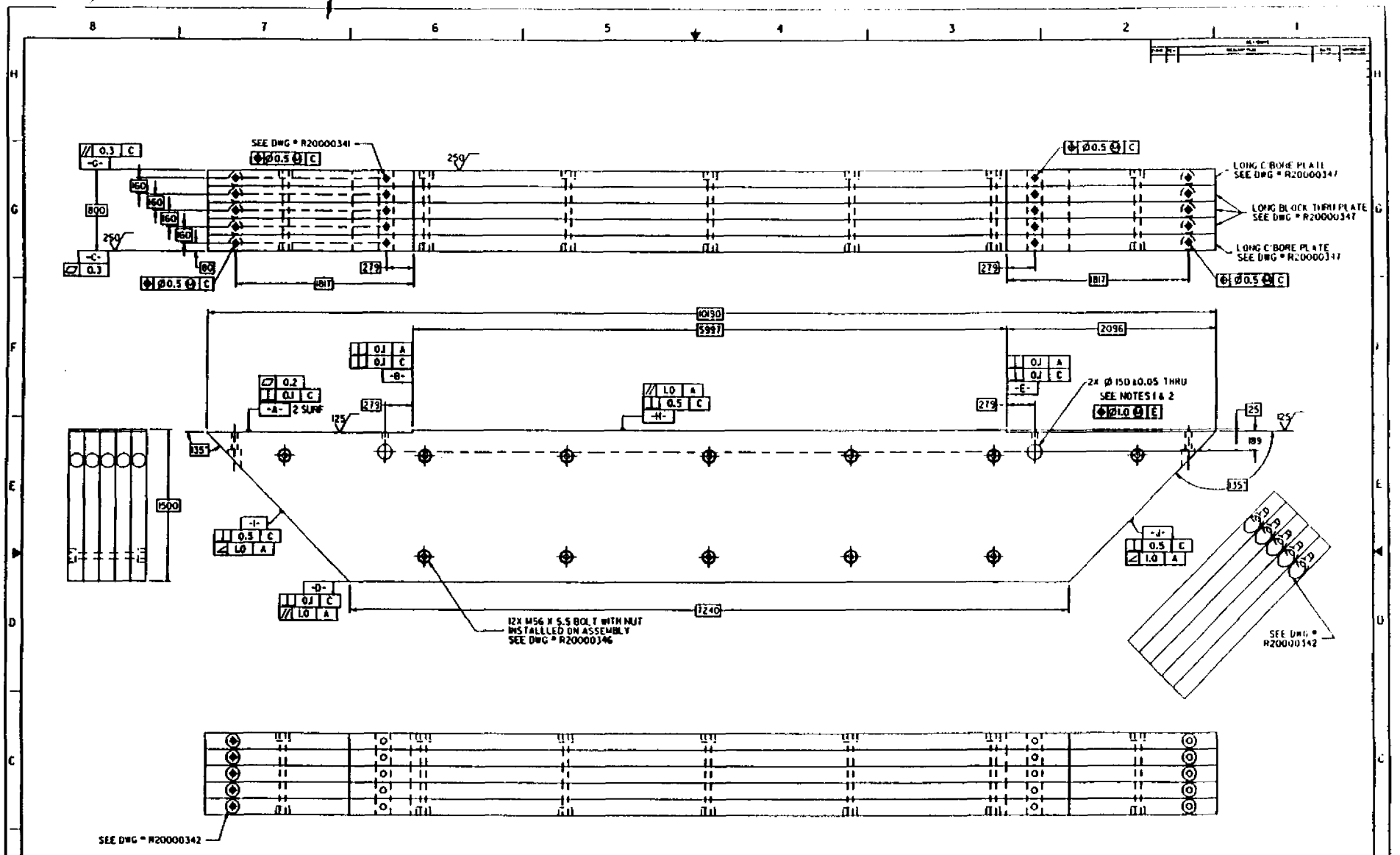

Figure 2-4

NOTES:

1. BORED TO Ø 150 AFTER PLATE BOLT UP
   Ø 150 ALLOY PIN SHRINK FIT INTO HOLE
2. BRING THE PIN TO LIQUID NITROGEN TEMPERATURE BEFORE INSTALLING IN A ROOM TEMPERATURE BLOCK

NUMBER REQUIRED: 148
(37 RINGS WITH 4 LONG BLOCKS)

BLOCK WEIGHT: 82.1 METRIC TONS
90.8 SHORT TONS

SSC

SDC MBT
CONCEPTUAL DESIGN
LONG BLOCK

R20000333

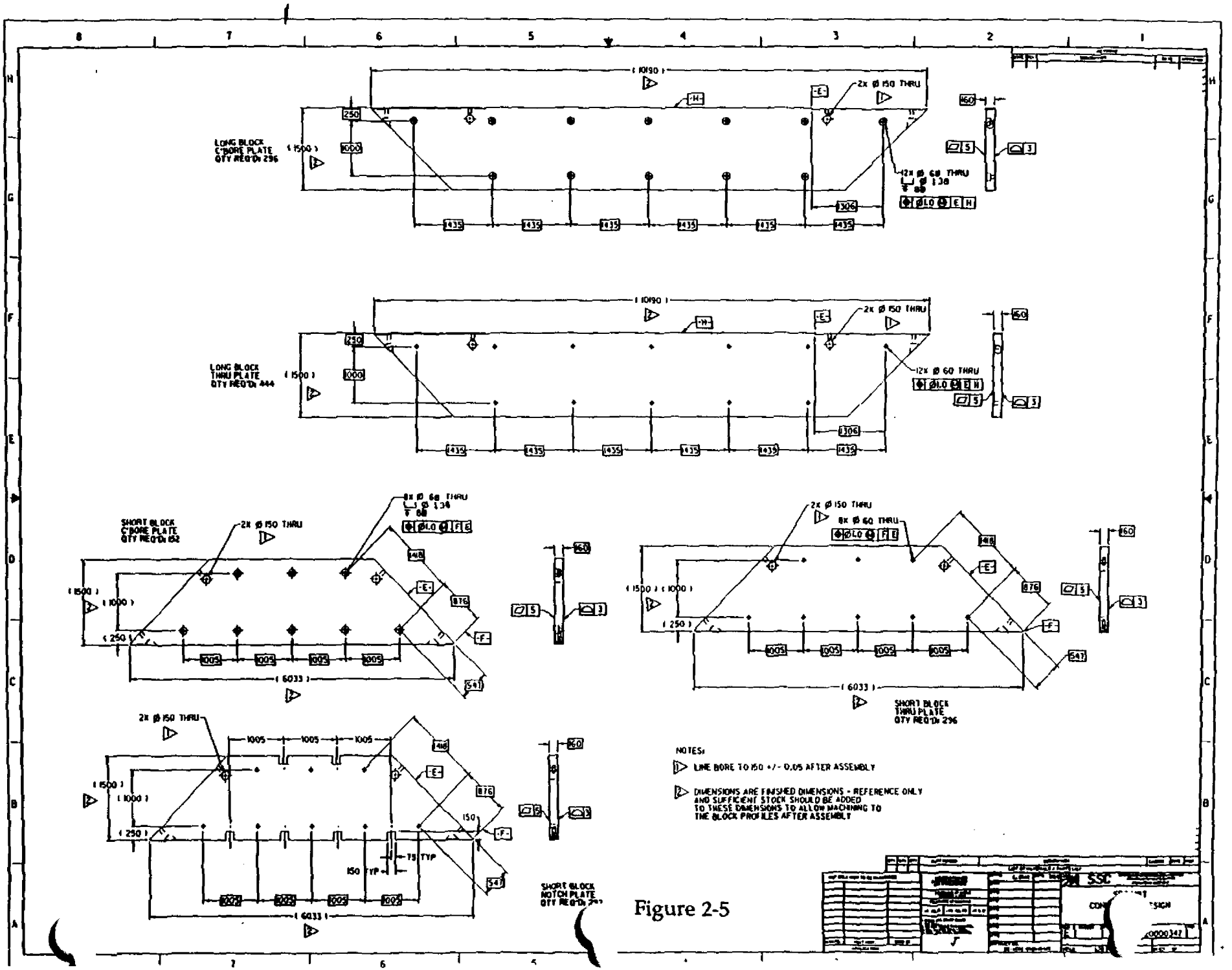
LONG BLOCK C'BORE PLATE QTY REQ'D: 296
LONG BLOCK THRU PLATE QTY REQ'D: 444
SHORT BLOCK C'BORE PLATE QTY REQ'D: 152
SHORT BLOCK THRU PLATE QTY REQ'D: 296
SHORT BLOCK NOTCH PLATE
2x Ø 150 THRU
12x Ø 60 THRU
8x Ø 60 THRU
NOTES:
LINE BORE TO 150 +/- 0.05 AFTER ASSEMBLY
DIMENSIONS ARE FINISHED DIMENSIONS - REFERENCE ONLY AND SUFFICIENT STOCK SHOULD BE ADDED TO THESE DIMENSIONS TO ALLOW MACHINING TO THE BLOCK PROFILES AFTER ASSEMBLY

Figure 2-5

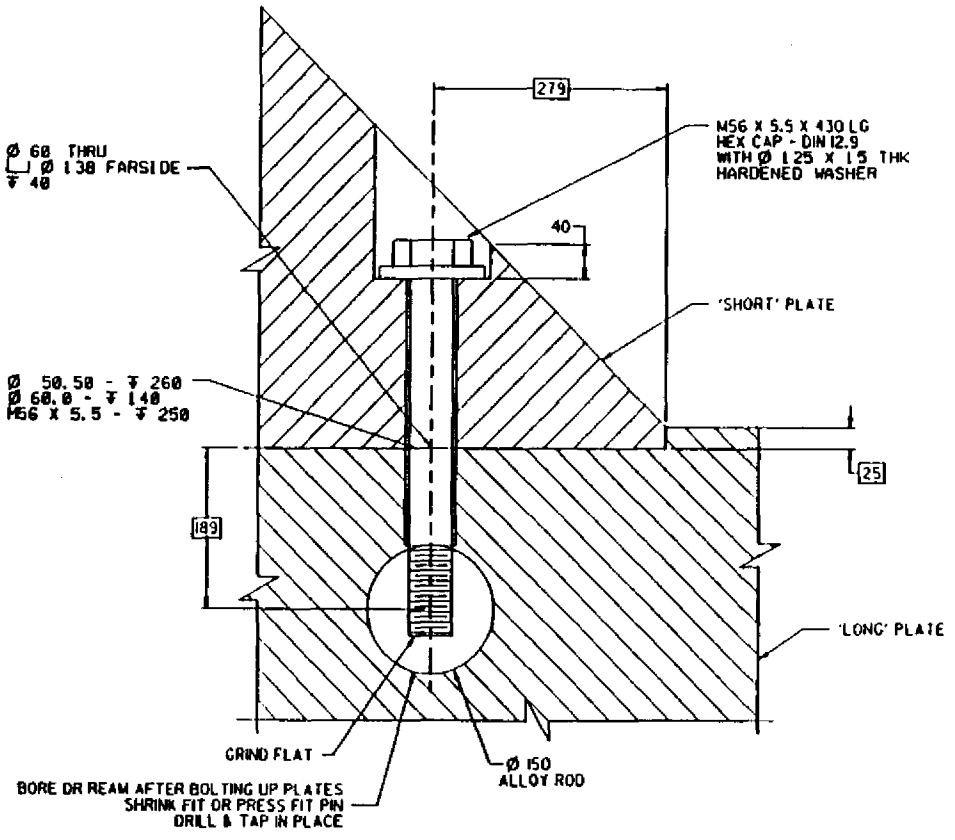

INSIDE BOLT DETAIL

Figure 2-6

REVISIONS				
ZONE	REV	DESCRIPTION	DATE	APPROVED

QTY	QTY	QTY	PART NUMBER	DESCRIPTION	CAGECO	ZONE	ITEM

LIST OF MATERIALS / PARTS LIST

REF ONLY - NOT TO BE MAINTAINED

DASH NO.	NEXT ASSY.	USED ON
APPLICATION		

UNLESS OTHERWISE SPECIFIED DIMENSIONS ARE IN MILLIMETERS

TOLERANCE OF WHOLE NUMBERS ±0.5

TOLERANCE OF DECIMALS

1. BREAK ALL SHARP EDGES 0.5 MAX.
2. DO NOT SCALE THIS DRAWING.
3. DIM. TO ANSI Y14.5 - 1982.
4. MACH. ALL MACH. SURFACES.

DRAWN	L. Okoy	DATE 6-14-9
CHKR		
APPD		
APPD		
APPD		
APPD		
APPD		
APPD		

CONTRACT NO. DE-AC02-89ER40486

SSC

SDC MBT
CONCEPTUAL DESIGN
INSIDE BOLT DETAIL

SIZE	CAGECO	DRAWING NO	REV
C		R20000341	

WBS

SCALE | WEIGHT | SHEET OF

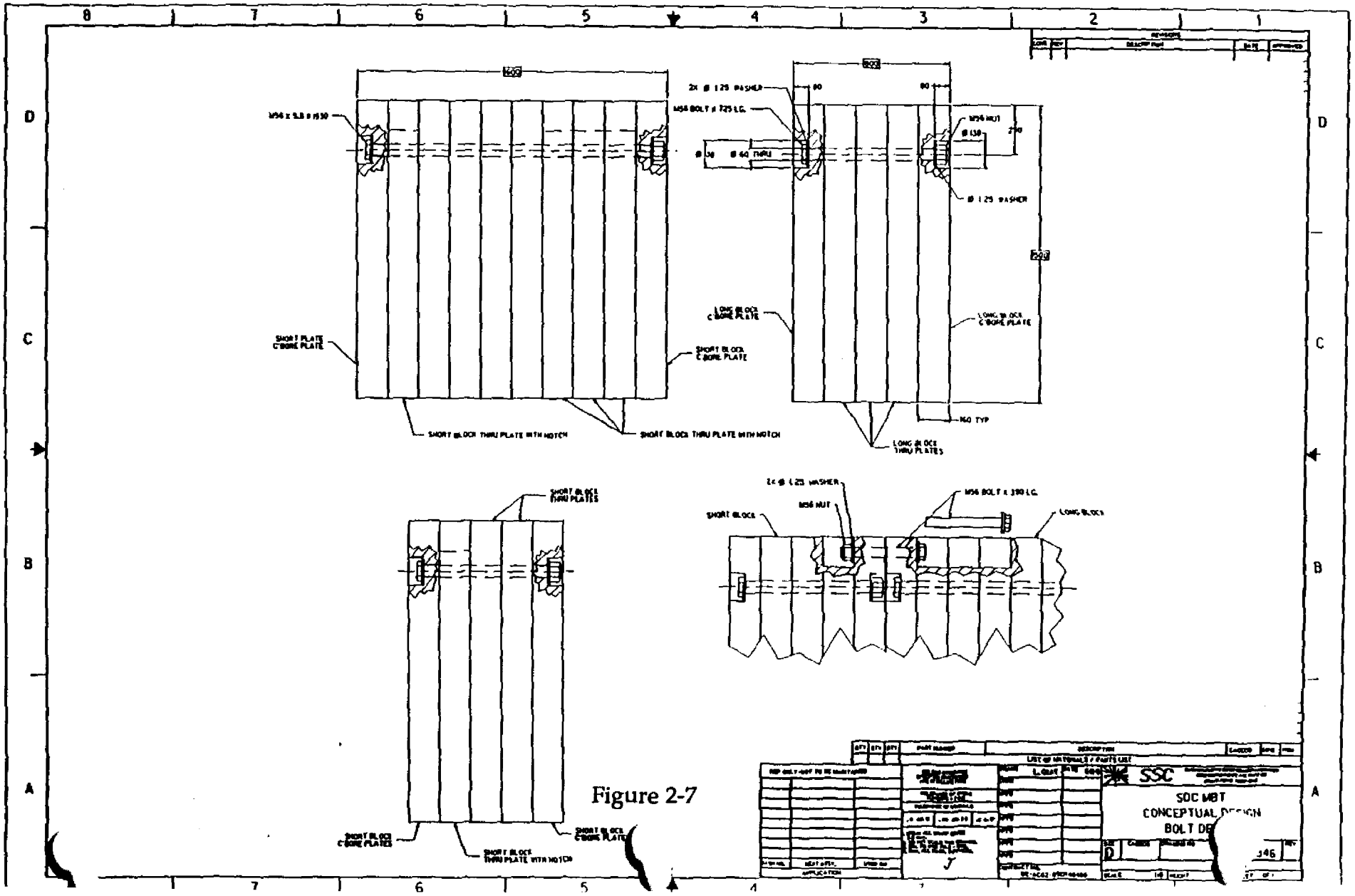
SHORT PLATE C'BORE PLATE
SHORT BLOCK C'BORE PLATE
SHORT BLOCK THRU PLATE WITH NOTCH
SHORT BLOCK THRU PLATE WITH NOTCH
LONG BLOCK C'BORE PLATE
LONG BLOCK C'BORE PLATE
LONG BLOCK THRU PLATES
SHORT BLOCK THRU PLATES
SHORT BLOCK C'BORE PLATES
SHORT BLOCK C'BORE PLATES
SHORT BLOCK THRU PLATE WITH NOTCH
SHORT BLOCKS
M56 NUT
LONG BLOCKS
SSC
SDC MBT
CONCEPTUAL DESIGN
BOLT DE

Figure 2-7

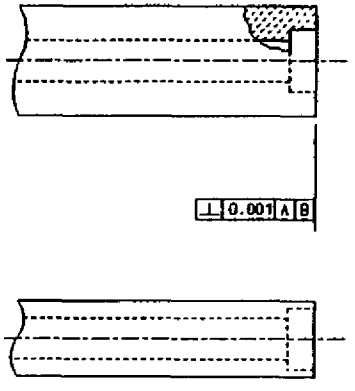

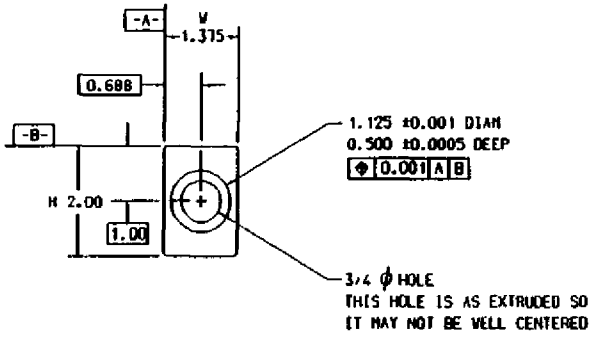

CONDUCTOR INFO
NOM. COPPER AREA - 2.3027 IN²
NOM. HOLE AREA - 0.4418 IN²
WEIGHT - 0.7438 LB/IN
IW - 0.4153 IN⁴
IH - 0.8958 IN⁴

CONDUCTOR BRAZE PREP

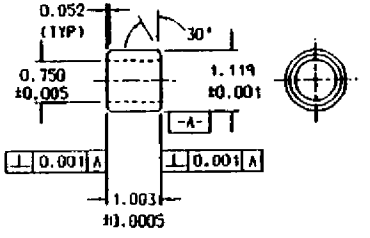

BRAZE TUBE INSERT

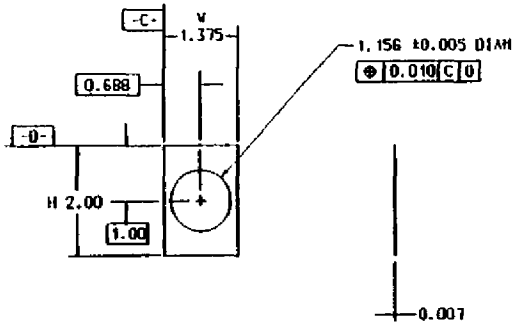

BRAZE PREFORM

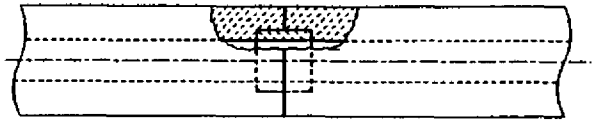

COMPLETED BRAZE JOINT

UW PHYSICAL SCIENCES LAB
SSC - SDC MUON MAGNET COILS
BRAZE JOINT LAYOUT
7/31/91 - JJC

Figure 2-8

PRODUCED BY JJC DRAWING FILENAME BRAZE
ON 08/01/91 AT 08:32 PLOTTED AT SCALE 1/1

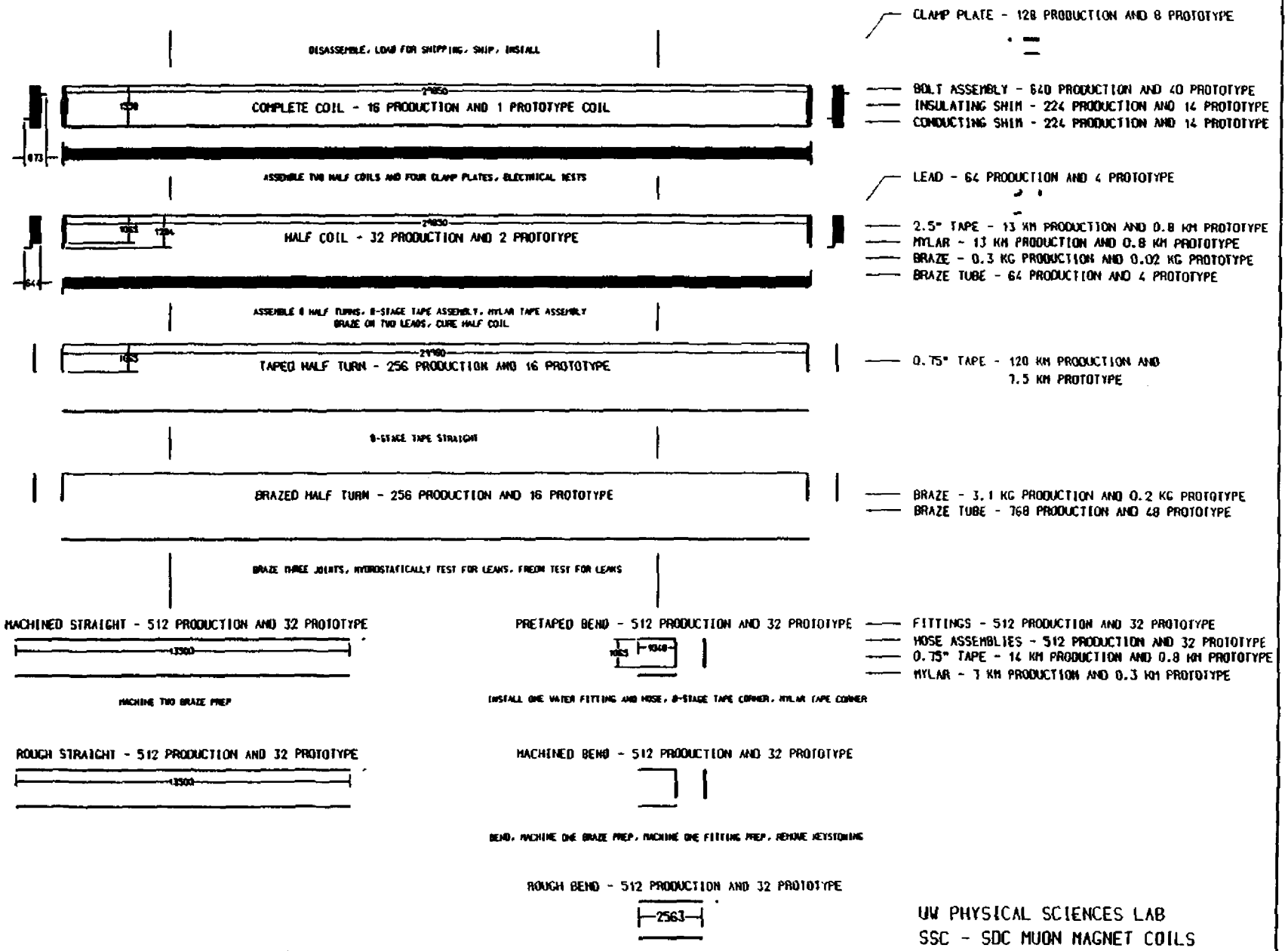

Figure 2-9

PRO JJC DRAWING FILENAME COILFIX
ON 08 91 AT 08:54 PLOTTED AT SCALE 1/1

3. UNIVERSITY OF WISCONSIN PHYSICAL SCIENCES LABORATORY (PSL) - TRIGGER SYSTEMS

Calorimeter Level 1 Trigger

A study of electronics pileup and resolution for calorimeter trigger signals is well underway. Three circuits have been designed, modeled and built on a breadboard to measure the expected quality of trigger signals. The circuits involve integration and baseline restoration over a high and low gain channel. The first circuit involves an integrator using an SE5539, the second an AD 848 and the third an AD 829. The most promising circuit is that based on the AD 829. This circuit is being adapted for use as an input device to the LBL Switched Capacitor Array and will be installed in the FNAL test beam. We are presently laying out a printed circuit board for this purpose.

A design has been developed for pattern logic to detect isolated electrons. The design includes setting a 2 bit Encoded Tower Type (ETT) for every trigger tower based on hadronic and electromagnetic energy. The ETT data from a region of 8 x 8 towers is input into 2 Pattern Recognition ASIC's (PRA), which use the 128 bits to search for isolated electrons at 2 different thresholds. The found isolated electrons are assigned to one of 49 possible 2 x 2 tower regions in the 8 x 8 tower grid. The PRA logic blocks of ETT decoding, Isolated Electron Detection, and Region Flag Word generation are designed.

A simulation of the isolated electron pattern logic has been developed and placed into a general SDC simulation program originally developed at U. Chicago. The program has been converted into UNIX and runs on the SSC Physics Detector Simulation Facility. At the moment it includes electron finding, jet finding, energy summing, and track matching.

Global Level 1 Trigger

A conceptual design of the Global Level 1 Logic has been produced. The specifications for the Global Level 1 Clock and Control have been prepared. Design work is beginning on a VME-based module that will simulate the function of the global level 1 processor (GL1P).

The GL1P Simulation Module (GL1PSM) emulates the control sequences of the GL1P. Its purpose is to aid in the debugging of Subsystem trigger circuits and to serve the basic functions of a trigger module for test experiments. The GL1PSM will not have the complicated decision logic found in the GL1P. In its place, there will be a single 16-bit memory lookup table. The contents of the memory lookup table will be downloaded under VME control.

The GL1PSM will have an internally generated 62.5 MHz clock, as well as being able to use an external ECL clock at a frequency up to 62.5 MHz. The GL1PSM can accept external triggers that cause the GL1PSM to issue an Accept, initiate a test sequence, or issue a reset a certain number of clock cycles after receipt. This number of clock cycles is set by a value into one of the control registers.

4. FERMILAB (FNAL)

Superconducting Solenoid

Cryogenics

Work was initiated on the piping and instrumentation diagrams for the support system, the coil-outer support cylinder, and the thermal shields. Calculations were refined for the heat load to the thermal shields and from the calculations a route was proposed for the liquid nitrogen tubing on the shields. An assembly drawing was initiated for the outer thermal shield, which is attached to the outer vacuum shell.

Studies were undertaken regarding the advantages and disadvantages of having two, independently controlled helium cooling circuits for the outer support cylinder and the thermal intercepts on the supports. We calculated flow rates, pressure drops, tube spacing and temperature distributions for a two-circuit system. The flow control valves for these circuits would be located in the control dewar on top of the detector. The two additional lines could be accomodated in the chimney without increasing its diameter.

In order to avoid penetrating the outer vacuum shell with the instrumentation feed-throughs (as shown in a figure in the June report), we redesigned the cryostat-to-chimney joint region, moving the instrumentation connectors to a section of chimney just above the EM calorimeter. This new design is shown in Fig. 4-1.

The engineering and design of the isogrid outer vacuum shell continued. In a meeting with our consultant, we decided that the full-length shell would be fabricated of four short cylinders, each of which is made of three isogrid panels. Only TIG welding would be used on the shell. The present isogrid design has an overall thickness of 2.2" and an effective thickness of 0.38". The consultant is working on the panel-to-panel joint, the chimney-to-shell joint and the shell-to-bulkhead bolted joint. We contacted a supplier of the 2219 alloy which will be used and learned that sheets 8' wide x 14.5' long are available from the mill at $2.65 per pound and 10 week delivery. The full-length shell would require 12 sheets this size.

Cold-mass Support System

The design of the support system was modified to include a truss structure on both ends of the cold mass. The truss on the chimney end of the cold mass would be attached with pins and welding to the outer support cylinder. The truss on the opposite end would slide axially to accomodate the thermal contraction of the cold mass and would, therefore, be a radial support only. This design has the advantage that the outer vacuum shell and annular bulkhead are the same on both ends on the cryostat.

A request for quotation was issued to Structural Composites Industries for the engineering of composite members for the truss structure. The support system is designed for 66 metric tonnes axially and 60 tonnes radially. The resulting design

parameters on the composite members are for a working load (with safety factor of 4) of 12,000 lb axially (tension or compression), maximum outer diameter of 1.5" and length of 22.5"

Magnetostatics

An earlier finite element magnetostatic analysis of different coil- calorimeter iron geometries was expanded to study the effect on the axial compressive coil force of reducing the 1/4" air gaps in the endwall to 1/8". The earlier study showed a significant effect when the gap was changed from 1/2" to 1/4". The new calculation showed that changing the, gap from 1/4 to 1/8" caused negligible change in the axial force. Another calculation showed a negligible change when the gap was reduced from 1/8" to zero.

Another set of four computational runs was made in which the endcap calorimeter iron terminated at different distances from the end of the coil. The resulting axial compressive forces were plotted as a function of coil-iron separation. The curve, Fig. 4-2, demonstrates that reentrant endcap geometries significantly reduce the compressive force on the superconducting coil.

We completed our study on the effectiveness of axial coil preload in reducing coil-outer support cylinder relative motion. Our conclusion was that, because of the axial distribution of the axial Lorentz force, preloading the coil against the support cylinder cannot prevent relative motion.

For a design in which the coil is epoxy bonded to the outer support cylinder without significant preload, as in the present KEK design, we found that the safety factor on shear failure of the bond is a function of the coil-iron geometry. We calculated the safety factor for five geometries; it was 28 for a total axial force of 140 tonnes and 140 for 1500 tonnes.

We also calculated that the friction force resulting from the radial Lorentz force on the coil. A friction coefficient of 0.2 was adequate to prevent relative motion only when the axial force was 140 tonnes or less.

Figure 4-1. The lower end of the chimney, with a section of the vacuum pipe enlarged to accomodate instrumentation connectors.

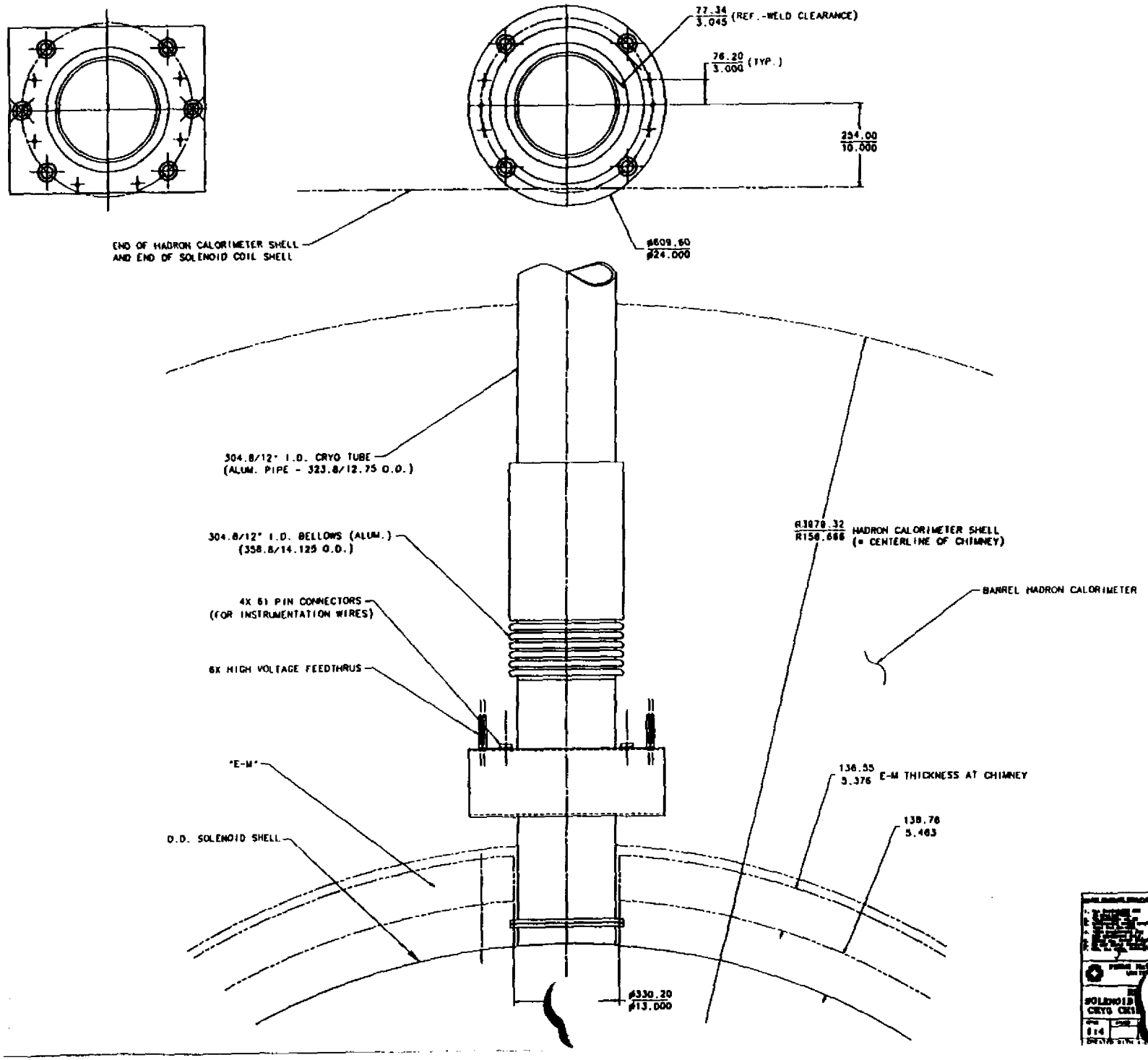

Figure 4-2. The axial compressive force on the superconducting coil as a function of the amount of re-entrant endcap c meter iron.

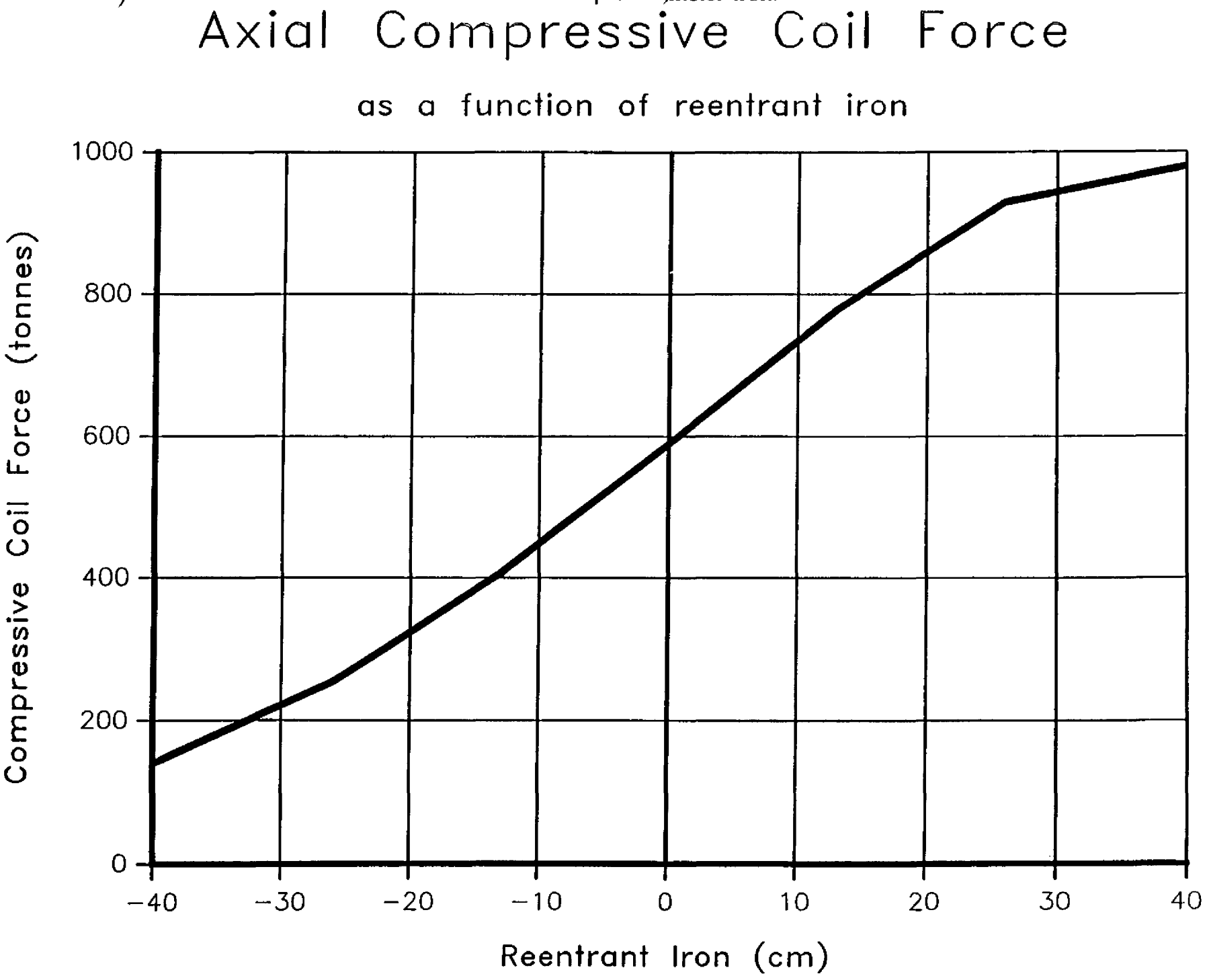

Calorimetry

Iron Calorimeter Design

Work continued on the design of the iron tile-fiber calorimeter option. Layout drawings were made that show the location of every phototube on the calorimeter wedges. We developed the support structure concept with calculations and FEM analysis. Steel weldments were designed to attach to the muon steel which would be used for rails to roll the calorimeter. The absorber cone was developed that attaches to the end cap sections such that we know how to fabricate the absorber, and attach it. We finished the conceptual design of three different assembly techniques for the steel in the hadronic sections. Brian Wheeler finished the detailed design work of several options for the PMT housings.

WBS and Cost Estimating Effort

By August 4 a relatively final version of the iron calorimeter WBS was developed. This will probably change again in the upcoming weeks to reflect the next revision. We collected cost information on almost every subsystem in the calorimeter, and made estimates based on past experience for the parts without vendor quotes.

Alternate EM Design

Progress was made in understanding the properties of the barrel and end cap EM sections. Calculations were made to determine what the wire tension has to be to support the lead and scintillator. We are in the process of putting actual plate weights into the calculation. We also created a data-base which calculates the size of all of the tiles in the EM section (as well as the other sections,) and the lead plates too.

Data Acquisition System

Baseline DAQ Costing

July efforts included refining cost estimates, descoping cost estimates and starting to consolidate backup material for cost estimates in preparation for the SDC Collaboration meeting in early August at LBL. Some additional time was spent on the preparation of the Data Acquisition System part of the SDC Technical Proposal.

Scintillating Tile Calorimetry, Scintillating Fiber Tracking Test Beam Project

The designs and PC artwork for an energy adder module, a data storage (SIRO) module, a test transmitter module and a track finder module (with Al Baumbaugh of the Research Division) were mostly completed. Prototype boards were ordered, designs were refined (e.g., PAL equation modifications, etc.) and some diagnostic software was started.

Calorimeter Flash Analog to Digital Converter

Work is continuing on the Integrator/Digitizer chip. A writeup was completed on the Orbit NPN transistor model. A design for the current splitter portion of the chip was submitted to Orbit in July. Twelve prototype parts are expected back in August. A specially designed PC board for testing the splitter has been received.

Our first design of a fast floating point adder chip has been fabricated by Orbit. Initial testing indicates that the chip works. The chip has an 8 bit mantissa and a 4 bit exponent for each of the two inputs. However, only 1 of the input exponent bits for each input is brought out to a pin for testing. It is assumed that the remaining exponent bits are also functional.

The Adder chip is the first chip design which we have submitted directly to Orbit for fabrication. Thus, we now have a working fabrication alternative to submissions through MOSIS. We plan to use Orbit for 1.2 micron designs and/or fast fabrication of devices.

Muon Support Alignment Systems

Work is progressing on the detailed design and analysis for a prototype truss, bearing, and rail system for a BW3+BW2 supermodule assembly and developing the supermodule kinematic support designs to allow x,y,z adjustments for alignment. Work continued on the setting up and testing of prototype remote chamber alignment monitoring systems.

On July 30, we visited MIGATRON, Inc. to bench test/evaluate the prototype electronics board for the high precision (RPS 8800) ultrasonic distance measuring system under R&D for us. Even without temperature compensation included, the system was demonstrating (stack measurement average) distance resolutions of 25 microns or less and short term stability of 75 microns. However, the system was NOT operating with the 1800mm range transducers and matched front end electronics of the final prototype system. Thus, we do not yet have a feeling for the capability of the system for long distance ranging. System delivery is now estimated as early September. In the meantime, we took home with us a precursor system #8000 on which we will measure resolution and stability on short ranging. In detailed studies with the original Selectron system, we have established that a toroid magnet wormhole of 67mm is just adequate for ultrasonic transmission/reflection measurements (for smooth walls).

The final stretched steel (final system- tungsten) wire setup has been established. Duplicate x,y,z target and proximity sensor systems have been setup in a cycling computer readout system. Thermal measurements are now included as well as fixed reference calibration sensing. We have been doing a series (power glitch interrupts) of long term (1 wk, 2 wks, etc) test measurements on stability.

In the work on target materials and shapes, we have concluded that 50mm dia. cylindrical targets (x,y) on the wire (z) are the most stable. Either a plastic target with a thin aluminum foil skin or a stainless steel cylinder will work about equally well in magnetic fields. We have successfully demonstrated that we can solve for the x and y

target displacements even though these sensors are coupled. One has to iterate the first order coordinate solution using a small hyperbolic or parabolic correction term in the opposing coordinate.

Our tests do indicate a small temperature dependence of the position sensing outputs; but with our temperature sensors we can essentially correct the readings. It appears that we can maintain measurement stabilities like 50 micron or better, especially in the z (wire) direction.

A second brand of linear output capacitatively coupled proximity sensor is being evaluated. It is basically comparable to the first, but each has some unique features. Both versions are being tested in fringe magnetic fields of 120 gauss (parallel or perpendicular to the sensor axis) with little effect. A batch of sensors has been measured and their calibrations are very uniform.

We have also been evaluating light beam position sensing photodiodes for relative transverse x, y position monitoring of chamber modules. This work has included the testing and optimization of LED light sources. We have found some far infrared diodes which provide good forward emission intensities. These are being coupled with different optical lens configurations to study resolution capabilities. A final configuration needs to be established for long term tests. Measurements using different sharp cutoff longpass (long wavelength) filters indicate that these IR systems can operate in variable ambient optical backgrounds with high source resolution. Resolution and short term stability tests have been very encouraging.

5. ARGONNE NATIONAL LABORATORY (ANL)

Design of a Lead Scintillator Plate Calorimeter

Barrel Calorimeter Mechanical Design

The barrel calorimeter revision has been completed to reflect the latest cost reduction efforts. Some detailed work has been done particularly in the region at the outside radius of the barrel. Figure 5-1 represents the latest thinking on a strong back which will provide structural support for intermodule connections, fiber routing, and photomultiplier tube containment. Some work has been accomplished on methods for carrying both tension and compression loads across intermodule boundaries at the inner radius.

A modification has been made to the bulkhead structure at the location of the shower maximum detector. Additional information about the sizes of scintillator in the SM detector has forced a redesign of the lead absorber plates both before and after SM to accommodate the increased space between bulkheads. This has been accomplished by a cast in membrane reinforcement of the lead. This is represented in Fig. 5-2.

Barrel and Endcap Calorimeter

End cap intermodule connections have been added to the design and their relationship to coil gravity load supports has been studied.

Coil Support

A considerable amount of work has gone toward integrating the supports for the coil into the barrel calorimeter. In conjunction with Fermilab coil designers, we have added a conceptual design for those supports into the barrel calorimeter design.

EM Test Section for Test Beam

All of the necessary components for the support and translation of the test module in the Fermilab test beam have been completed and are being fabricated. This includes the enclosure and support for the photomultiplier tubes.

The electronic controls for stepping motors are also near completion.

FEM Analysis

Work that was started on the 3D analysis of the half barrel has been halted due to a computer fault. This has forced a rethinking and different approach to circumvent the problem until it can be resolved.

A model of the barrel calorimeter module has been remeshed and the loads obtained from the Westinghouse 2D analysis will be redistributed on this model to get preliminary data on internal stresses in the module.

Some work has also been done on the model of the end cap EM section. Output indicates that the lead stresses are similar to those encountered in the barrel.

A publication search program is also being conducted to allow us to better understand the long term creep characteristics of pure lead.

Barrel Design

a) HAC1 3D Analysis: Cases have been performed for 12 o'clock and 3 o'clock positions. In the 12 o'clock position, the maximum displacement is 0. 053 mm, and the maximum streses are 15,881 psi in the bulkheads, and 496 psi in the lead. In the 3 o'clock position the maximum cantilever deflection is 0.159 mm, and the maximum stresses are 33,000 psi in the bulkhead, and 291 psi in the lead. All of these numbers are higher than desired, and design iterations will be performed to reduce the stresses and deflection. It is likely that the 3 o'clock cantilever case is an unrealistically stringent design case, because the adjacent modules support one another, thus preventing deflections as large as 0.159 mm.

b) Full Barrel 2D Model and Design: For the "no-backiron" case performed last month, the fastening forces between HAC2 module front plates have been tabulated. A preliminary fastening system has been designed. Shown in drawing D-412.4138A73.R1, this system utilized 0.25-20 14" long grade 8 bolts that pass through the first two HAC2 absorber plates, and tap into the corresponding plates of the adjacent module. The bolts are placed along tower boundary lines, so that their disturbance to the fiber readout plane is minimal.

EMC Test Module

The aluminum inserts (1D33635-39, Rev. 2) are 75% complete. Approval of final dimensions was received on July 26. Finishing of the inserts to these dimensions is in progress. The mold lip (1D33596), frame clamp bars (DWS-7291A&B), lifting eyes, Belville washers, and fiberfrax paper were all fabricated and/or procured, and shipped to Argonne. Sketches for the aluminum perimeter plates (DWS-7891A through G) were made and sent to Argonne. Temperature probes were obtained for the next casting.

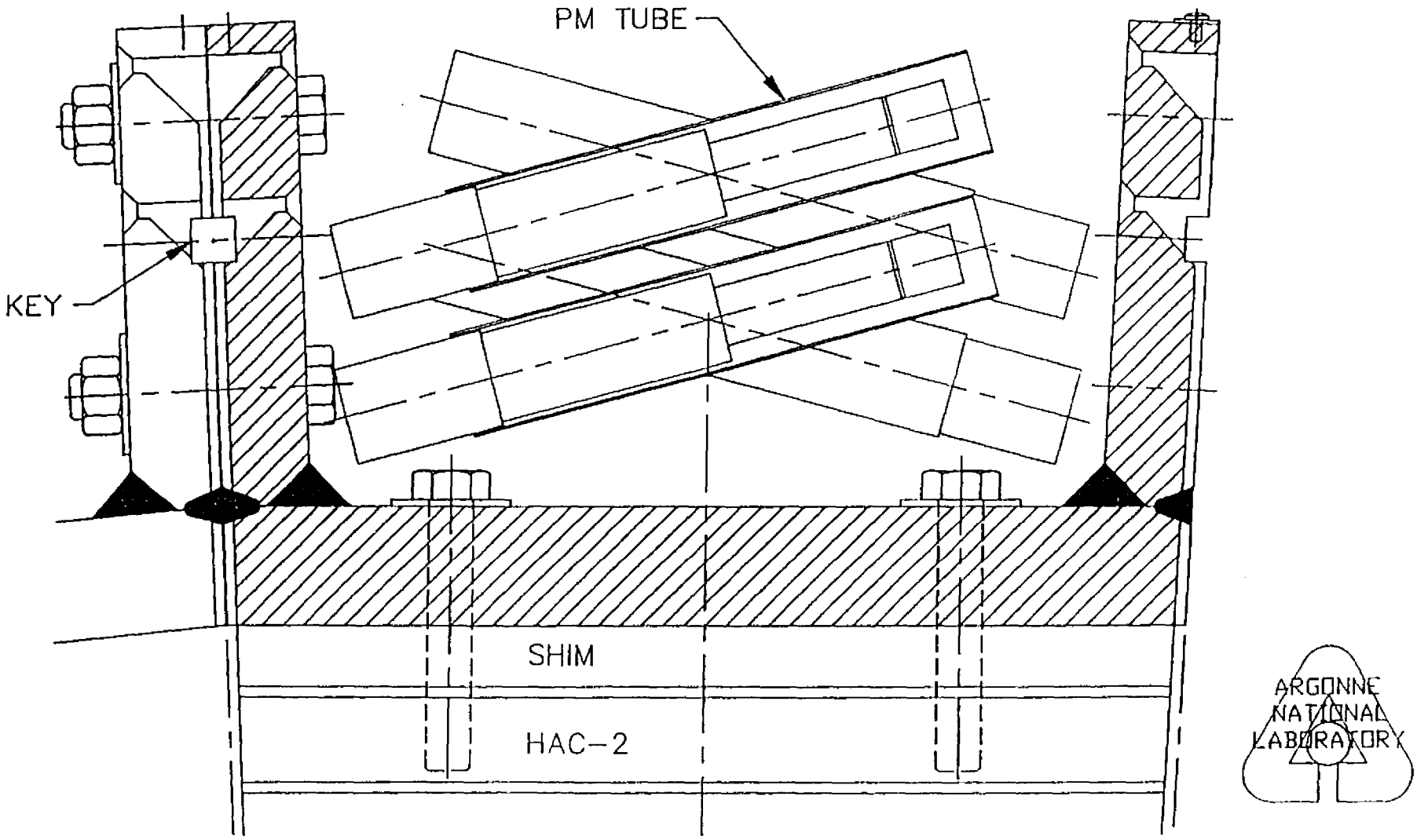

(J) Support Channel–Module

Figure 5-1

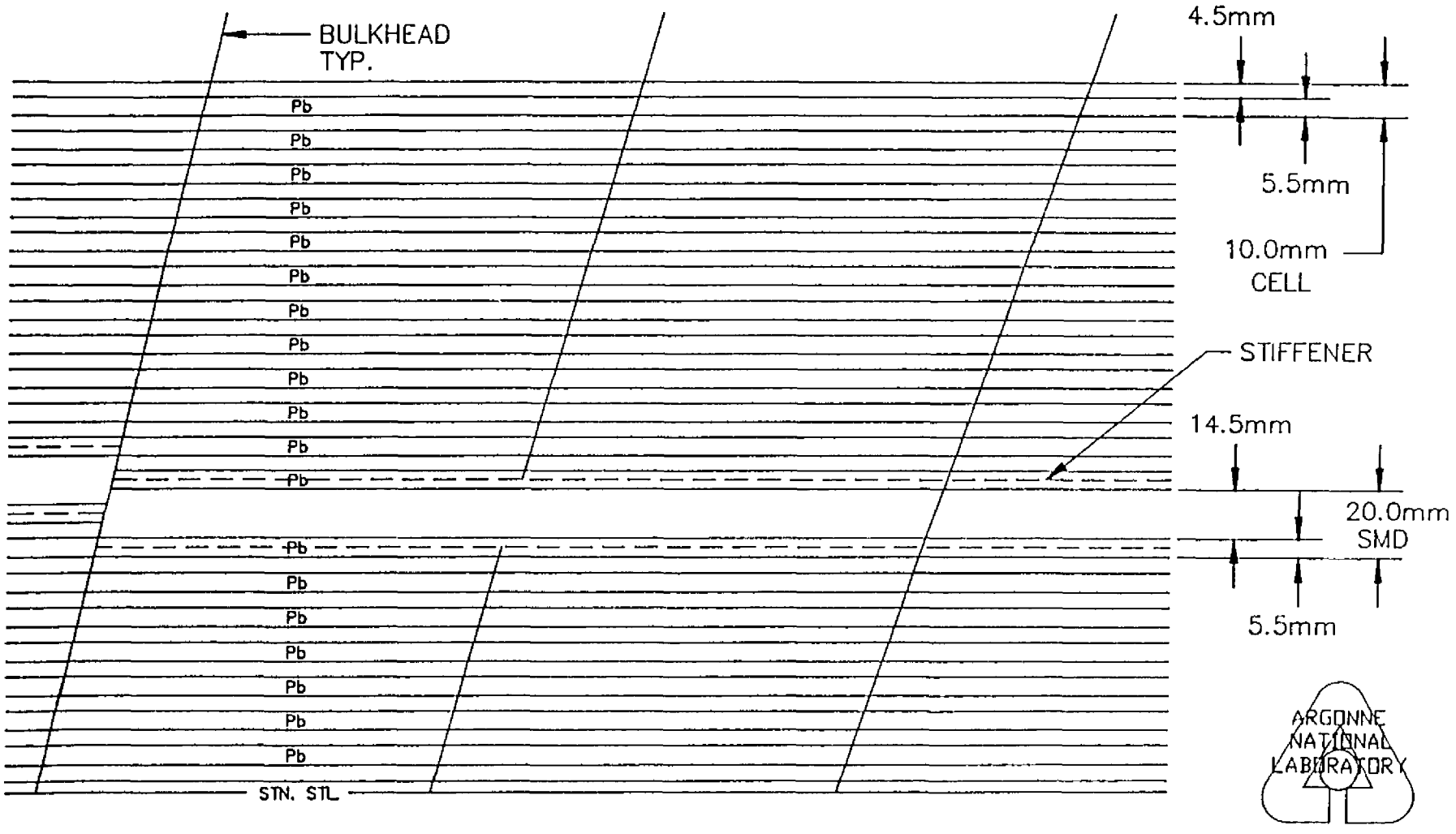

(A) Barrel EM Structure

Figure 5

6. WESTINGHOUSE SCIENCE AND TECHNOLOGY CENTER (WSTC)

The entire effort over the past month has been in the areas associated with costing and scheduling of the barrel calorimeter, end cap calorimeter and central straw tube tracker.

The month of July was spent in updating the costing and schedule information based on comments from the June collaboration meetings. These comments included corrections to the mix of labor categories between EDIA and production, component costs, organizational rates and schedule considerations.

All information based on the cost and schedule of the three subsystems were provided to the collaboration. This complete package was provided on PRIMAVERA program output and computer discs for translation to other data bases. Included in the package was the estimated schedule for installation of each subsystem into the detector. In order to make descoping/concept modification decisions, spreadsheet files were also developed which consisted of the estimates/equation logic for each subsystem. These spreadsheets will be used during the August collaboration meeting for descoping discussions.

7. UNIVERSITY OF MICHIGAN

SDC Trigger Development

Summary

Work has continued on triggering with superlayers of straw tubes. The work is proceeding in both simulation and the development of Application Specific Integrated Circuits (ASICs). The first all-digital implementation has been designed, fabricated, and initial tests are underway. Results to date indicate that the unit functions as designed. A cosmic-ray test stand to exercise the chips with real tubes is complete and will be used to inject actual straw tube signals into the trigger chips.

Chip Development

The circuit that is being tested is a single stage synchronizer based on 2ns delay elements. It has 15 delay elements in the momentum selection portion of the circuit and 30 delay elements in the total drift time section. This gives it a range of up to 30ns in the timing difference of radial wires and up to 60ns of maximum drift time. Values less than these extremes are programmable within the chip. The locking of the delay element timing to an external clock is provided as well as numerous diagnostic points. We have tested the delay cell and locking circuits and have found them to function over the range of 1.3ns to 4.0ns, consistent with the CAD) simulations. The mean timers have been found to work and the drift time and momentum restriction circuitry has been partially tested. No design errors have so far been found. Testing is continuing.

Trigger Algorithm Simulation

We have continued to work on trigger simulation in the framework of GEANT, a fast emulation of a stiff track trigger, and with a parameterized global trigger being simulated at Chicago. The utility of a stiff track signal for electron identification has been demonstrated (namely that a 10 fold reduction of the QCD 2 jet rate of false electrons can be effected) and the stiff track momentum resolution requirements (approximately 10% or better) have been shown. This matches the characteristics of the proposed straw track trigger well. We have assessed the effect of material on the trigger with regard to occupancy and additional false rate. At the level of material proposed no significant variations in false rate have been seen. The uncertainty rests with the low statistics inherent in the slow GEANT simulations. This work is continuing along with a program to determine the triggering efficiency for electrons which show significant losses as the amount of material is increased ahead of the trigger. We continue to pursue a trigger based on 8 straw tubes per superlayer. Numerous connection arrangements are being investigated as a means of optimizing the trigger characteristics and fabrication ease for the ASICs.

Cosmic-ray Test Stand

The cosmic-ray test stand is mechanically complete with scintillator trigger counters, straw tube layer, amplifier-discriminators, and cabling. We plan to connect this stand

to a LeCroy 1879 Fastbus TDC in the near future and begin testing the straw tube pattern. Our plan for testing trigger chips is to use the auxiliary card connection of the LeCroy TDC for pickoff of the straw outputs, form the trigger with one of several options, and reconnect the trigger results back into unused channels of the 1879. We will first exercise the chips that arrived in July. Later versions will also be tested. The auxiliary cards that we plan to use are already in hand.

Muon Trigger

The efforts in the area of the muon trigger have been driven by the need to consider descoping options for the detector subsystem. We have begun simulations based on a design with one layer of scintillators with tubes at both ends. In this scheme the drift tubes must provide all the momentum selection. The tradeoff (other than cost) is that the ϕ coordinate from the scintillators can be more precise than the scintillator segmentation (32 bins in ϕ) from the differential timing and the η segmentation of the muon trigger can be naturally aligned with the calorimeter segmentation for isolation restrictions if desired.

Simulation of muon trigger ASICs is continuing on the CAD system at Michigan. As trigger algorithms for muons are developed, trigger chips that implement the design will be fabricated. We anticipate such a chip in the fall of 1991.

8. LOS ALAMOS NATIONAL LABORATORY (LANL)

Cost and Schedule Activities

Integration of the program schedule and resource files has been completed. The prepared OPEN-PLAN neutral files will be transmitted to LBL on July 31, 1991. The LANL sub-project must be linked with the other silicon tracker program activities being compiled by LBL. More effort will be required to achieve a completely integrated schedule/resource plan with all the appropriate sub-project interconnects resolved. Future efforts will be directed toward minimizing the integration task involved with up-loading program revisions.

Silicon Tracking System Configuration Studies

System integration activities performed this reporting period were in the following areas:

- forward region silicon planar array structural interfaces
- alignment
- power/electronics interconnects.

Forward Region Structural Analysis

A conceptual structure of Forward Region Planar Array 15 was analyzed to determine its static and dynamic stiffnesses as well as its response to temperature change if it were kinematically mounted at three points on its outer edge. This particular array was chosen because it represents the worst case for the forward region structures.

Three concentric rings of graphite/epoxy composite connected by three equally spaced radial webs compose the substructure to which the silicon detector strips are attached. A kinematic mount is located at the outmost end of each web. The inner ring, which has a minimum radius of 180 mm, is similar to a conventional wide- flange beam in cross-section. The inmost flange is cut away in an alternating pattern to form castellations to which the inner ends of the internal array of silicon strips are attached. When the structure is subjected to a temperature change, the castellations, which appear to be short cantilever beams, act as complaint members to accommodate differential contractions due to differences in material CTE. The outer ring has a maximum radiusof 465 mm and is configured the same way to accommodate differential contractions of the external array of strips. Adjoining ends of the strips are attached to an intermediate ring which has a mean radius of 285 mm. This ring, which is closed- cell structure 12 mm x 30 mm in cross-section, provides cooling for the strips. The strips are arranged on the substructure in an alternating pattern so that half are mounted on the upstream (axial or z-direction) face and half are mounted on the downstream face.

Static analyses show that when the structure is mounted in a vertical attitude, with one of its kinematic points at the uppermost position, its maximum sag is approximately 22 microns in a downward radial sense. This is indicated as the delta y value for node 1 in Fig. 8-1. A finite element model of 1/3 of Forward Region Planar Array 15 may be seen as Fig. 8-2 and demonstrates the static deformation associated with gravity loading.

Alignment Studies

A metrology laboratory to test alignment concepts for silicon trackers is being developed. During the past quarter we have made some progress towards this goal. Precision glass spheres are a key alignment tool for many alignment tasks, but we had not been able to purchase precision spheres for proof of concept tests, because they were too expensive. Recently, we located a supplier that will make spheres at reasonable cost, and we have ordered several spheres. With Los Alamos Laboratory funds, we ordered an electronic autocollimator for the metrology laboratory and expect to have it available soon to make precision angles and position changes. In addition, several Zygo laser interferometers and piezoelectric drivers are now available from another LANL program for use in the metrology laboratory; we are learning to remotely operate them using a PC. Small optical hardware for setting up optical experiments has been collected, and with a few purchase orders to supplement this equipment, we will soon have enough equipment to do some reasonable testing. A schematic of the test setup we envision can be seen in Figure 8-3. We have continued to survey techniques for making precision measurements of large structure shape changes. We still believe that TV holography is the best approach. During the next few months work will be performed towards bringing TV holography into our metrology laboratory as well as setting up and making measurements with the other equipment that we now have.

Power/Electronic Interconnects

Power distribution cabling and data readout chip arrangement for the central region is intimately connected with the structural and detector electronic cooling system design. Configuring the high speed power and data transmission interconnects, on and off the silicon detector, presents a significant thermal problem as well as packaging and electro-magnetic interference problems. A secondary issue relates to the assembly and disassembly of the silicon shell assemblies for maintenance reasons. LANL and LBL are jointly developing design concepts for these specific issues. Modularization of the on-board data readout electronics is being undertaken with the objective of minimizing the thermal resistance of the package, while providing means for avoiding undesirable electromagnetic coupling with the silicon strips. Completion of this activity is essential to configuring the central region design arrangement.

Power Cabling/Electronic Readouts

The shielding requirements of the electronic hybrid structure were analyzed and the results applied to the design of a two- layer prototype. Referring to Figure 8-4, the nominal dimensions of the two-level hybrid are: insulator thickness (It) = 25

um, ground plane thickness (Mt) = 75 um, stripline thickness (t) = 5 um, stripline width (w) = 25 um, stripline pitch (p) = 50 um, and stripline insulator thickness (b) = 55 um. Using aluminum as the conductor material, the electrical, thermal, and radiation length where evaluated for the following insulating materials.

Material	Zo	Attenuation	Thermal Resistance	Radiation Length
	(ohm)	(dB/cm) @ 100 MHz	(C/W/cm^2)	(%)
Kapton	47	3.4	1.03	0.31
AlN	30	5.3	0.017	0.44
BeO	34	4.7	0.017	0.44
Alumina	29	5.6	0.061	0.47
SiC	14	11.7	0..017	0.44

Tracking System Interfaces

The activities related to establishing design interface issues within the calorimeter volume continued this report period. LANL submitted an alternative support arrangement for the silicon tracking system that uses a "tangent-bar" support concept. This support method has been successfully used in the optics field as a kinematic support. The concept supplied for inclusion in the SDC detector would rely on attachment to a rigid shell or ring support. The array of concentric shell assemblies contained in the straw drift-tube detector must be designed to not only support the tracker, but maintain the exact alignment as well.

Materials Science Studies

The use of a cyanate ester resin system instead of an epoxy for the advanced composite materials composing the cooling rings is under consideration. The cyanate ester resin exhibits much better moisture absorption and desorption properties as well as greater radiation hardness than highly cross-linked epoxy resins. The moisture performance of a pure cyanate ester resin, RS-3, and a highly cross-linked epoxy, 934, may be seen in Figure 8-5. The maximum processing temperature of the cyanates is the same as epoxies and the cost is also comparable. In addition to having maximum moisture absorption nearly a factor of 6 lower than epoxies, the cyanates demonstrate only a marginally lower elastic modulus, on the order of 3 GPa and a bit larger coefficient of thermal expansion (CTE), on the order of 40 ppm/C°. These characteristics can be used with ultra-high modulus graphite fibers to yield a laminate CTE approaching zero or 2.6 ppm/C°, that of silicon, as desired. Fabrication of test specimens to verify the aforementioned attributes of these materials is in progress.

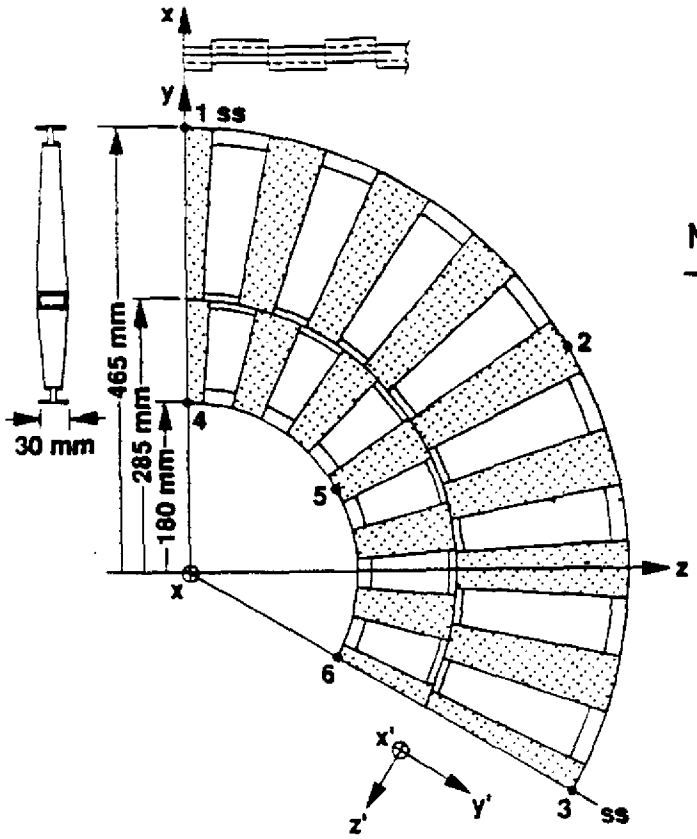

Gravity Sag Displacements (μm)
(vertical orientation)

	w/o Wafer Stiffening			I-Beam Wafer		
Node	Δx	Δy	Δz	Δx	Δy	Δz
1	0	-21.94	0	0	-14.97	0
2	0	-11.14	6.26	0	-7.74	4.33
3 (L)	0	21.75	0	0	15.05	0
4	0.01	-21.87	0	0.04	-15.23	0
5	0	-12.89	7.28	0.01	-9.13	5.15
6 (L)	-0.02	22.03	0	-0.04	15.31	0

Figure 8-1. Static displacements resulting from gravity loading.

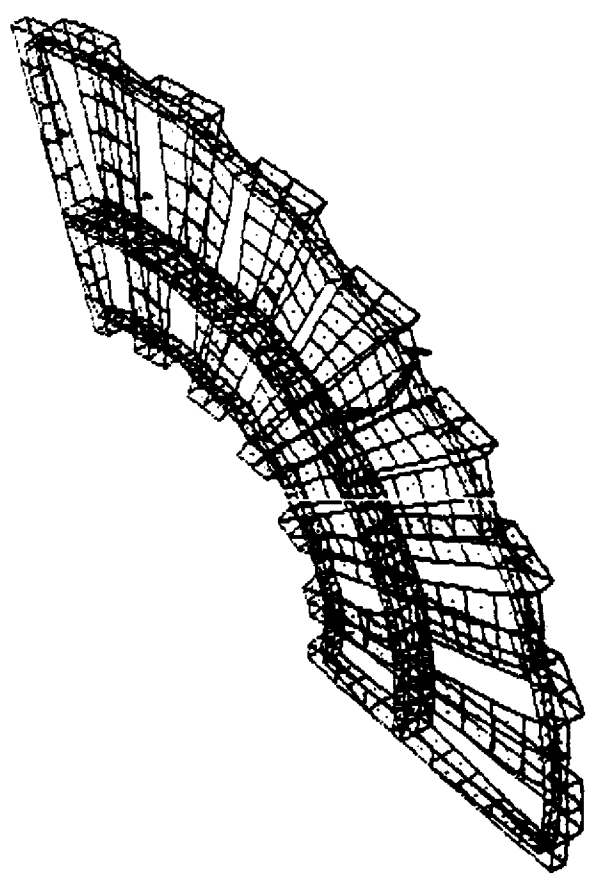

Figure 8-2. Deformed finite element configuration due to gravity loading.

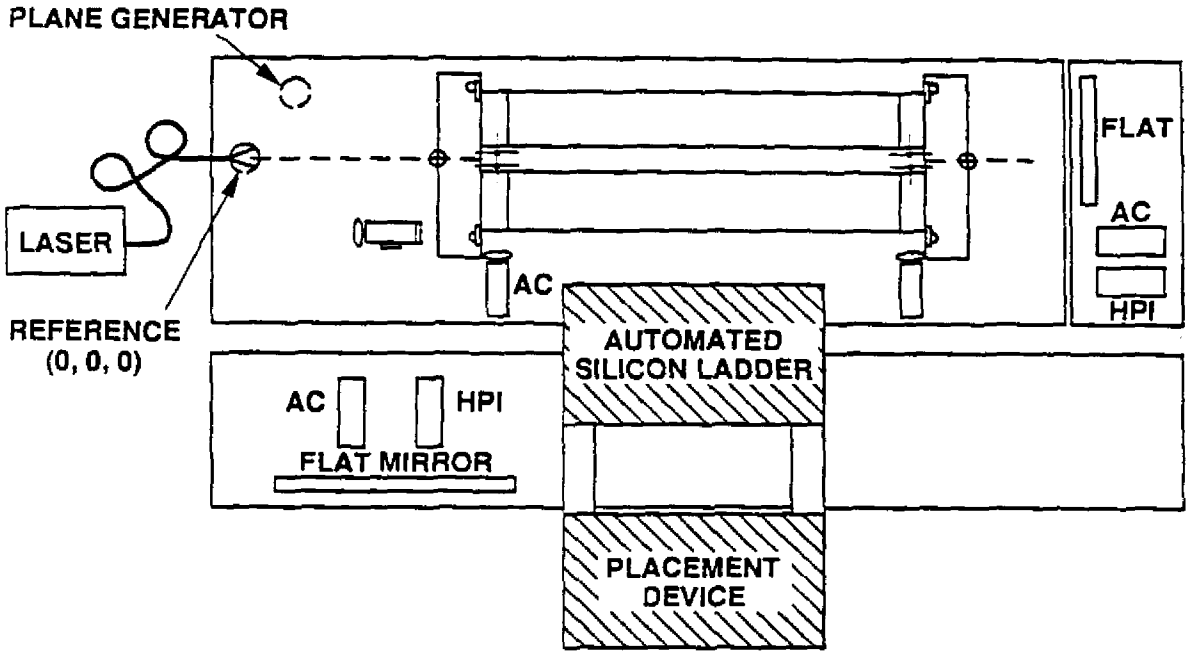

Figure 8-3. Alignment concept schematic.

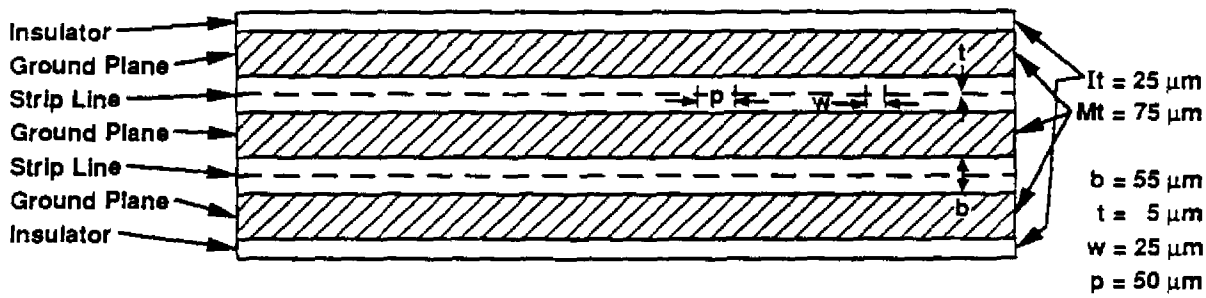

Figure 8-4. Two layer hybrid circuit sketch.

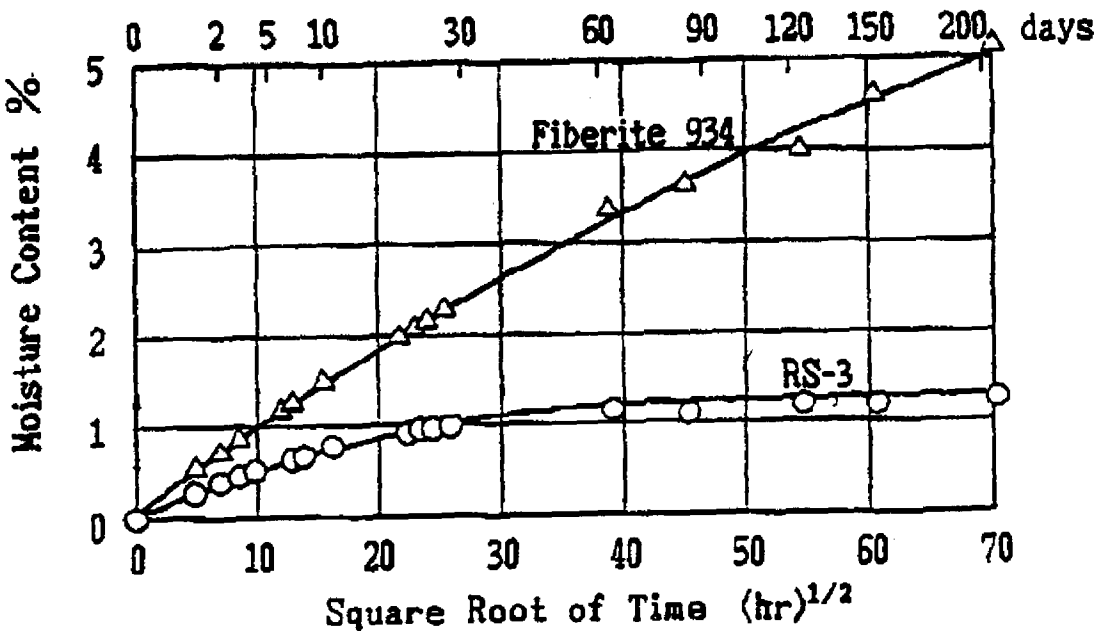

Figure 8-5. Moisture absorption of cyanate ester and epoxy resins.

9. ICF – KAISER ENGINEERS (KE)

Activities this month consisted of continuing the development of conceptual tools and fixtures for the assembly of t.he various components of the detector in the hall. Construction planning and t.he preparation of monthly assembly sequence drawings were also. continued.

A conceptual design *of* fixtures and methodology for the installation of the muon steel barrel coil segments and the muon chamber guides was developed.

The assembly procedures for the forward toroids were revised and a conceptual design of the rolling supports of the forward toroids was made.

The temporary supports of octants 4 and 6 *of* the muon steel barrel were also revised and simplified.

Schedule

Figure 1 shows the latest version of the construction schedule *of* the detector *for* the Underground portion only. This schedule is being coordinated with the construction-sequence drawings that follow and it is being revised as the construction sequence methods are developed.

Construction Sequence

Figures 2 through 42 show the construction sequence through month 38. There are two types of drawings shown. The monthly progress drawings are coordinated with the schedule. Interleaved with the progress drawings are sequences that show construction methods for some of the operations. These drawings are not yet totally coordinated so that there are discrepancies that will be corrected as the job progresses. These discrepancies occur due to the trial and error method utilized in the design as well as the changes in the data received from the different participants in the collaboration.

The drawings shown were developed during the month of July and therefore do not represent a complete set. The drawings that are repeated from last month have been extensively revised.

Month O: This drawing (fig 2) shows the hall at beneficial occupancy. It has been revised to include the air conditioning ducts.

Figure 3 shows the muon steel barrel supports with the hydraulic aligning system. This system is being revised at present and will include horizontal tie bars or beams between the supports.

Month 6: This drawing (Fig. 4) is self explanatory. It has been revised to incorporate both the air conditioning ducts as well as the stairs and air conditioning ducts.

Figure 5 shows the barrel bottom layer of plates already installed and plates for octants 4 and 6 in the process of being installed. In the background, the assembly frame, utilized as a form for the rest of the octant plates, is being assembled.

Figure 6 shows the assembly frame already in place and plates for octants 3 and 7 being installed. Previously the crossover bridges had been installed.

Figure 7 shows plates for octants 2 and 8 being installed. The walkways shown are bolted temporarily to the barrel plates and will be used for fastening the toe bolts that hold the plates together.

Figure 8 shows the octant 1 plates being installed.

Month 9 (Figure 9) shows the status of the barrel steel assembly on month 9. This drawing has been revised to include ductwork and stairs.

Figure 10 shows forward toroid number 2 being assembled. The bottom plates are placed on temporary cribbing and also on the Hillman rollers supports. After assembly, the hydraulic jacks placed on the Hillman rollers will lift the toroid and the temporary cribbing will be removed.

Figure 11 shows the forward toroid number 2 complete.

Drawings 12 and 13 show the forward toroid number 1 support and roller system. This support system was developed at a later date and differs from what is shown in other drawings. Each toroid weighs in the neighborhood of 2000 metric tonnes, so it requires four 600 tonne capacity Hillman rollers to be able to move it.

Figure 14 shows the forward toroid steel assembly almost complete.

Figure 15 shows the steel for the forward toroids completed and muon chamber uFW3 being installed. Forward toroids number one and two are constructed separated by enough distance as to be able to have access to bolting and for assembly of the interleaving muon chamber. Later the toroids are moved to their proper separation and bolted together as a unit.

Month 12 (figure 16) shows the muon barrel completed and the start of the installation of the muon chamber guides and of the barrel steel coils.

Figure 17 shows a coil segment being lowered to the hall floor. The picture illustrates the large size of this component and the problem of handling it through the construction shaft. The method of handling these coils on the surface and through the construction shaft has not been fully addressed.

Figure 18 shows the installation of muon chamber guides inside the muon steel barrel. The tool used for this purpose is very conceptual and needs further development. The concept attempts to show the problem of operating heavy objects inside the muon steel where there is no crane access. This tool is to be used in the installation of muon chamber guides that may weigh several hundred pounds, barrel

steel coil segments that weigh in the order of 8000 pounds, plus conduit, cable and gas lines for the muon chambers.

This tool has to be provided with walkways for installation workers and be flexible to reach most of the octants in the barrel.

Figures 18 and 19, show the method used to install muon barrel coil segments on the outside of the barrel steel.

The concept here is that the coil segment (which has to fabricated and shipped in one piece) is attached to a hollow shipping frame large enough to avoid excessive coil deflection and which will allow a worker to crawl inside it to bolt the coil in place and to later free the coil from the support frame. Two cranes are needed simultaneously for this operation.

The inner coil segments are installed by the installation frame described above. Figure 20 shows the support beam with the coil being attached to the installation frame. The installation frame is later rolled into the barrel steel for the coil installation (see Figure 21). The tool is provided with rotation capabilities and with hydraulic cylinders that allow the tool operator to position the coil segment in its final location.

Figure 22 shows the installation tool rotated 45 degrees to enable it to install a coil segment in octant 2. The figure also shows the crane holding a walkway for bolting to the barrel steel. This walkway will be later used for the installation of muon chamber truss guides as shown in Figure 23.

Month 15: This drawing (figure 24) is self explanatory.

Month 18: This drawing (Figure 25) shows the muon chambers installed in octant 8, otherwise the picture is self explanatory.

Figure 26 shows a muon chamber panel being installed on octant 4. The tool used for this purpose includes guides that match with the barrel guides. One end of this tool is bolted to the barrel steel temporarily until the muon chamber is rolled onto the barrel steel. Two trolleys are used to pick up the tool and rotate it into position.

Figure 27 shows the method of pick-up of the tool and chambers when vertical panels are to installed. The crane in this case utilized the main hook and an auxiliary hook to control rotation.

Figure 28 shows the tool as it is used to install a panel on octant 2.

Month 19: (Figure 29) shows the central calorimeter being lowered to the hall floor, while progress is being made in the assembly of the end toroids.

The central calorimeter weighs in the order of 4000 metric tonnes. In order to lower the calorimeter to the hall floor, a system was designed to make this operation as inexpensive as possible. The system consists of a frame on top of which the calorimeter is rolled. This frame is held by four hollow hydraulic jacks that operate

on a bundle of cables. (see Figure 30). The frame is then lowered to the hall floor by slow reciprocating motions of the jacks (see Figure 31).

The calorimeter and its supporting frame are detached from the jacking system and rolled over to the steel barrel (see Figure 32). The frame is designed to match the height and rail system of the permanent calorimeter supporting frame.

Figure 33 shows progress up to Month 21.

Figures 34 through 36 show the method of installation of the rear absorber, muon chambers and the Cerenkov counter on the end toroids. We have been informed that both the muon chambers and the forward calorimeter/absorber system are being re-designed, so no further work is planned on this system until the revised design is received.

Month 24 through month 38 are self explanatory and are shown on figures 37 through 42.

SDC SCINT CAL DETECTOR CONSTRUCTION SCHEDULE

MONTHS

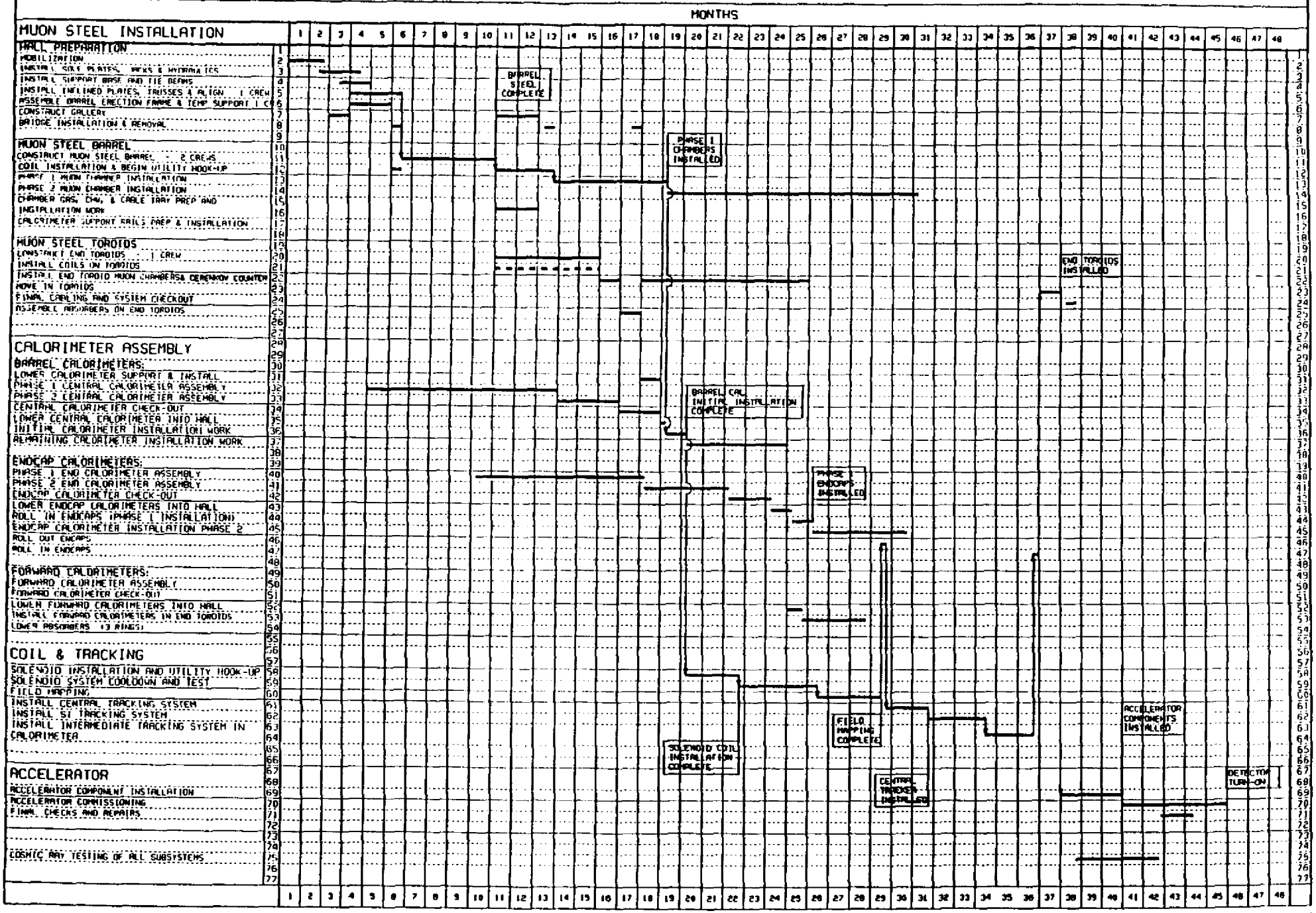

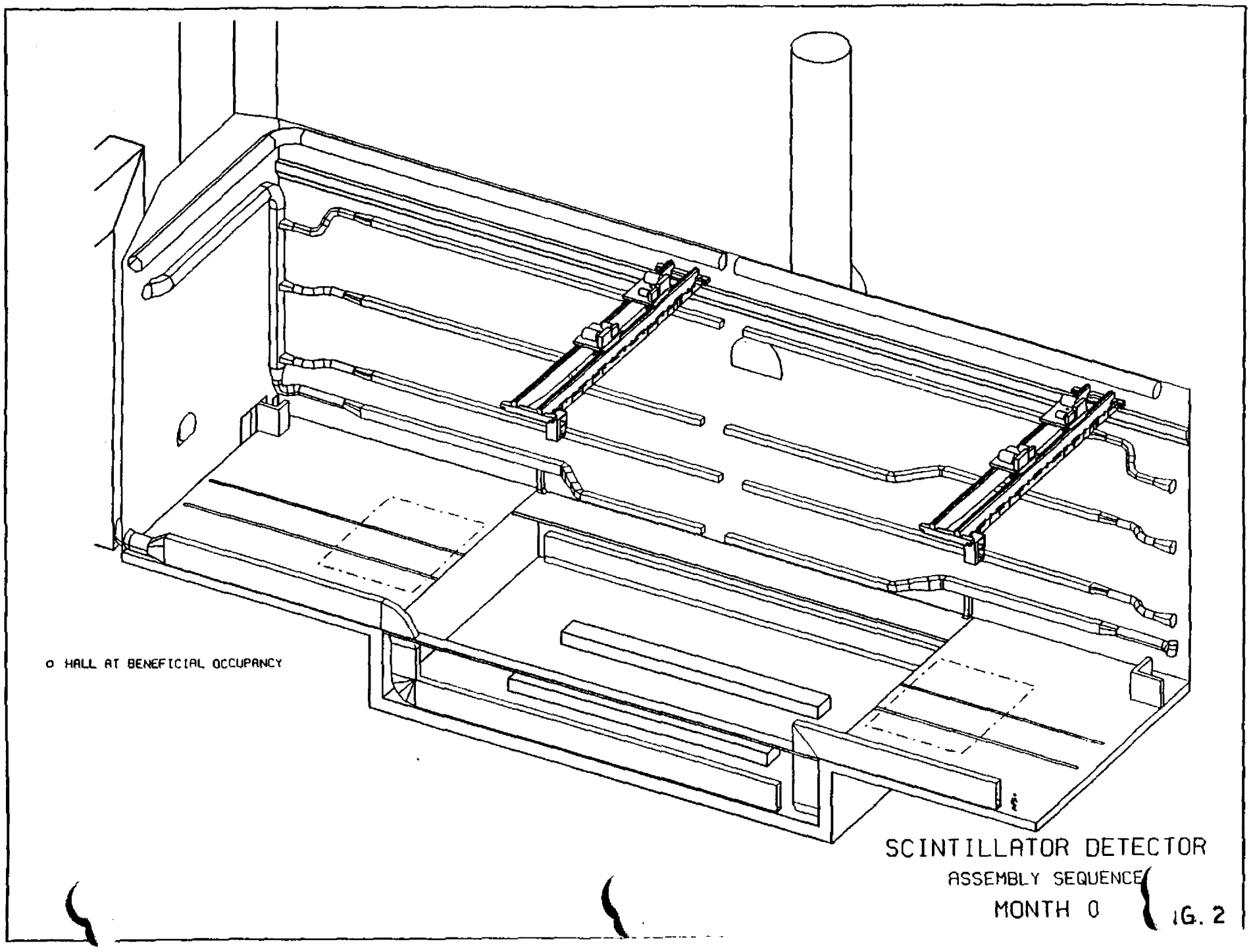

SCINTILLATOR DETECTOR
ASSEMBLY SEQUENCE
MONTH 0

FIG. 2

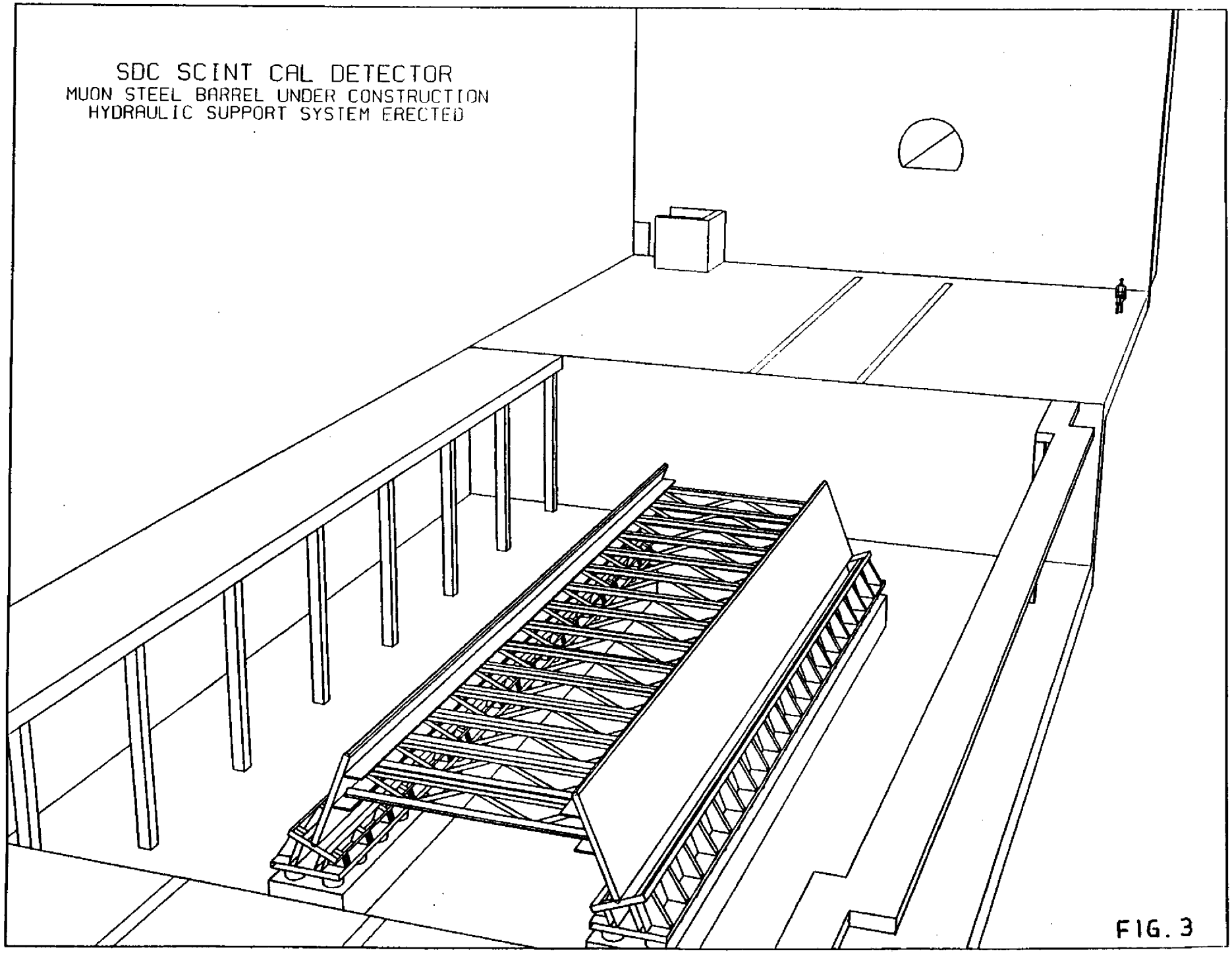
SDC SCINT CAL DETECTOR
MUON STEEL BARREL UNDER CONSTRUCTION
HYDRAULIC SUPPORT SYSTEM ERECTED

FIG. 3

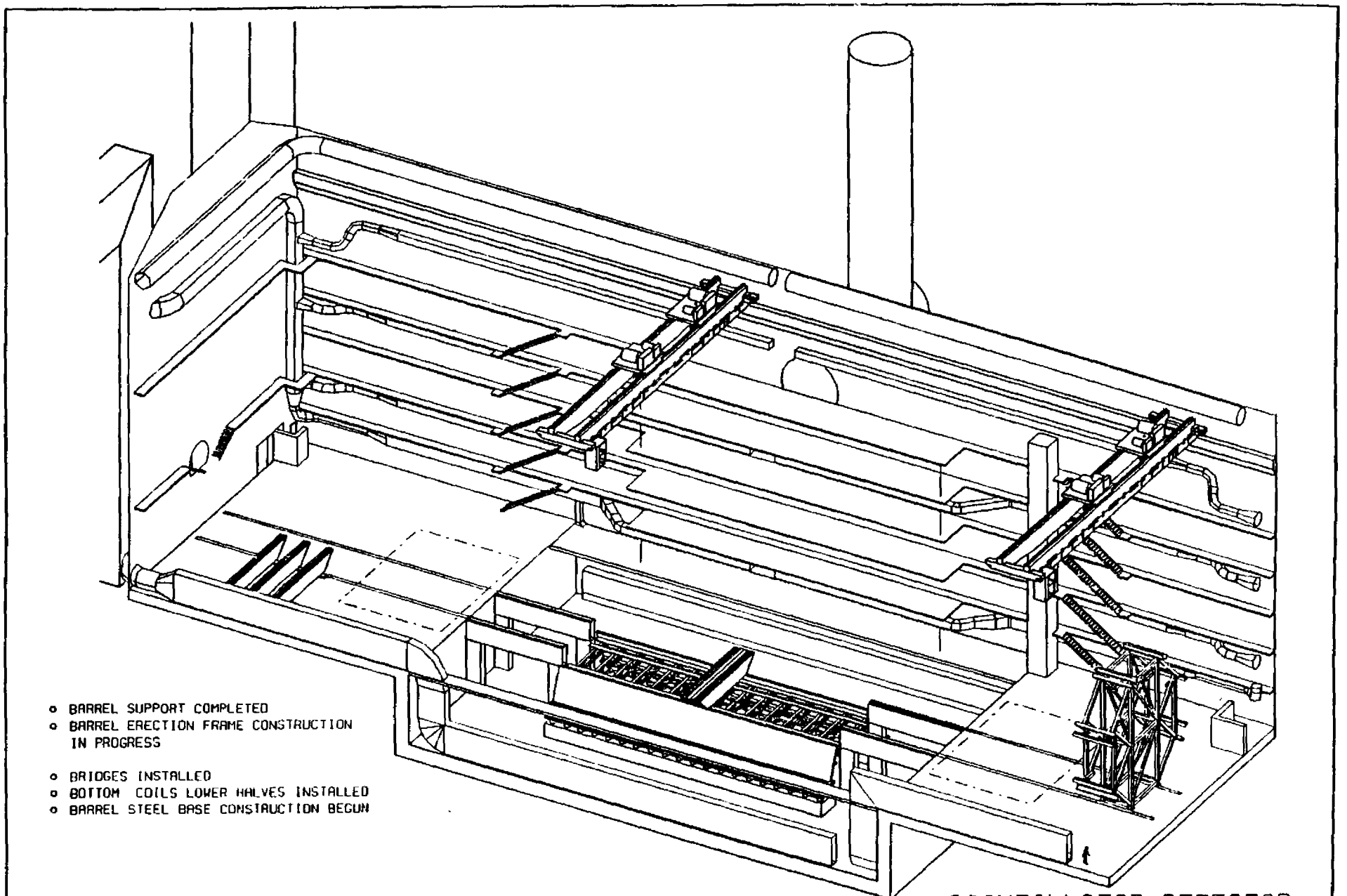

SCINTILLATOR DETECTOR

ASSEMBLY SEQUENCE

MONTH 6

Fig. 4

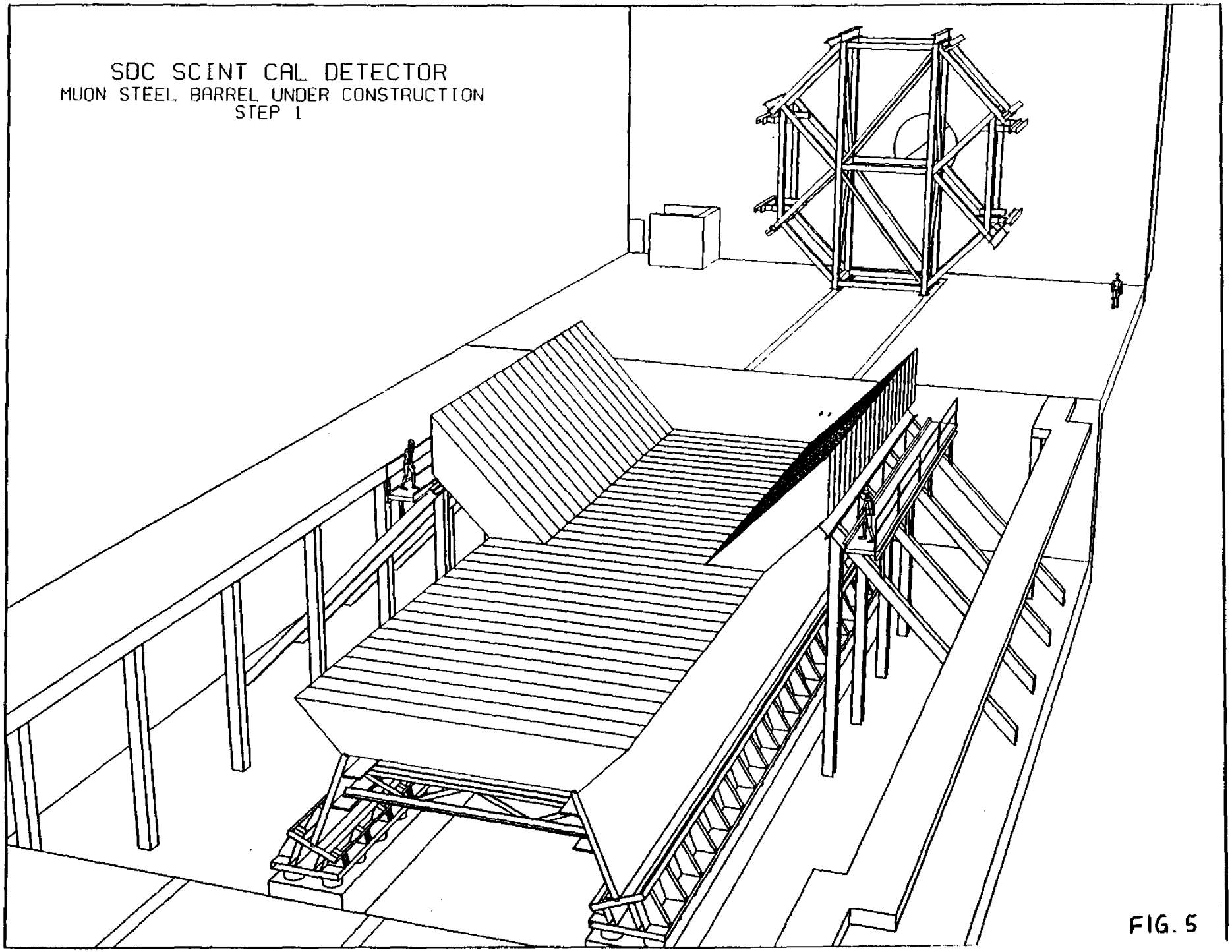
SDC SCINT CAL DETECTOR
MUON STEEL BARREL UNDER CONSTRUCTION
STEP 1

FIG. 5

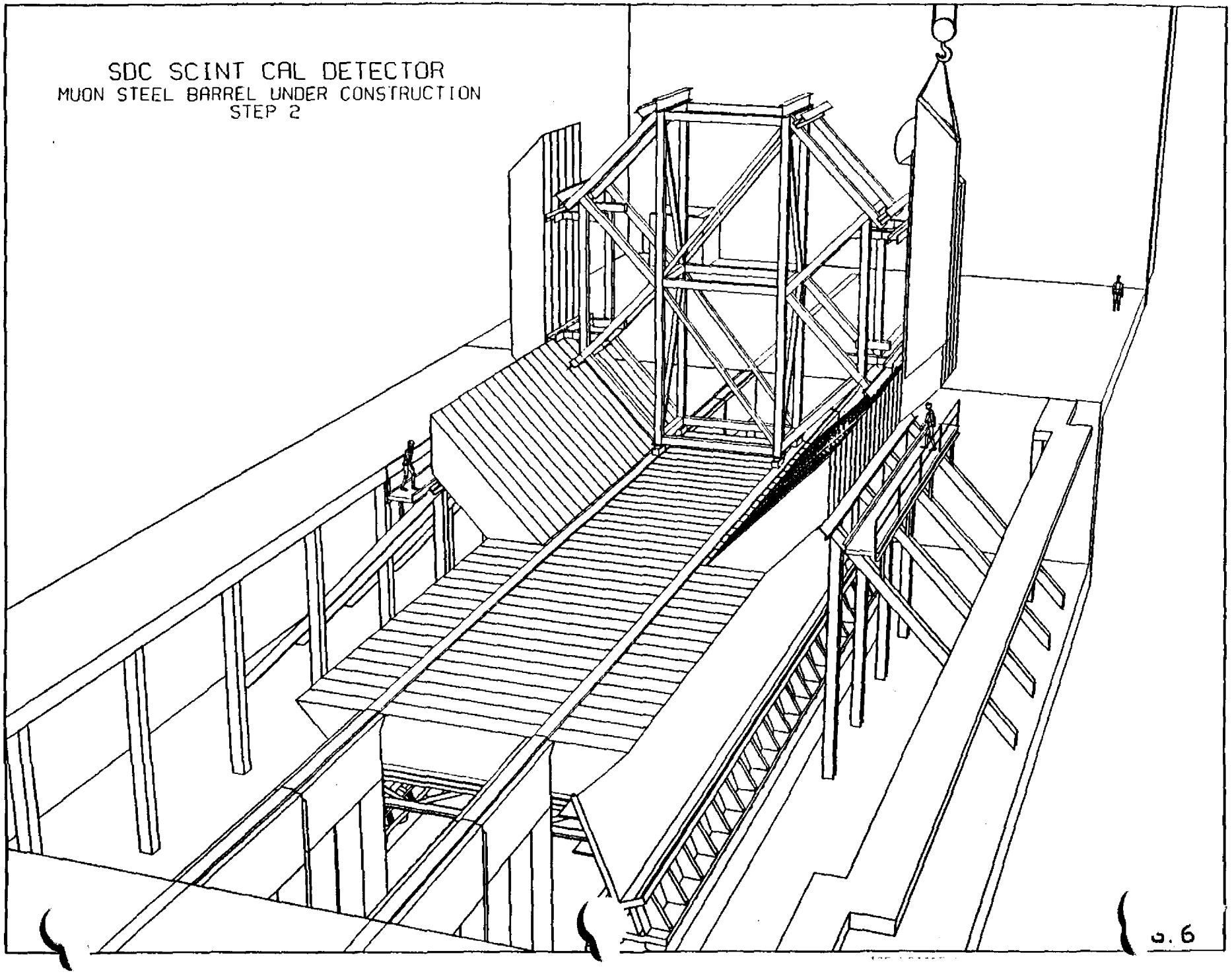
SDC SCINT CAL DETECTOR
MUON STEEL BARREL UNDER CONSTRUCTION
STEP 2

5.6

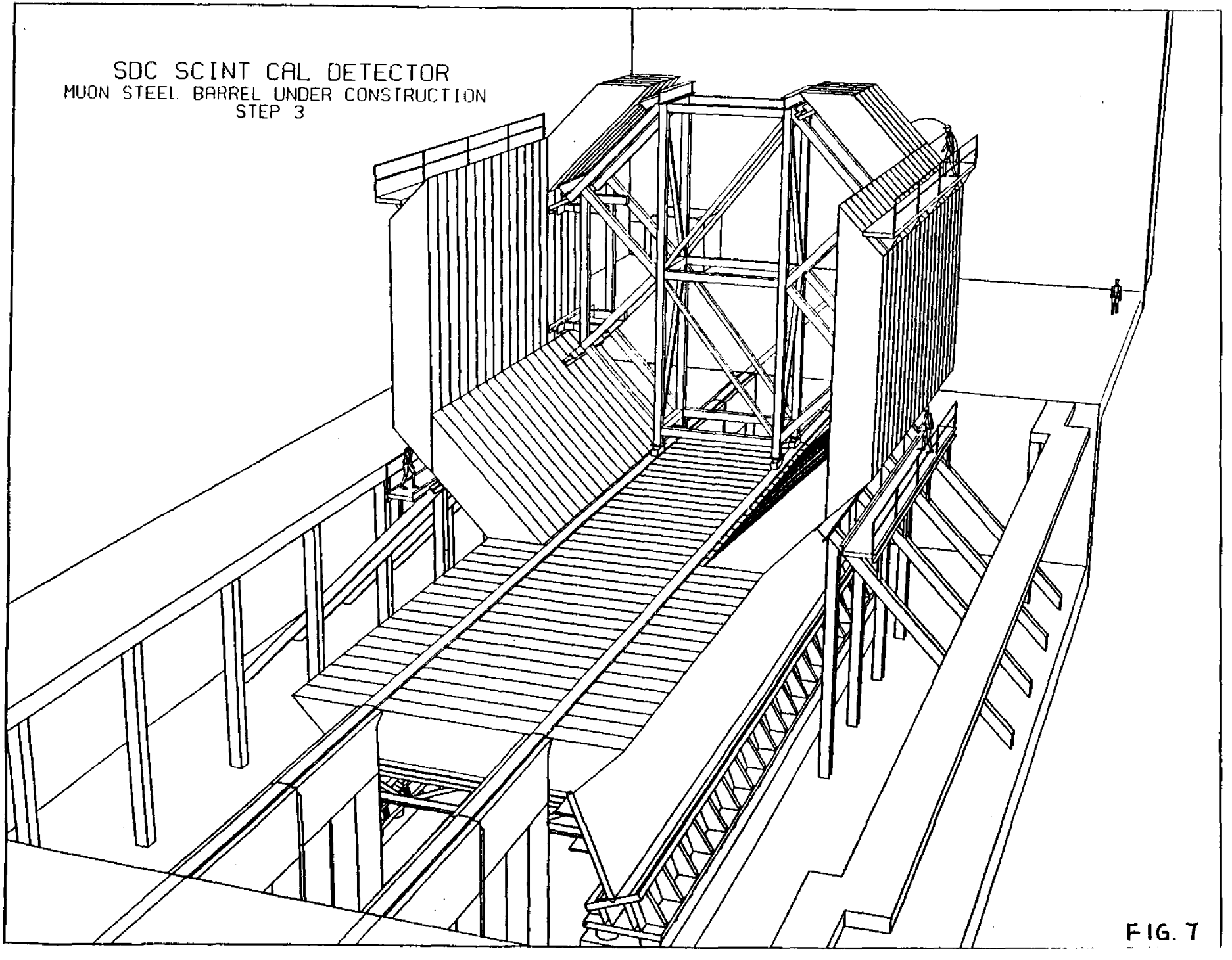
SDC SCINT CAL DETECTOR
MUON STEEL BARREL UNDER CONSTRUCTION
STEP 3

FIG. 7

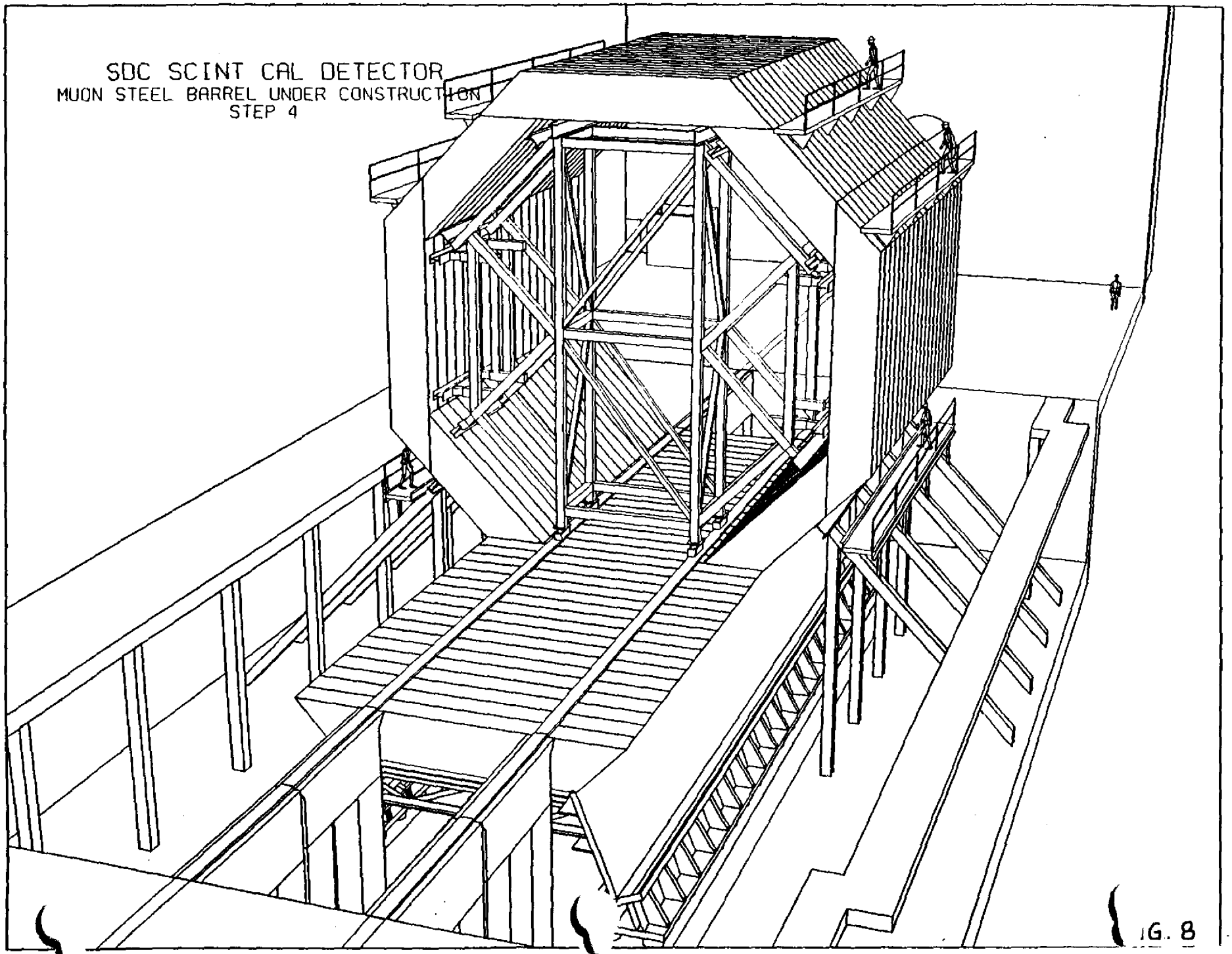
SDC SCINT CAL DETECTOR
MUON STEEL BARREL UNDER CONSTRUCTION
STEP 4

IG. 8

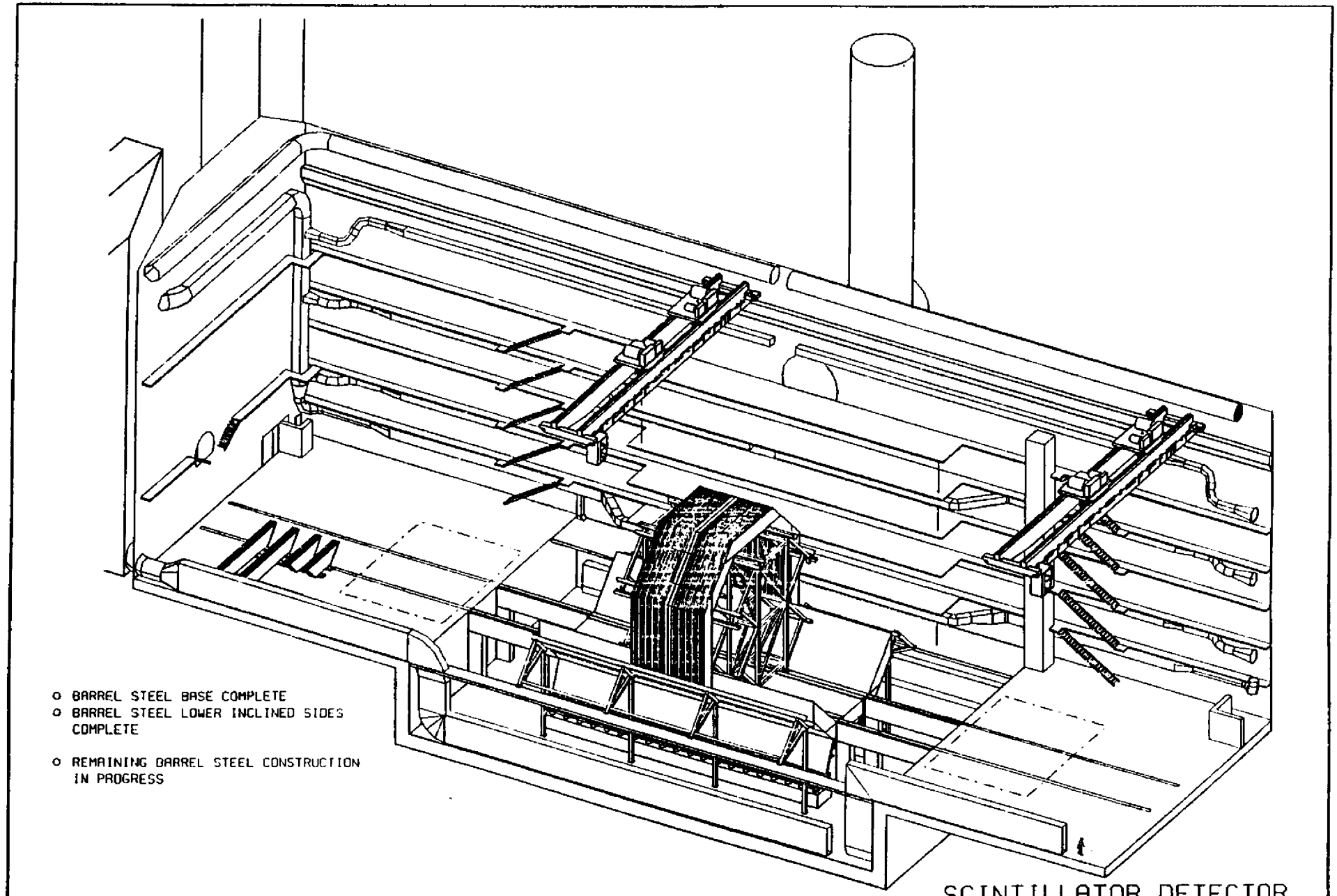

SCINTILLATOR DETECTOR

ASSEMBLY SEQUENCE

MONTH 9

FIG. 9

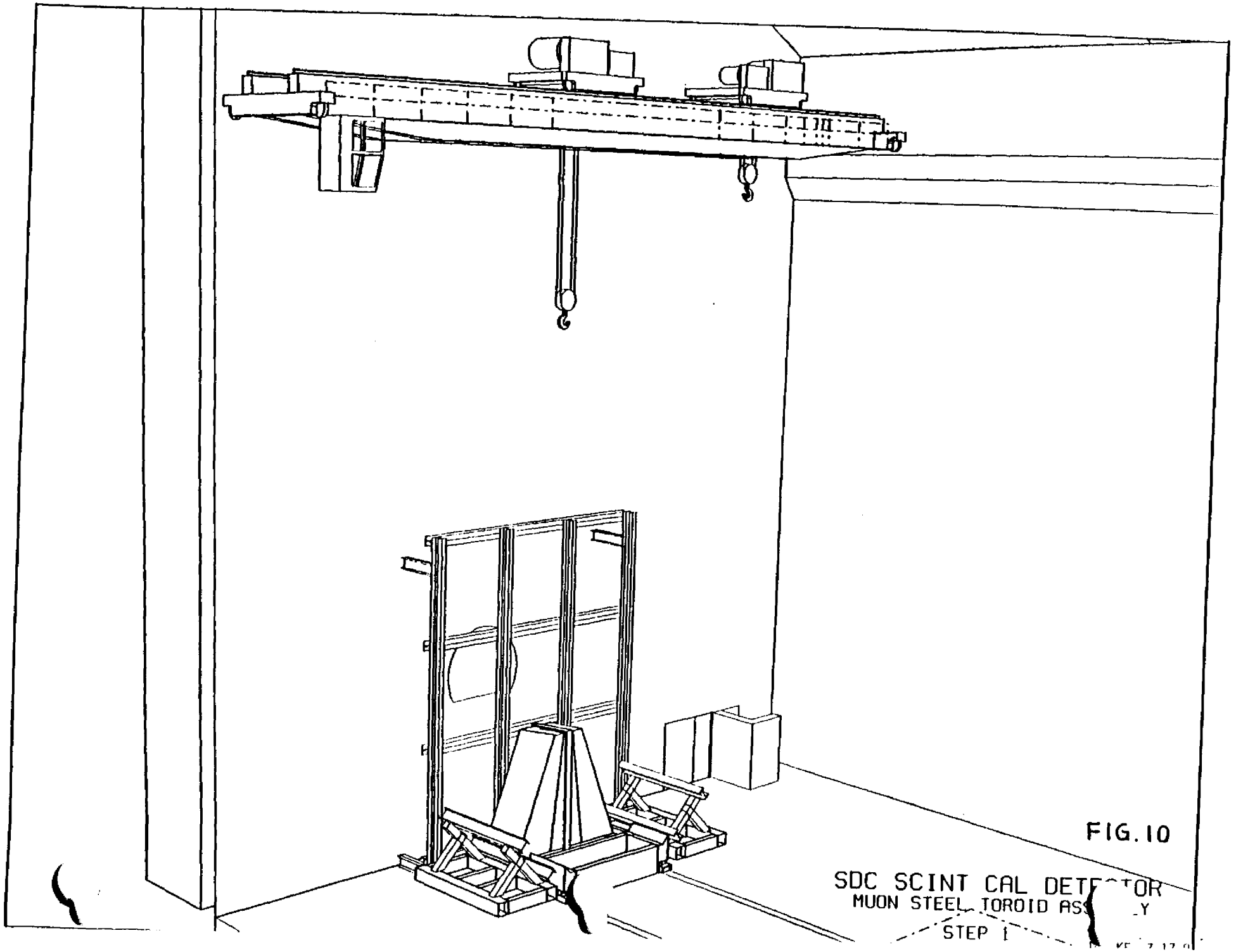

FIG. 10

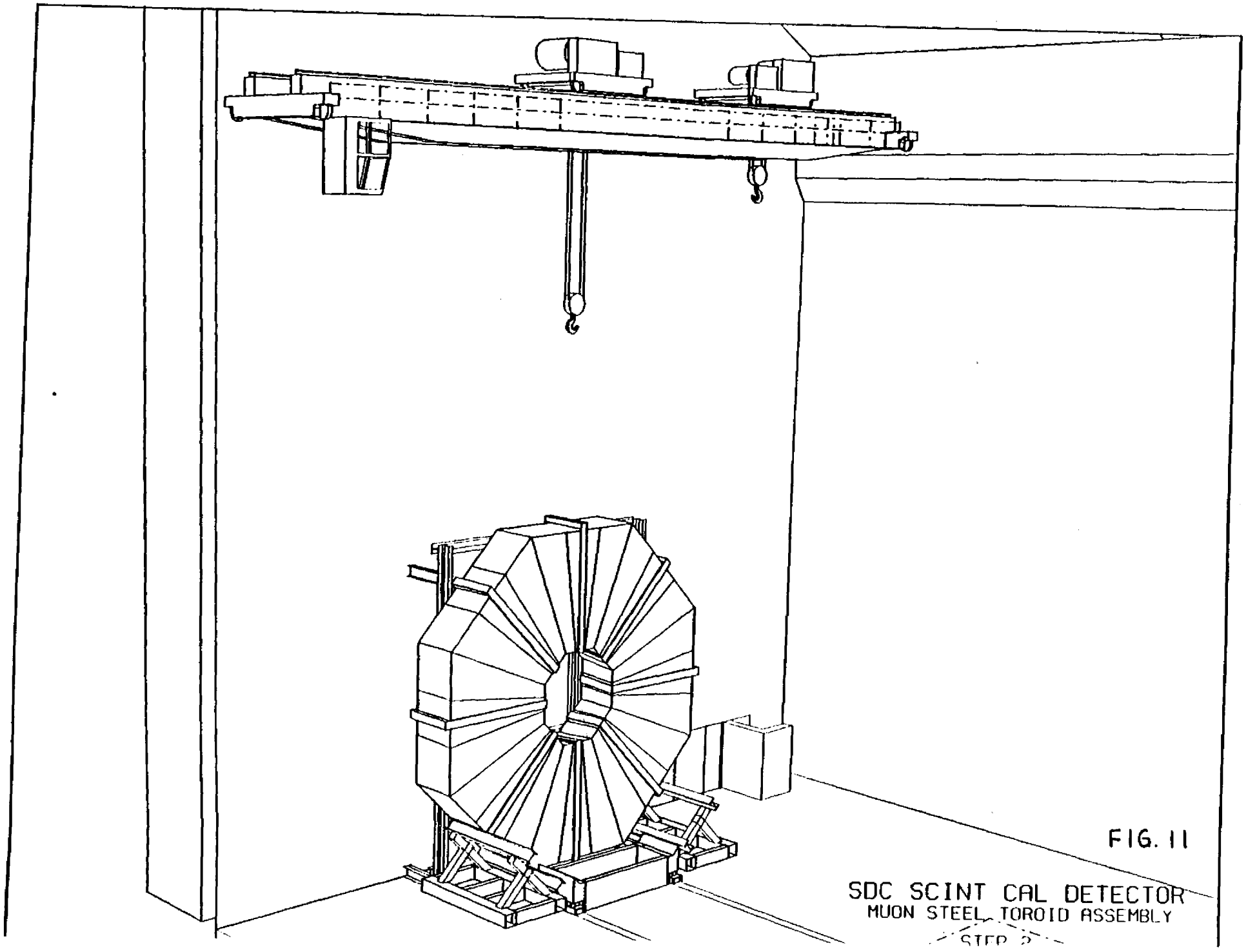

FIG. 11

SDC SCINT CAL DETECTOR
MUON STEEL TOROID ASSEMBLY
STEP 2

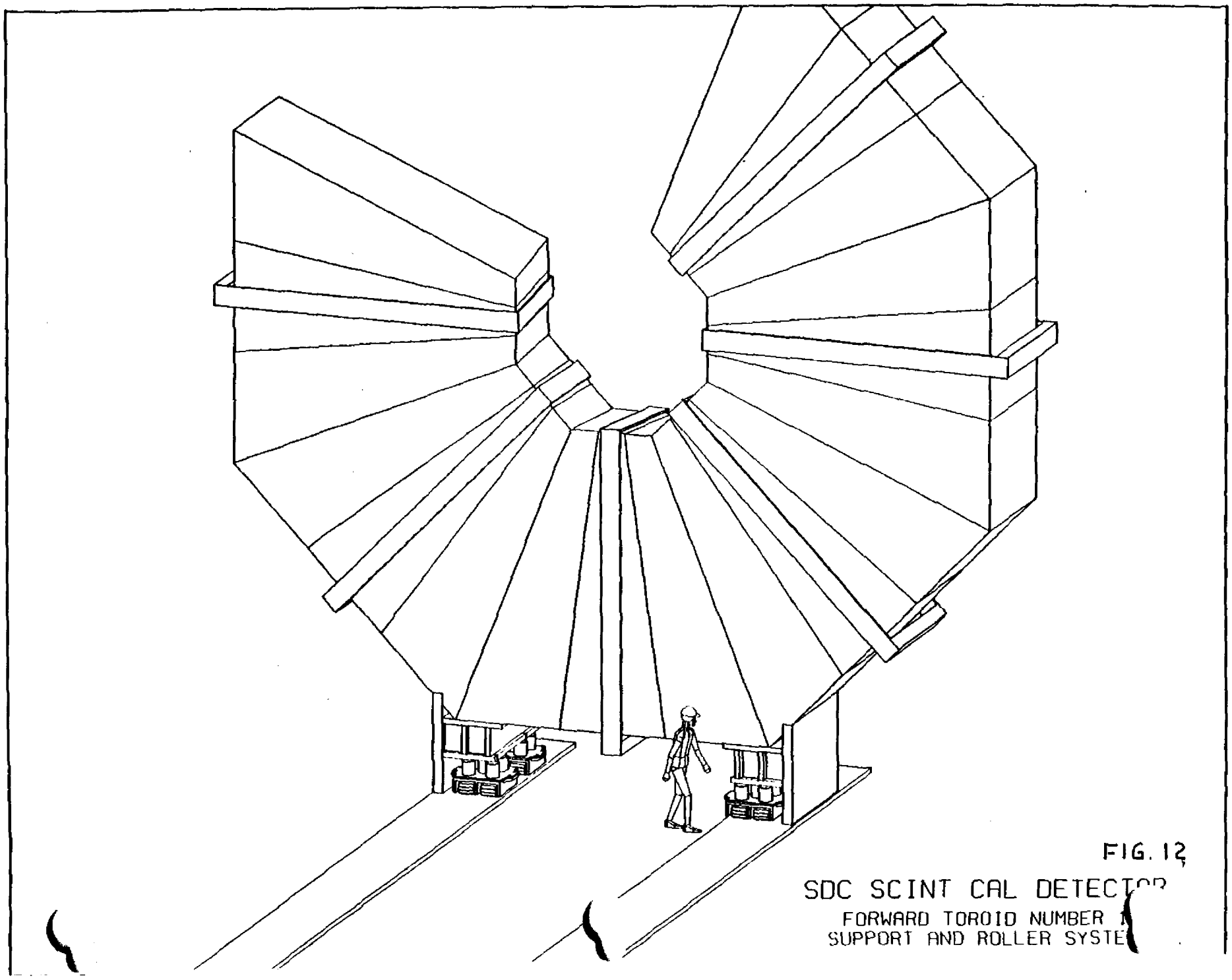

FIG. 12

SDC SCINT CAL DETECTOR

FORWARD TOROID NUMBER 1

SUPPORT AND ROLLER SYSTEM

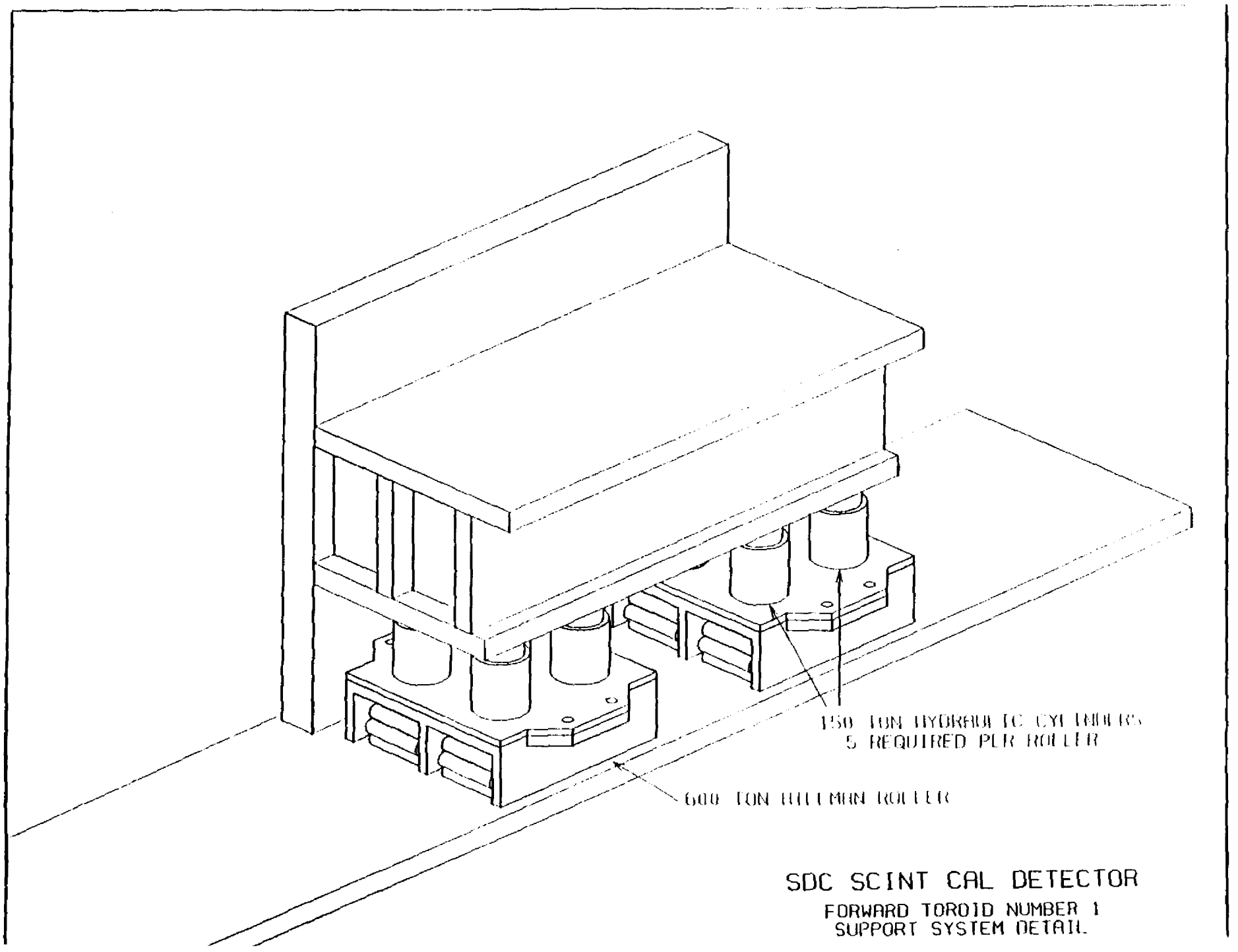

SDC SCINT CAL DETECTOR

FORWARD TOROID NUMBER 1
SUPPORT SYSTEM DETAIL

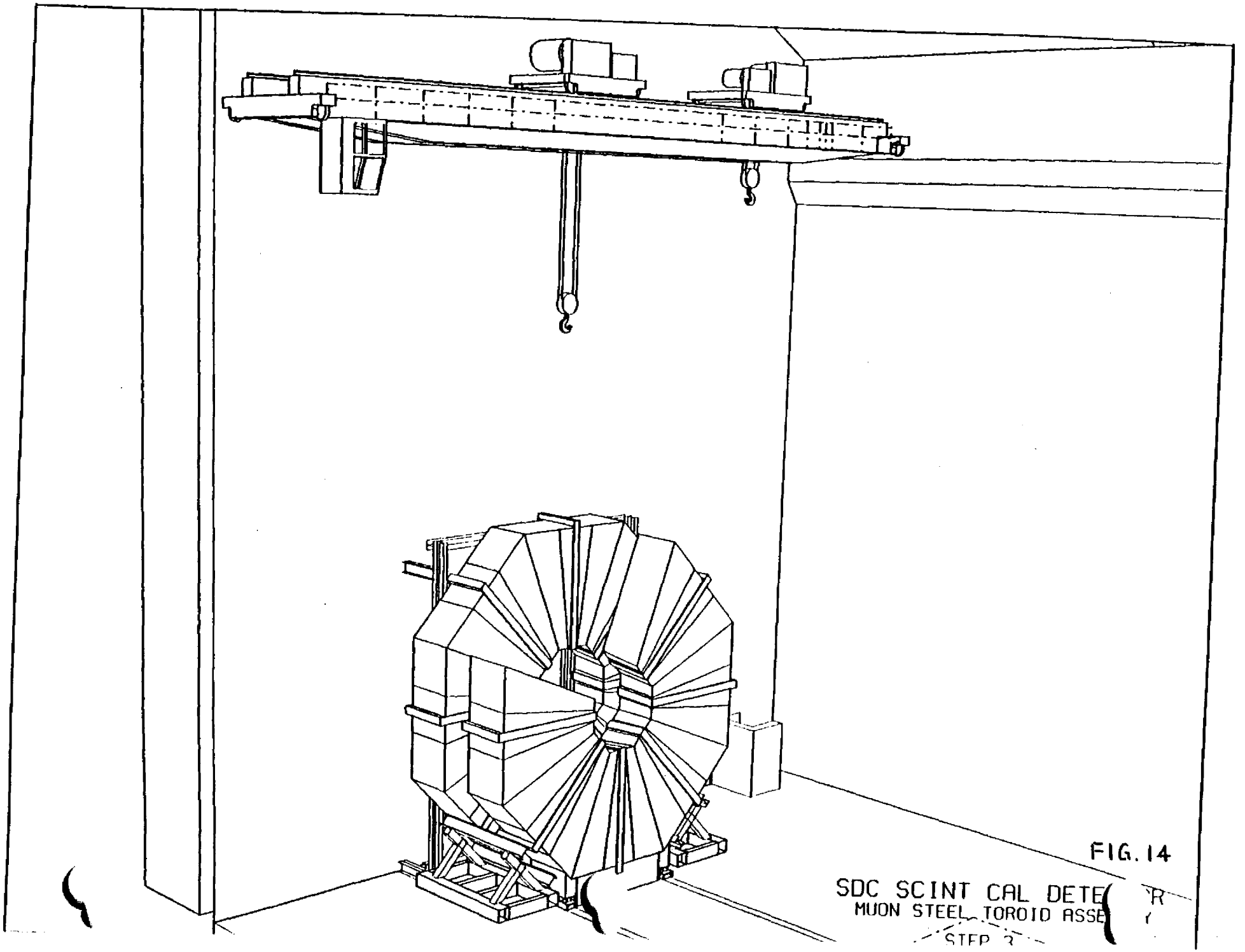

FIG. 14

SDC SCINT CAL DETE R
MUON STEEL TOROID ASSE

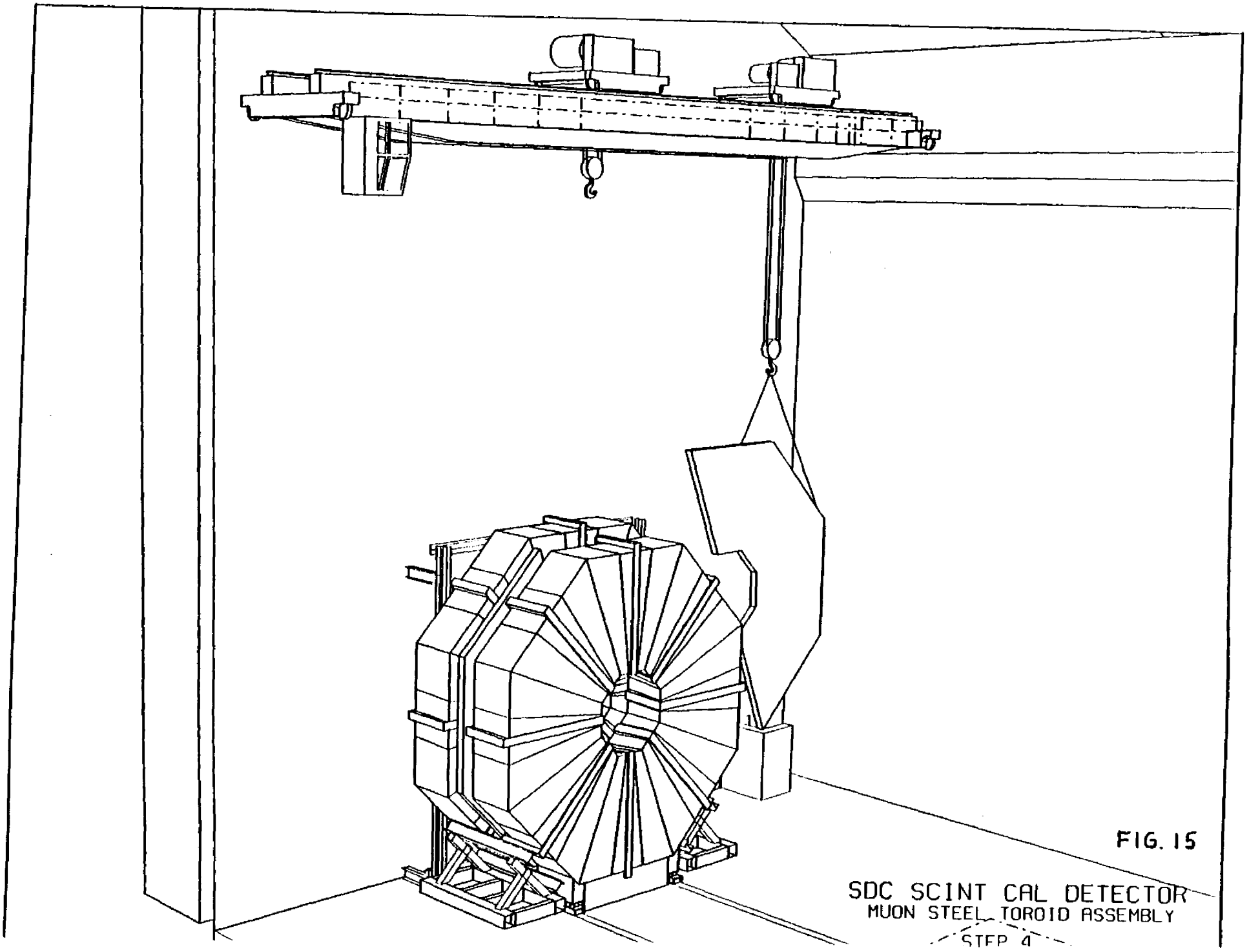

FIG. 15

SDC SCINT CAL DETECTOR
MUON STEEL TOROID ASSEMBLY
STEP 4

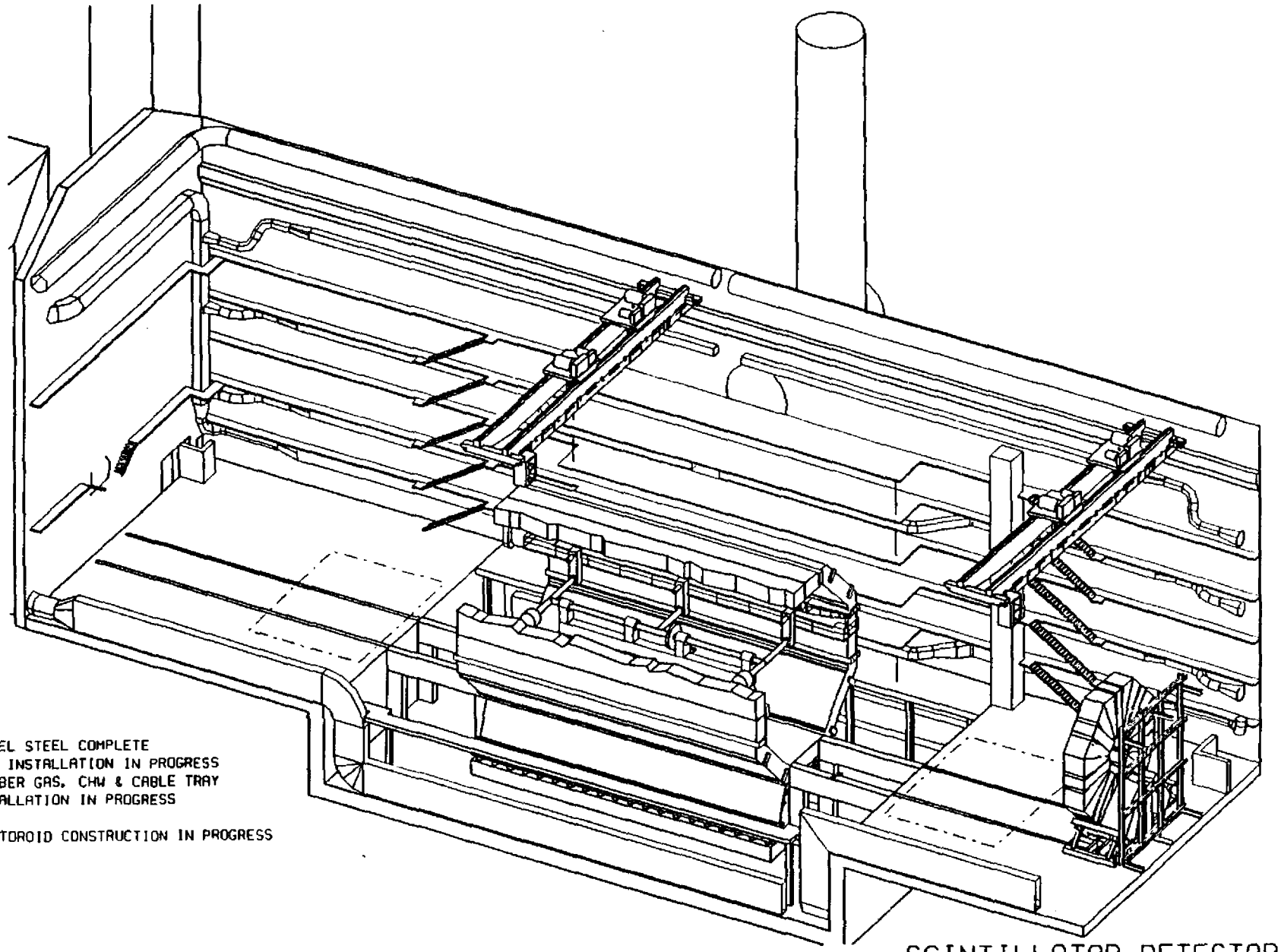

- o BARREL STEEL COMPLETE
- o COIL INSTALLATION IN PROGRESS
- o CHAMBER GAS, CHW & CABLE TRAY INSTALLATION IN PROGRESS
- o END TOROID CONSTRUCTION IN PROGRESS

SCINTILLATOR DETECTOR

ASSEMBLY SEQUENCE

MONTH 12

3.16

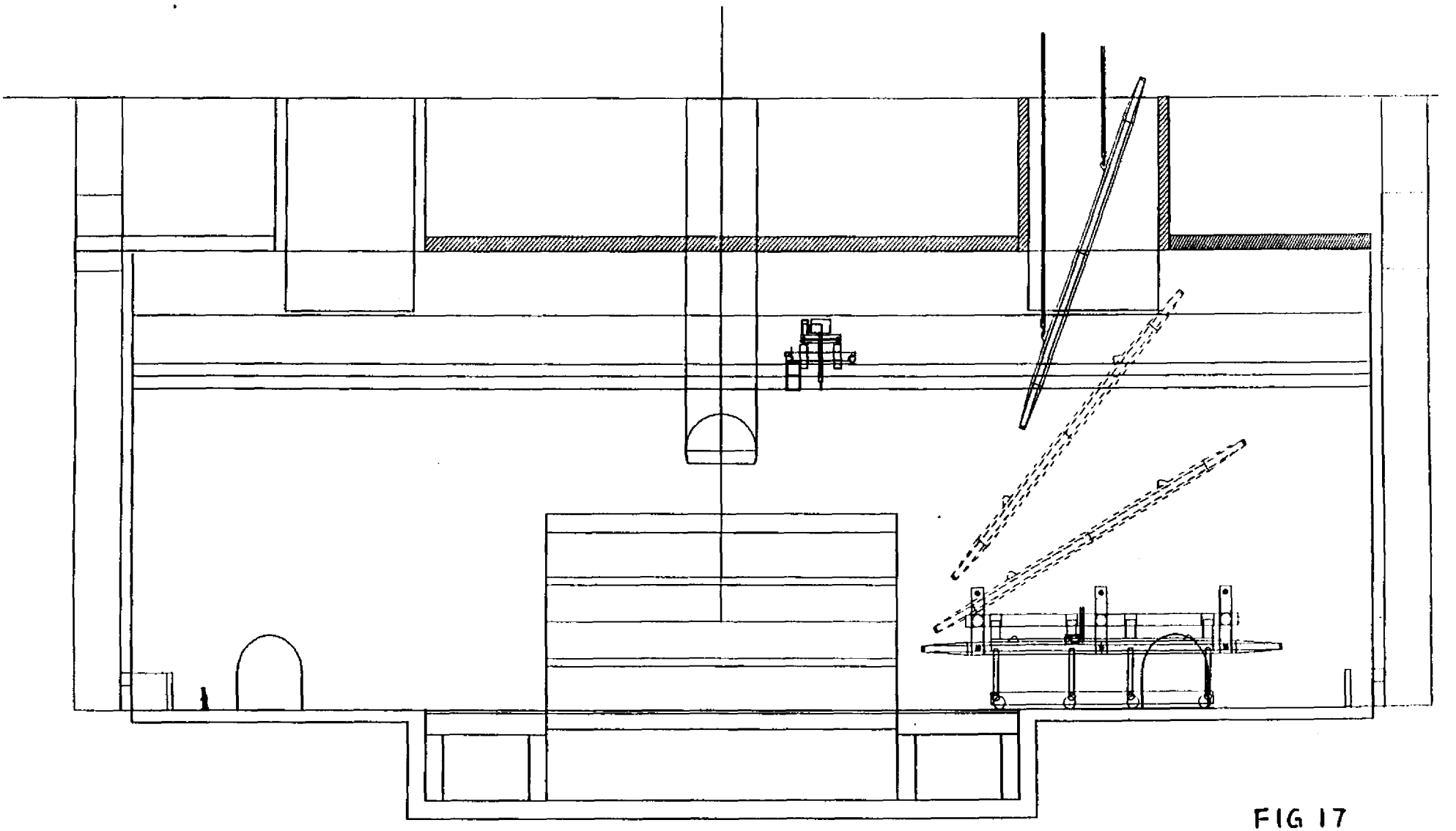

FIG 17

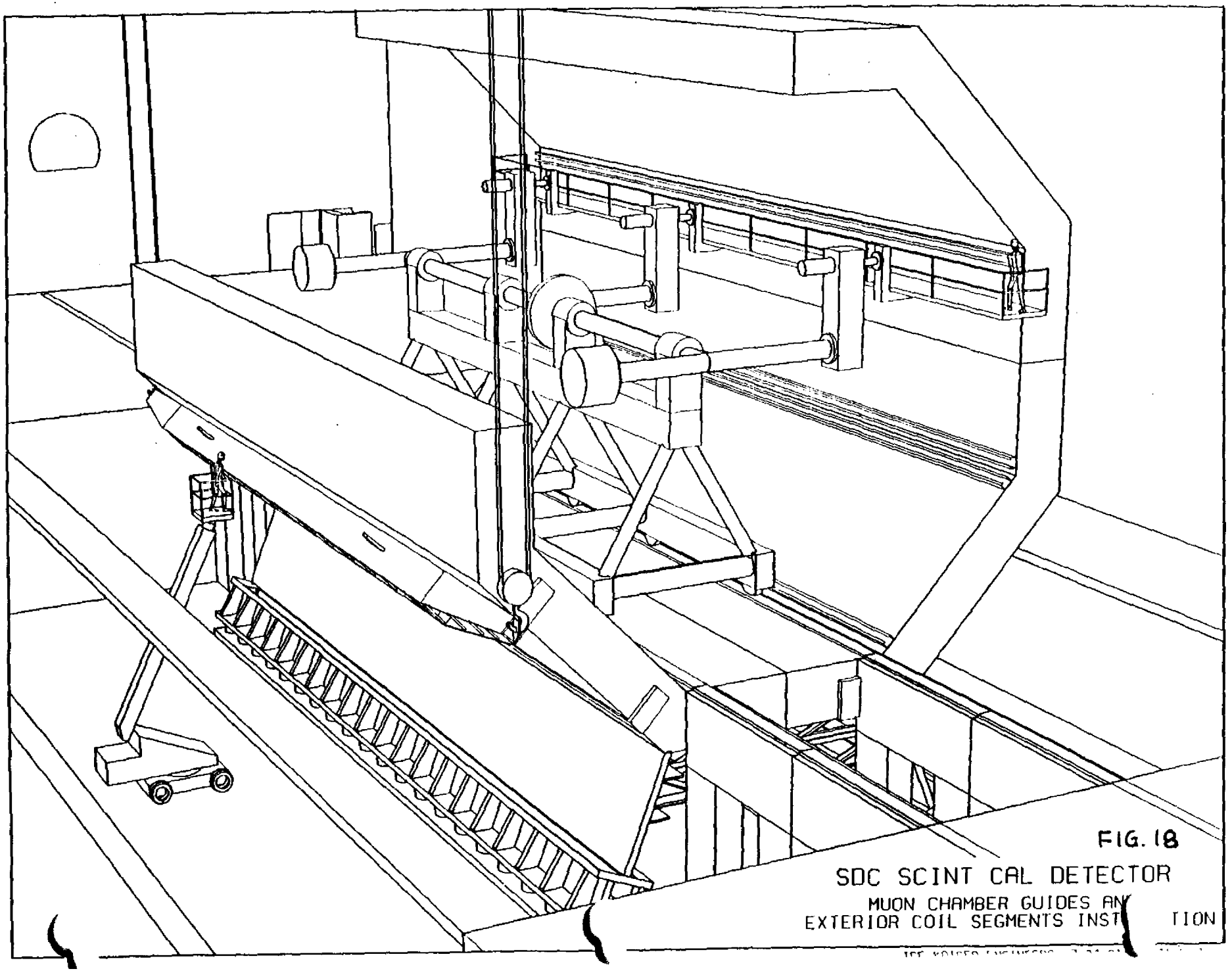

FIG. 18

SDC SCINT CAL DETECTOR

MUON CHAMBER GUIDES AN

EXTERIOR COIL SEGMENTS INST TION

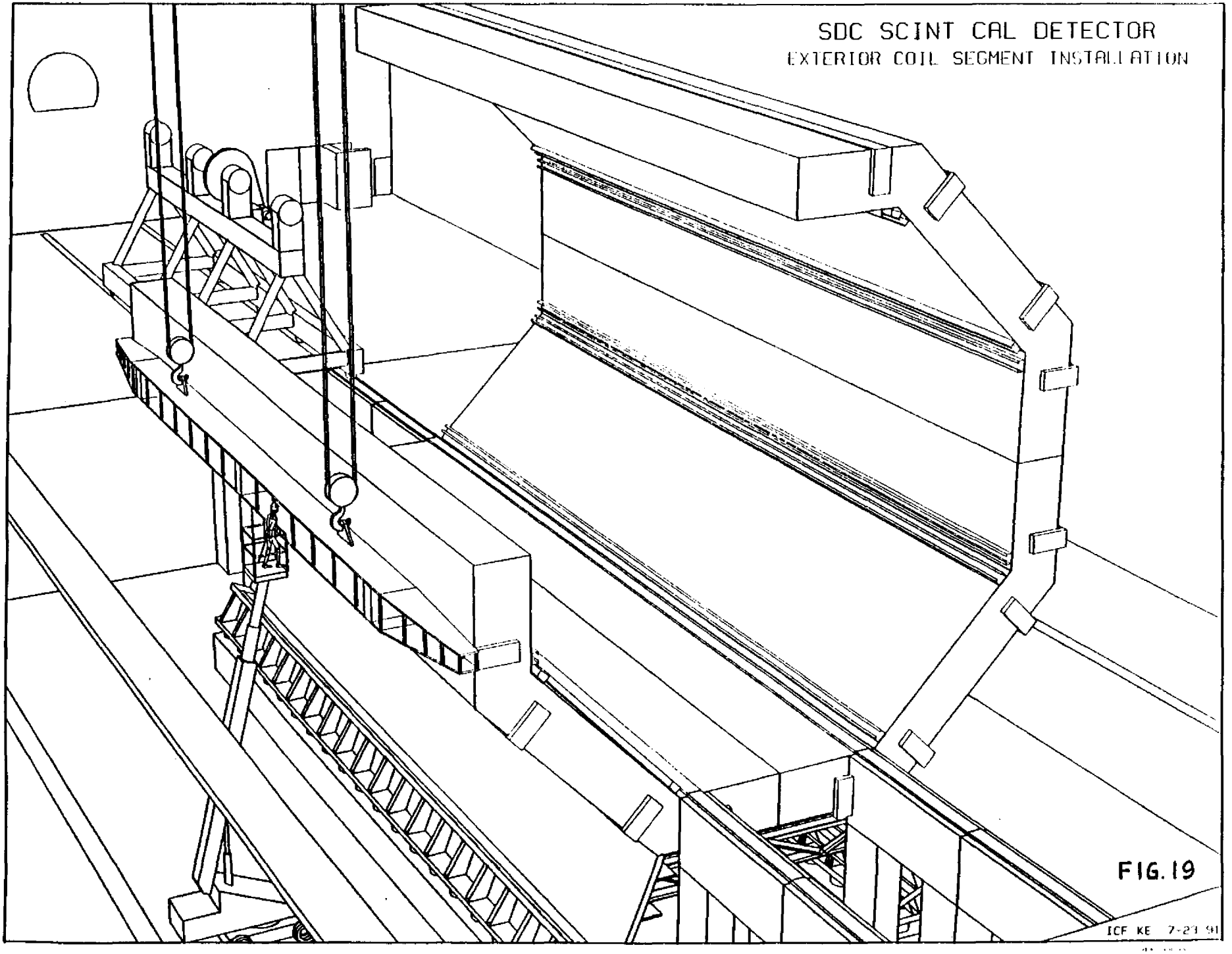
SDC SCINT CAL DETECTOR
EXTERIOR COIL SEGMENT INSTALLATION
ICF KE 7-23-91

FIG. 19

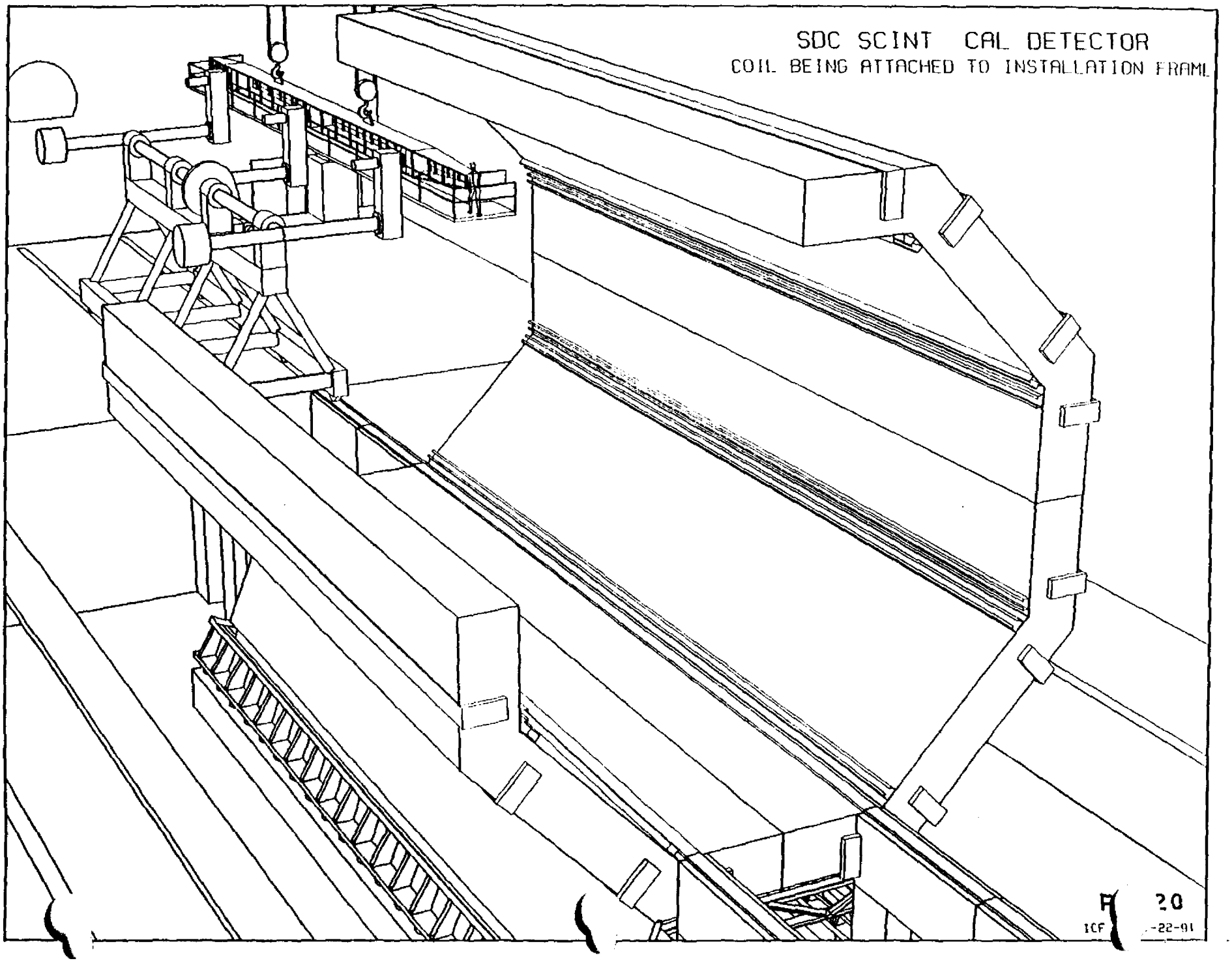
SDC SCINT CAL DETECTOR
COIL BEING ATTACHED TO INSTALLATION FRAME
20
ICF
-22-91

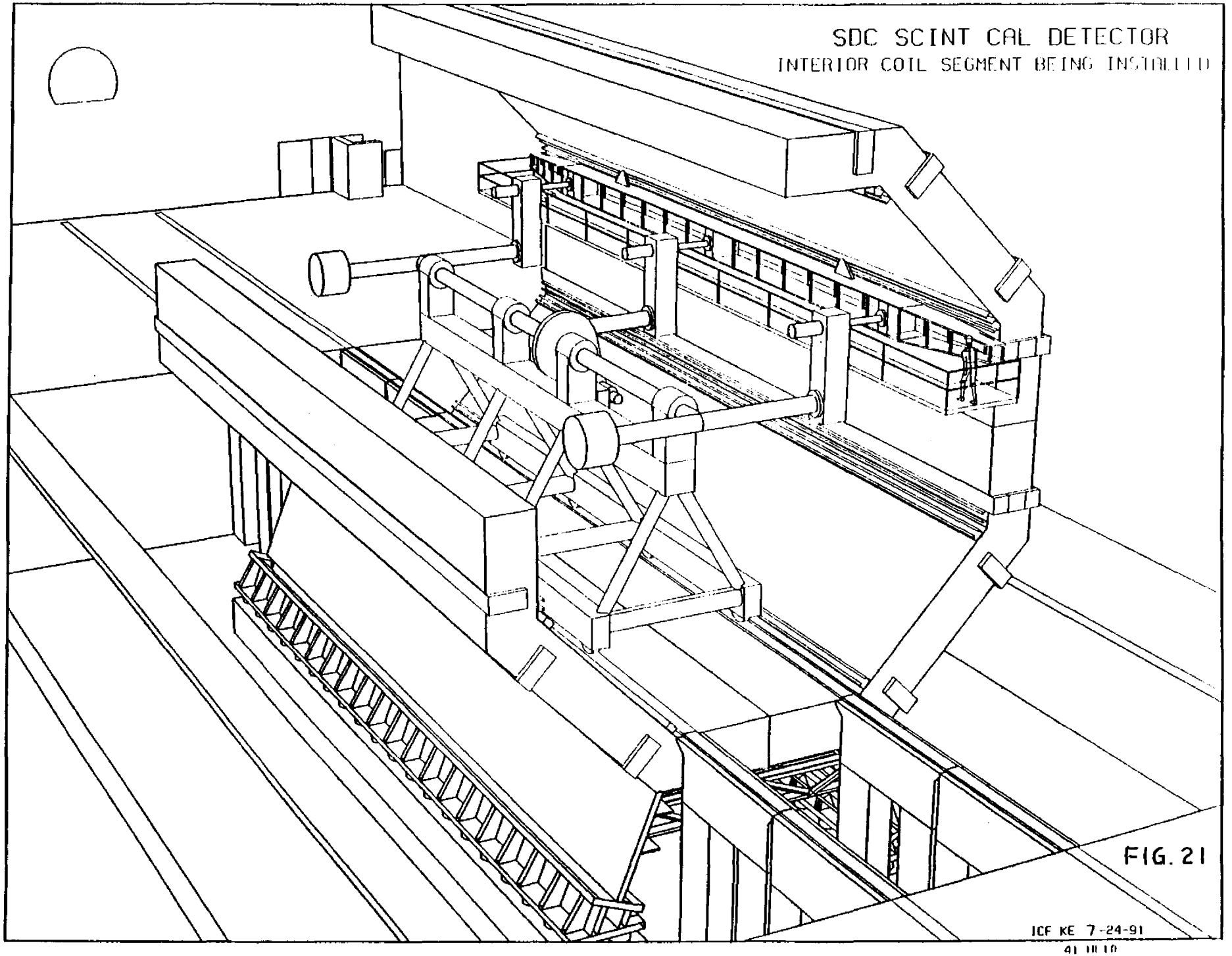
SDC SCINT CAL DETECTOR
INTERIOR COIL SEGMENT BEING INSTALLED
ICF KE 7-24-91

FIG. 21

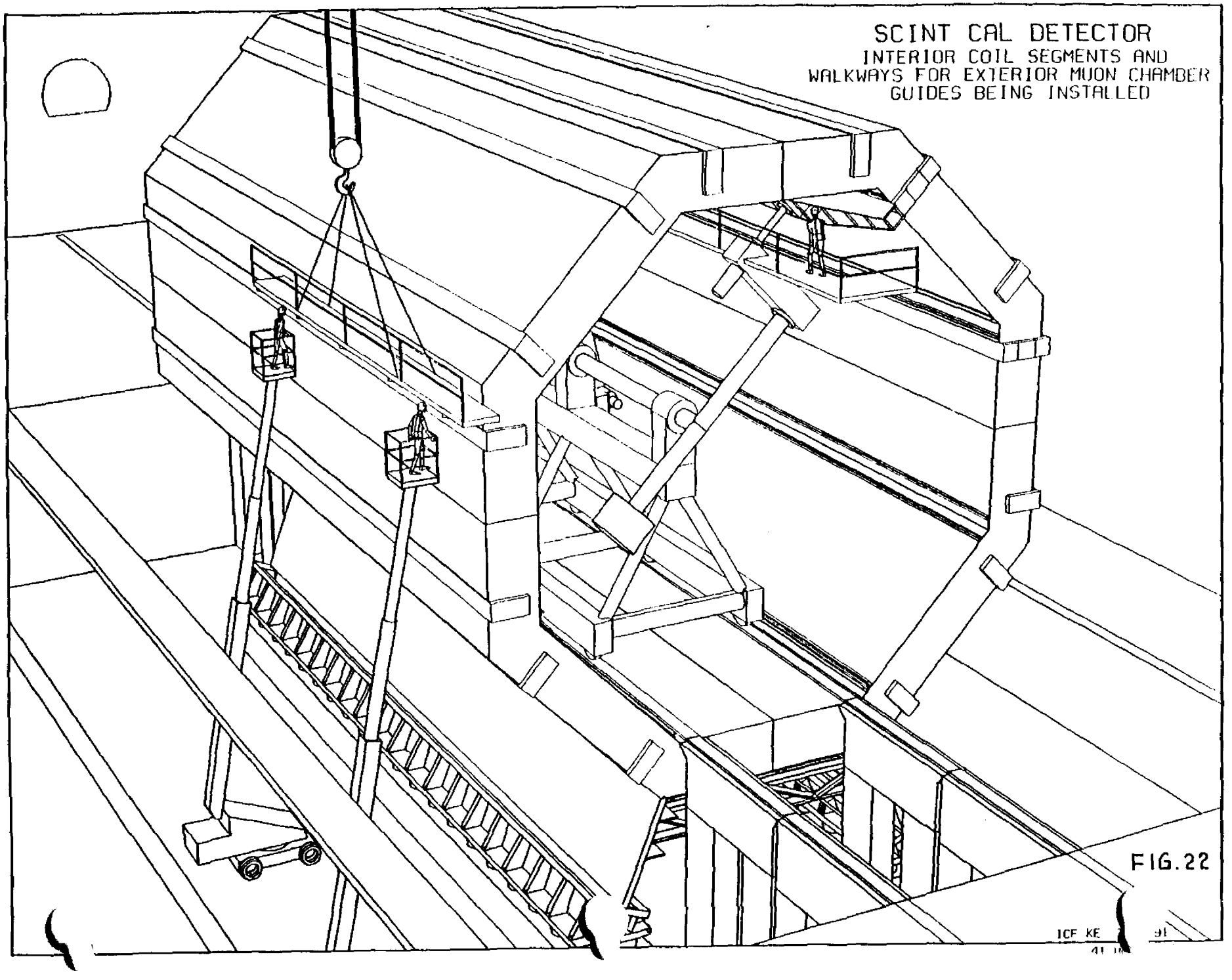
SCINT CAL DETECTOR
INTERIOR COIL SEGMENTS AND
WALKWAYS FOR EXTERIOR MUON CHAMBER
GUIDES BEING INSTALLED
FIG.22

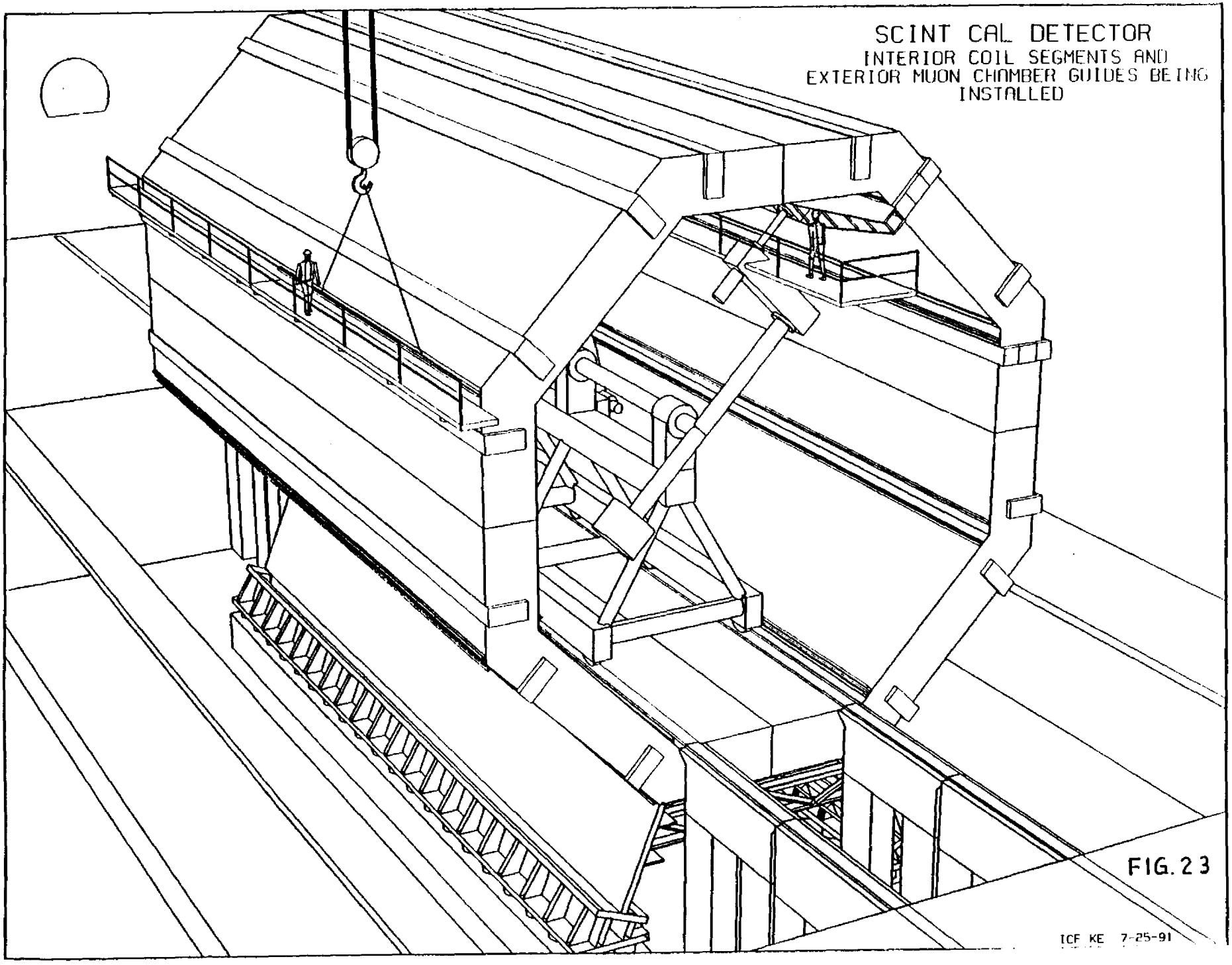
SCINT CAL DETECTOR
INTERIOR COIL SEGMENTS AND
EXTERIOR MUON CHAMBER GUIDES BEING
INSTALLED
ICF KE 7-25-91

FIG. 23

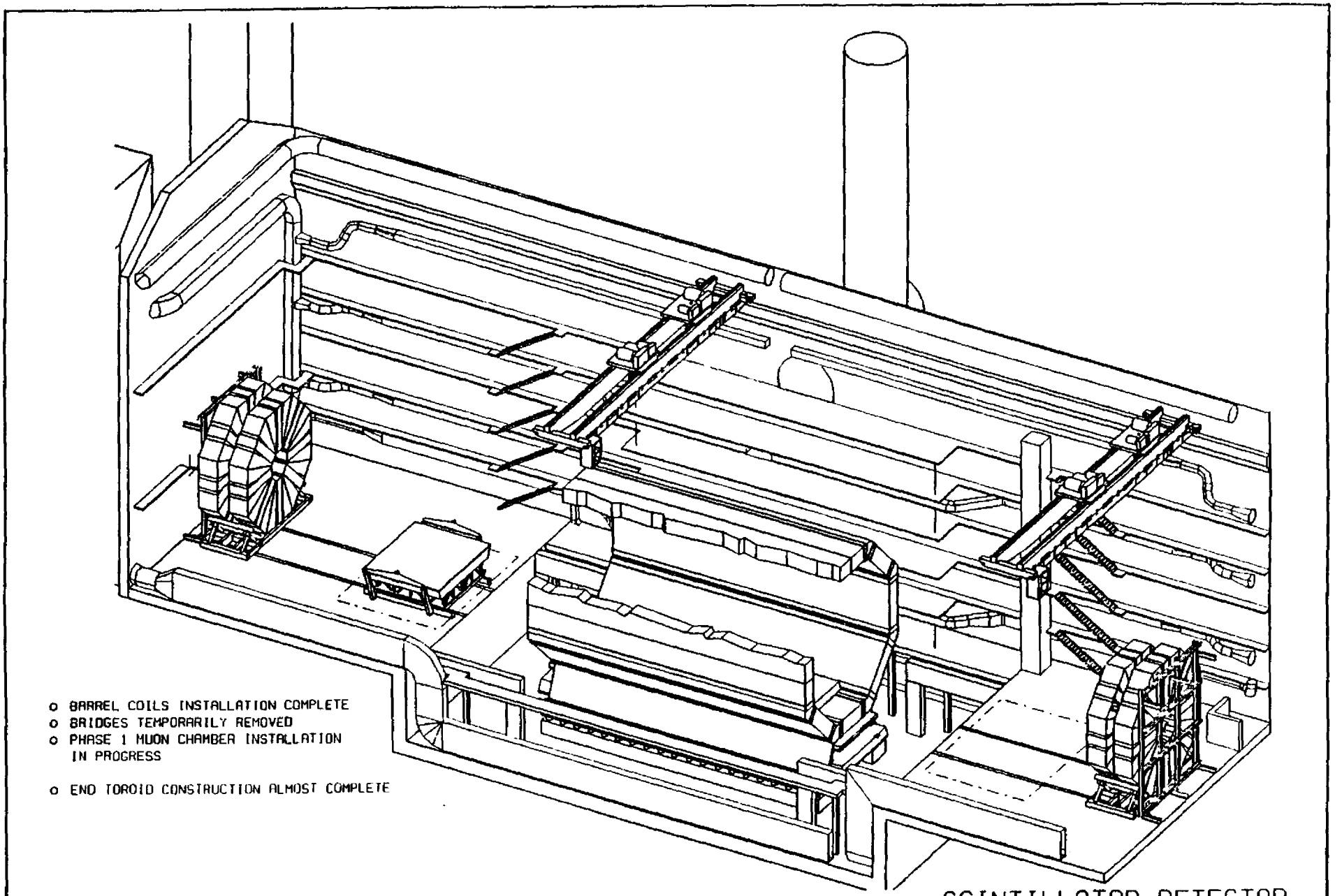

SCINTILLATOR DETECTOR

ASSEMBLY SEQUENCE

MONTH 15

FIG. 24

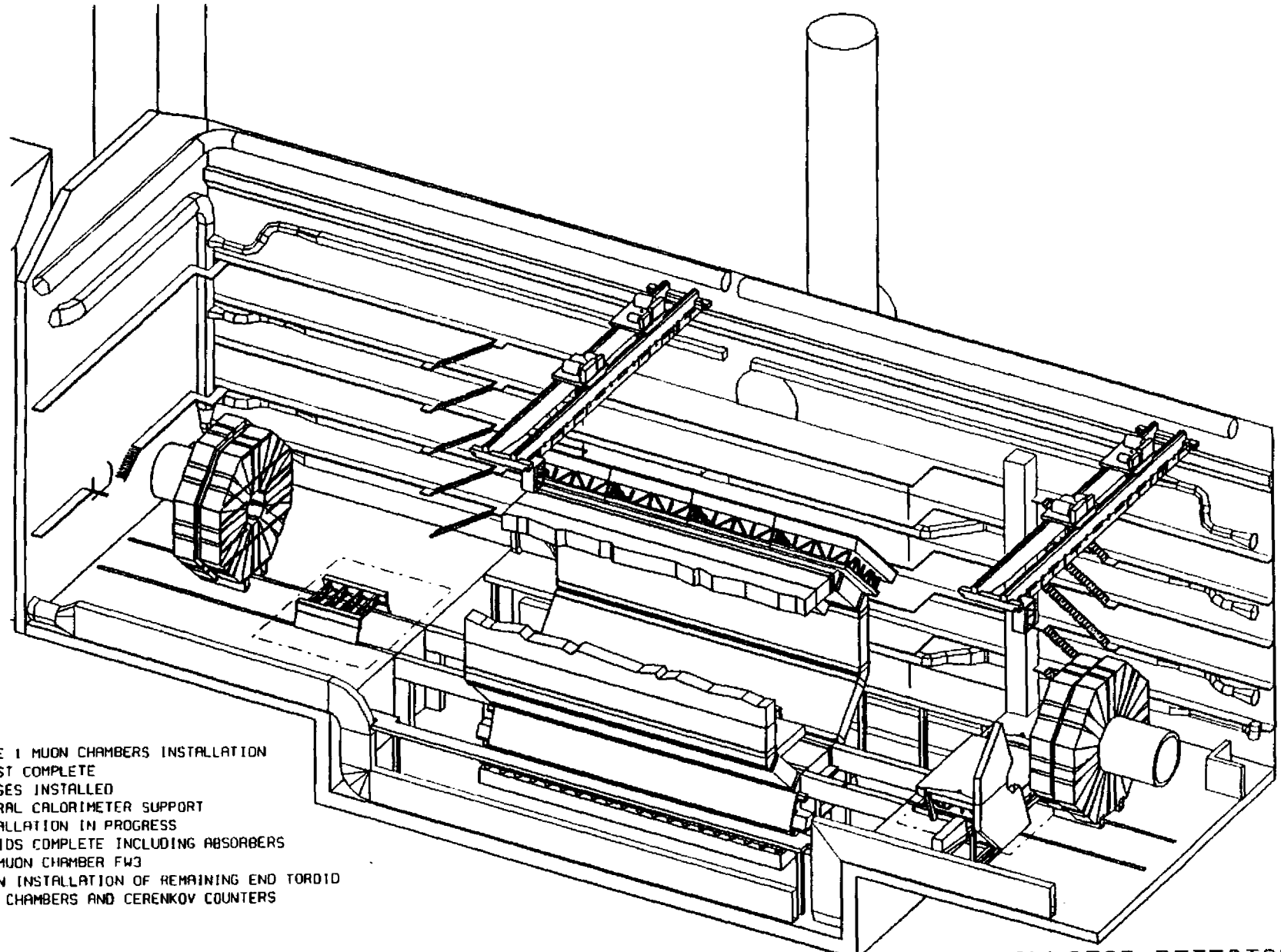

- o PHASE 1 MUON CHAMBERS INSTALLATION ALMOST COMPLETE
- o BRIDGES INSTALLED
- o CENTRAL CALORIMETER SUPPORT INSTALLATION IN PROGRESS
- o TOROIDS COMPLETE INCLUDING ABSORBERS AND MUON CHAMBER FW3
- o BEGIN INSTALLATION OF REMAINING END TOROID MUON CHAMBERS AND CERENKOV COUNTERS

SCINTILLATOR DETECTOR

ASSEMBLY SEQUENCE

MONTH 18 FIG. 25

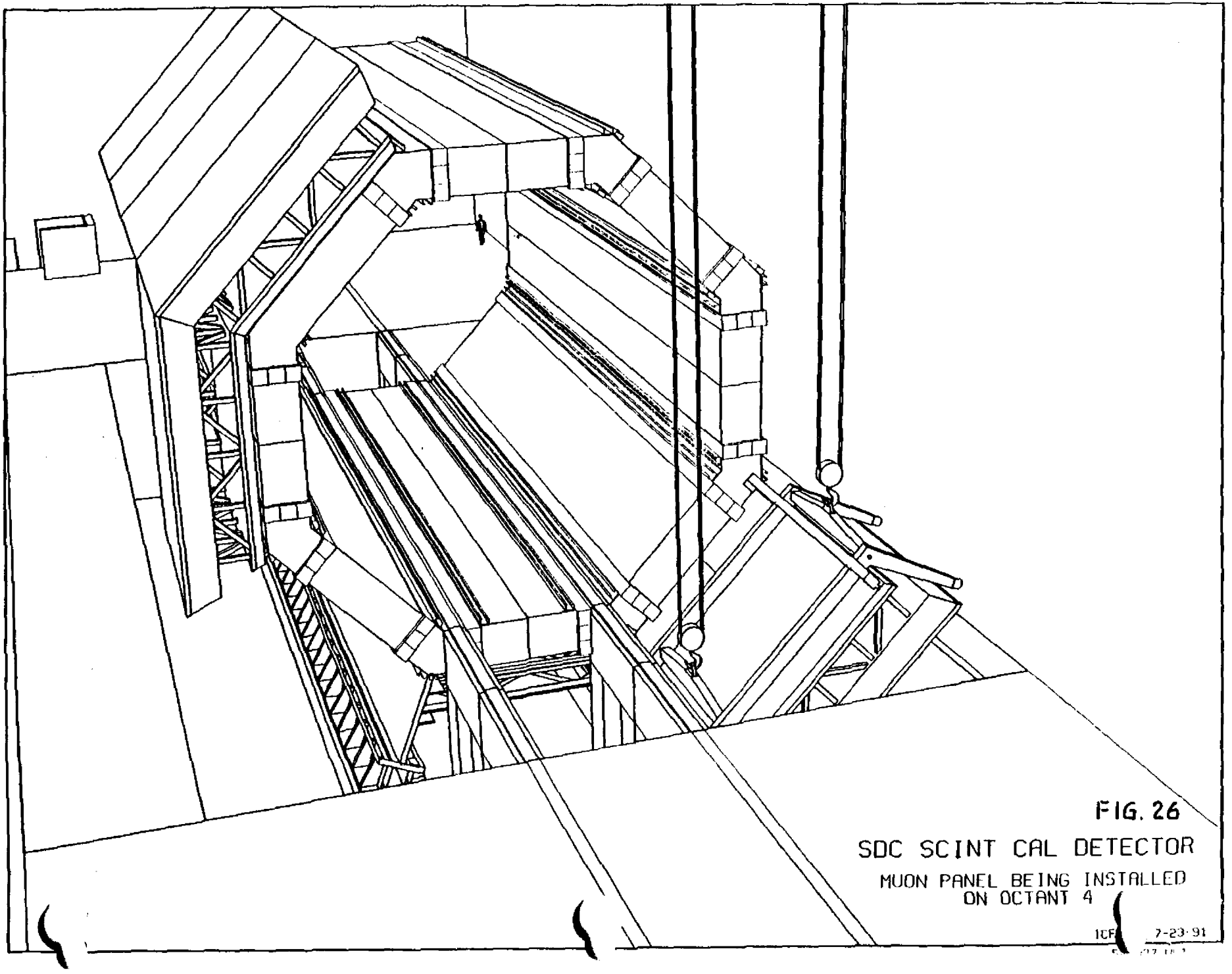

FIG. 26

SDC SCINT CAL DETECTOR

MUON PANEL BEING INSTALLED
ON OCTANT 4

ICF 7-23-91

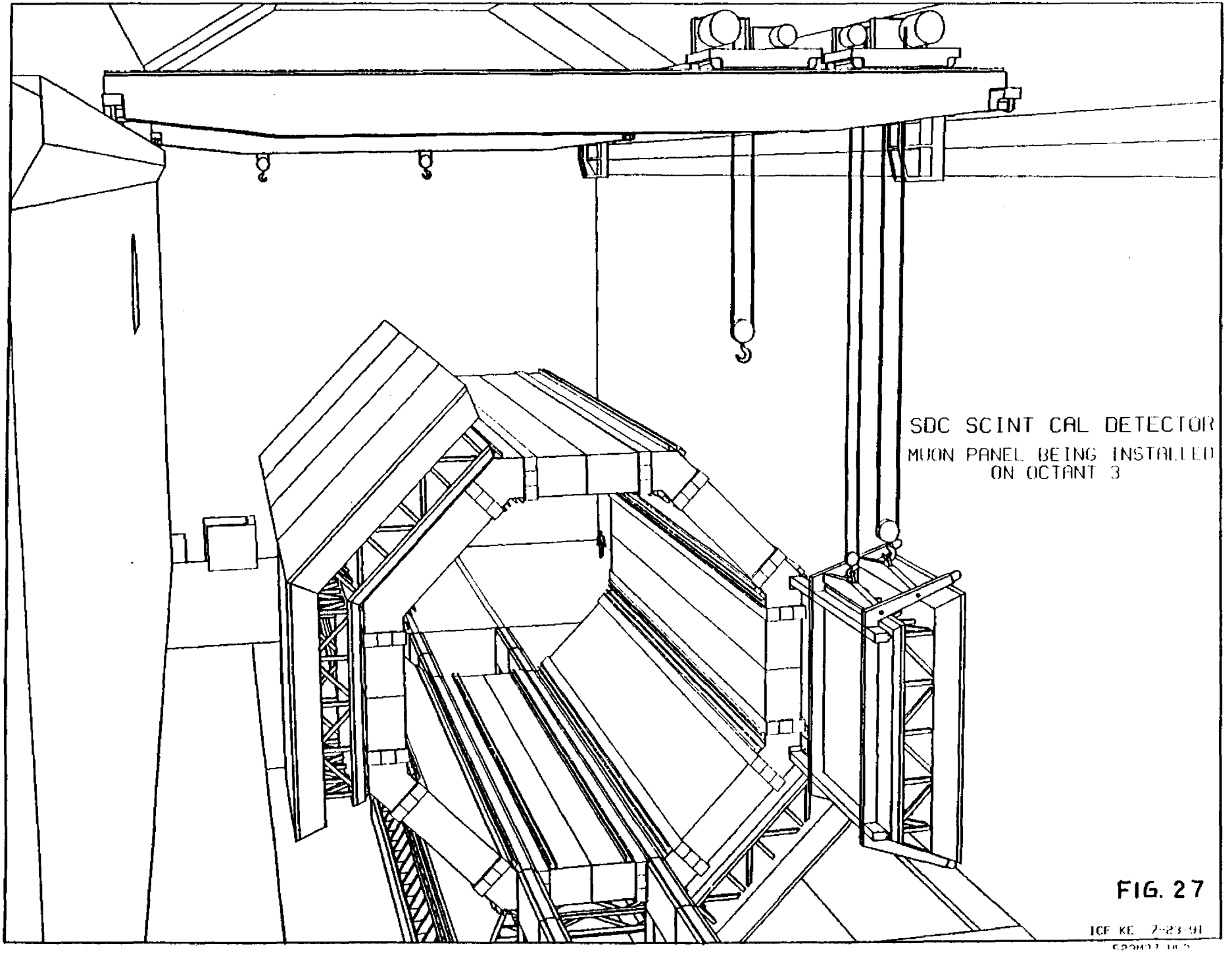

FIG. 27

ICF KE 7-23-91

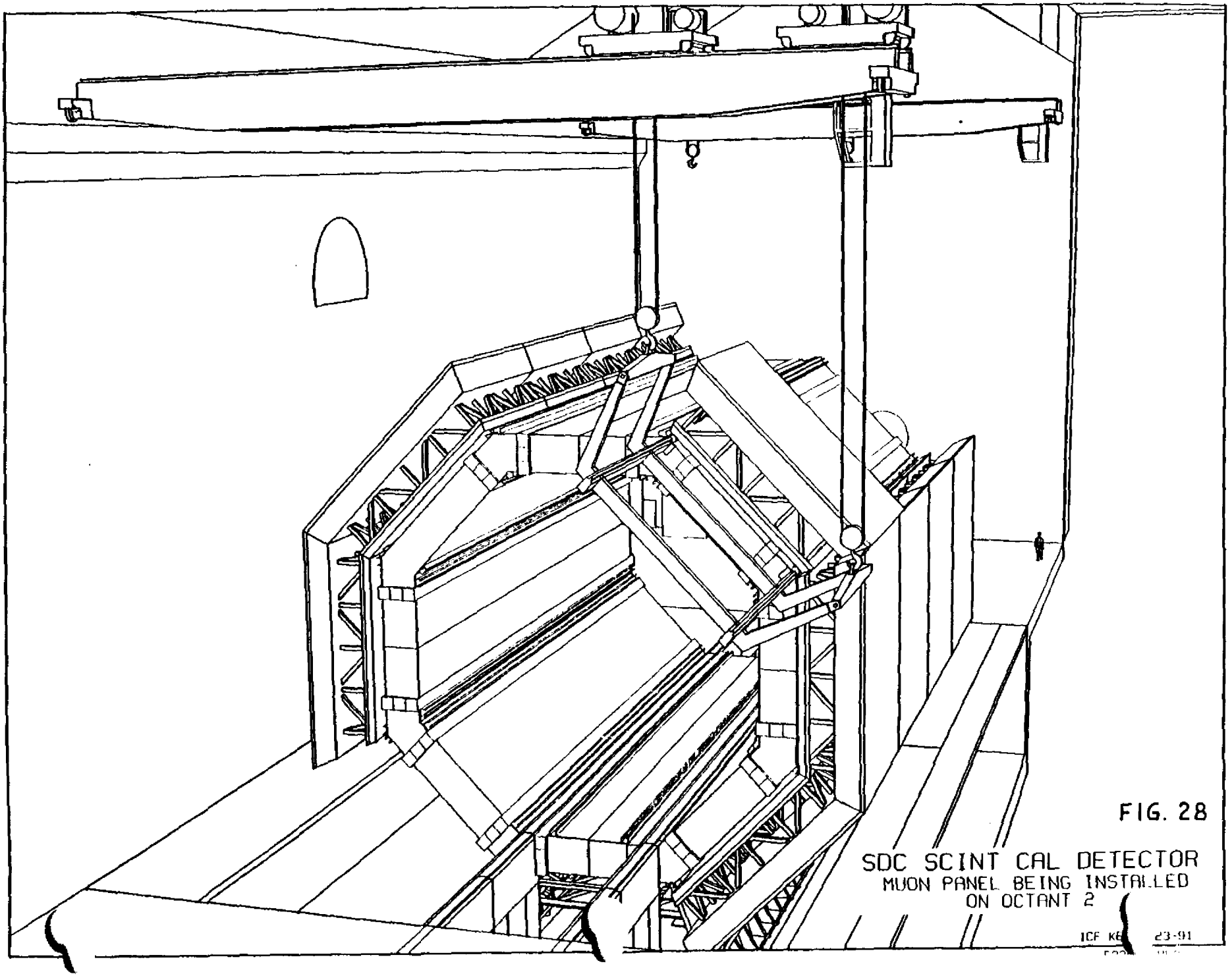

FIG. 28

SDC SCINT CAL DETECTOR
MUON PANEL BEING INSTALLED
ON OCTANT 2

ICF KE 23-91

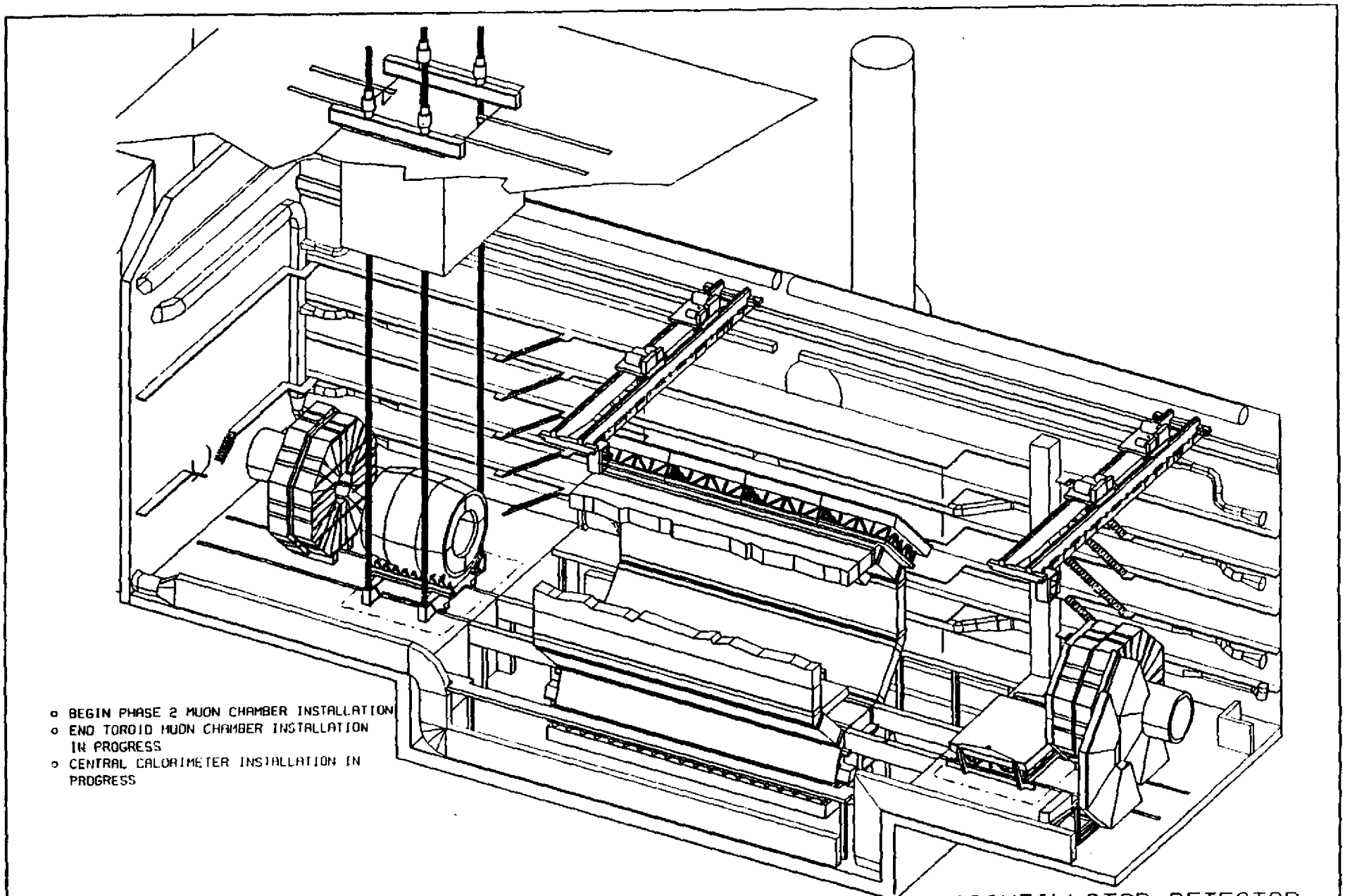

SCINTILLATOR DETECTOR
ASSEMBLY SEQUENCE
MONTH 19

FIG. 29

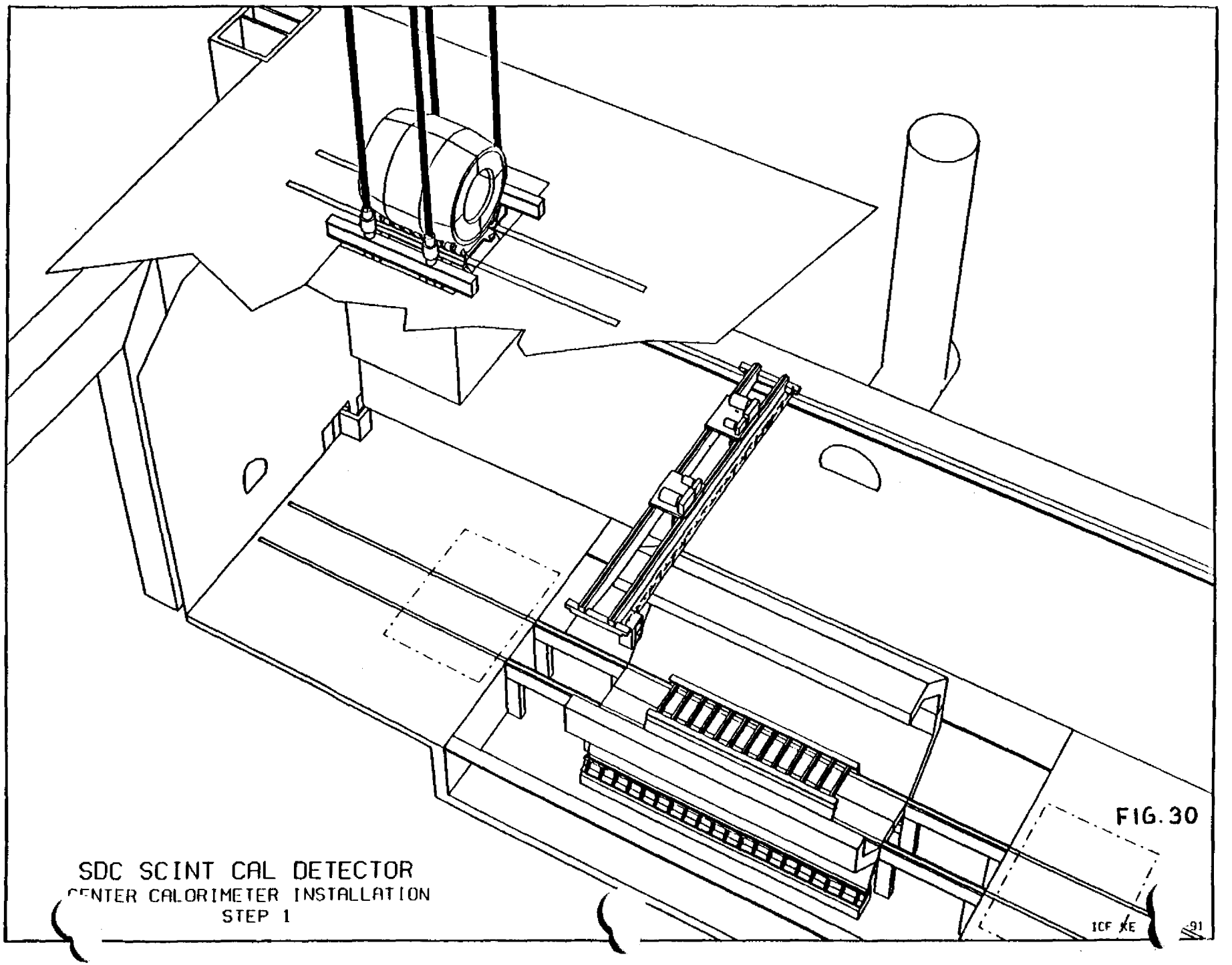

FIG. 30

SDC SCINT CAL DETECTOR
CENTER CALORIMETER INSTALLATION
STEP 1

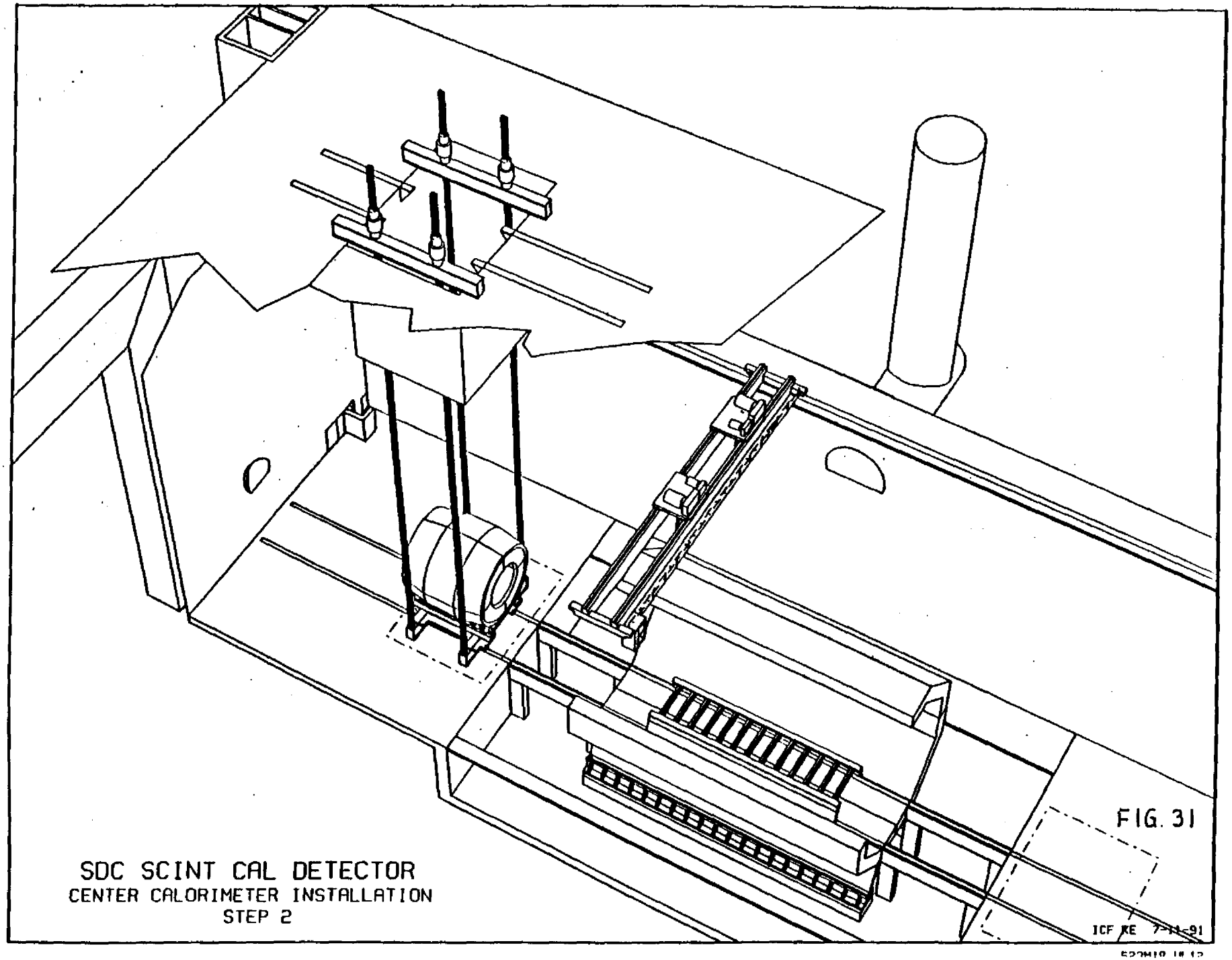

SDC SCINT CAL DETECTOR
CENTER CALORIMETER INSTALLATION
STEP 2

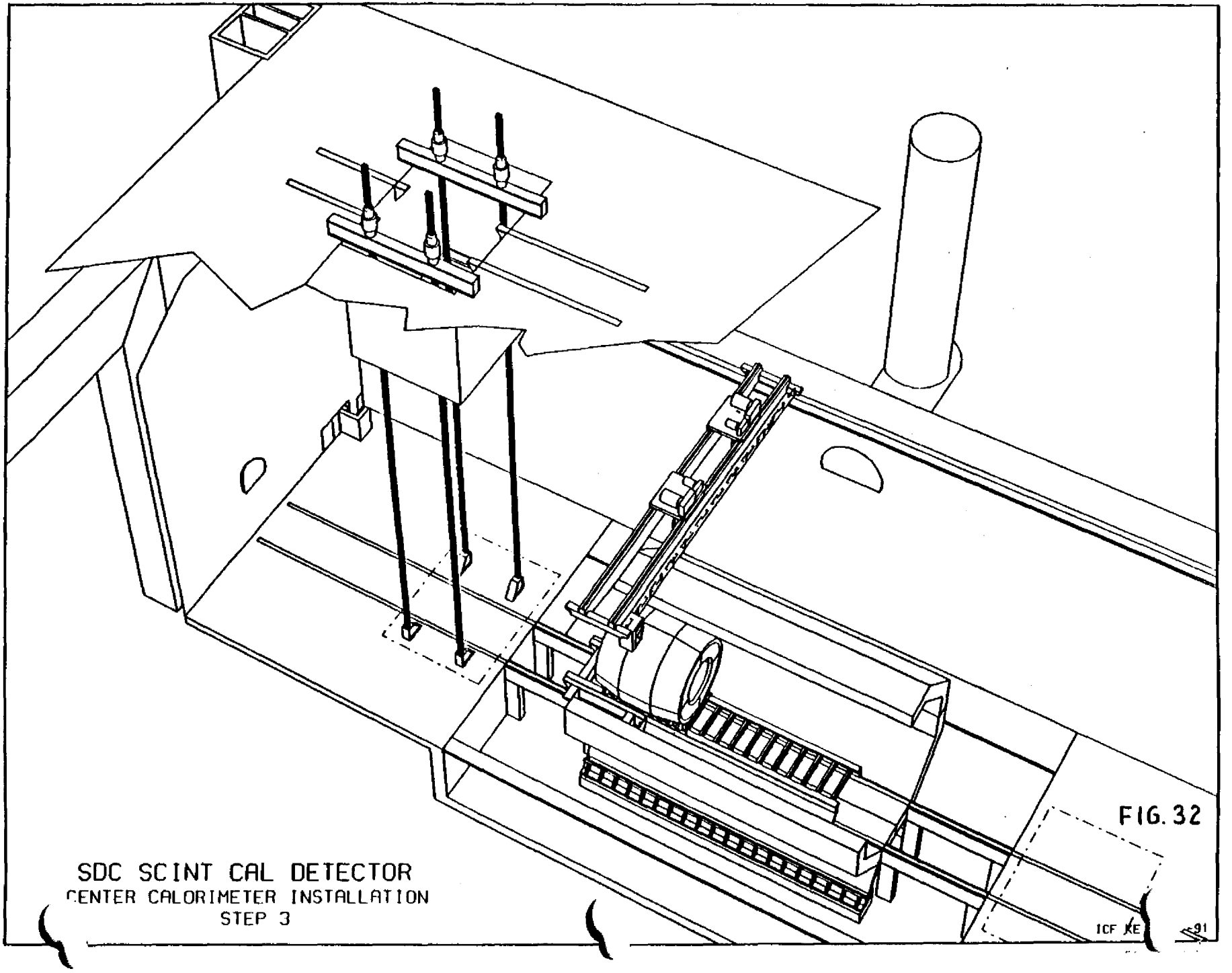

FIG. 32

SDC SCINT CAL DETECTOR
CENTER CALORIMETER INSTALLATION
STEP 3

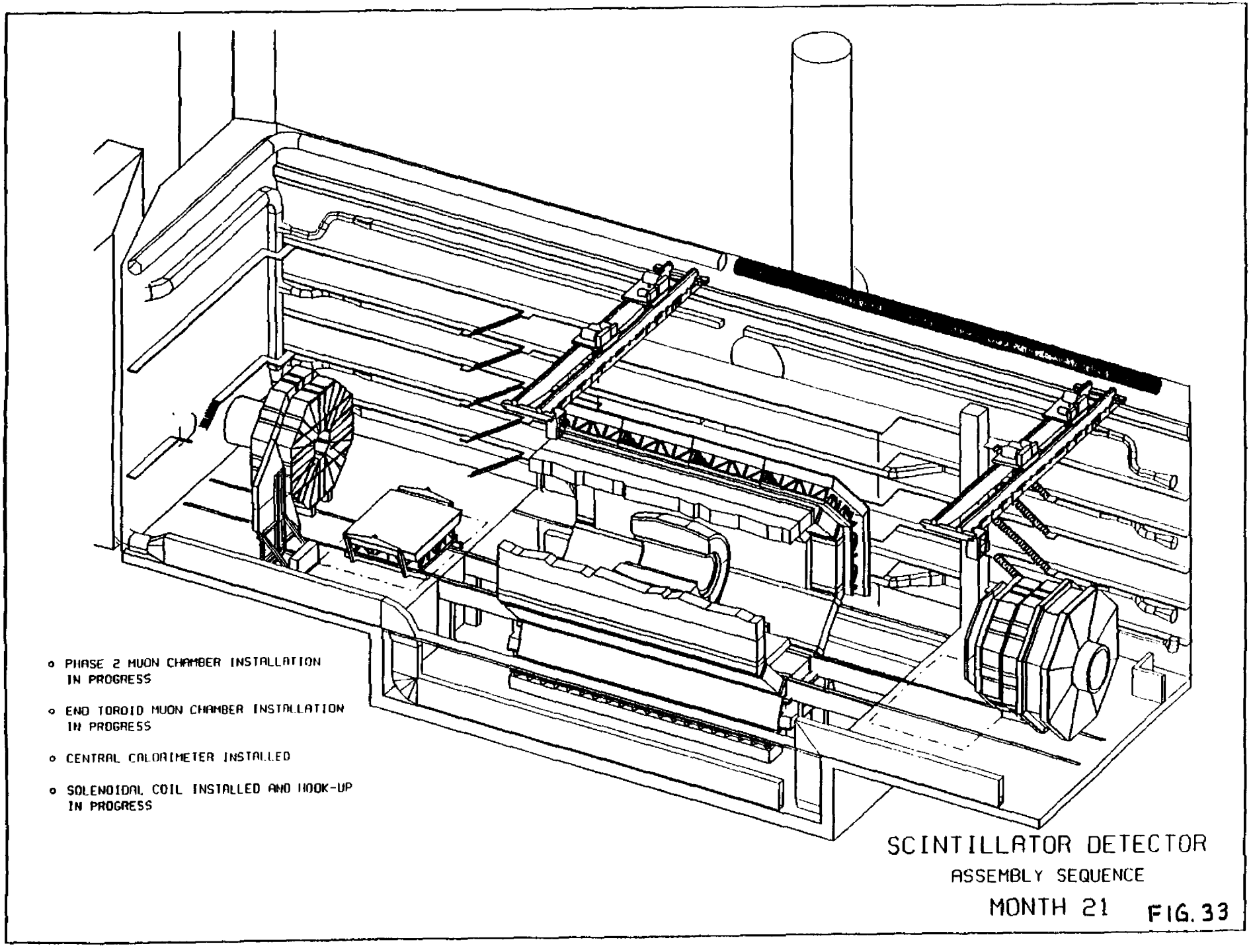
o PHASE 2 MUON CHAMBER INSTALLATION IN PROGRESS
o END TOROID MUON CHAMBER INSTALLATION IN PROGRESS
o CENTRAL CALORIMETER INSTALLED
o SOLENOIDAL COIL INSTALLED AND HOOK-UP IN PROGRESS
SCINTILLATOR DETECTOR
ASSEMBLY SEQUENCE
MONTH 21

FIG. 33

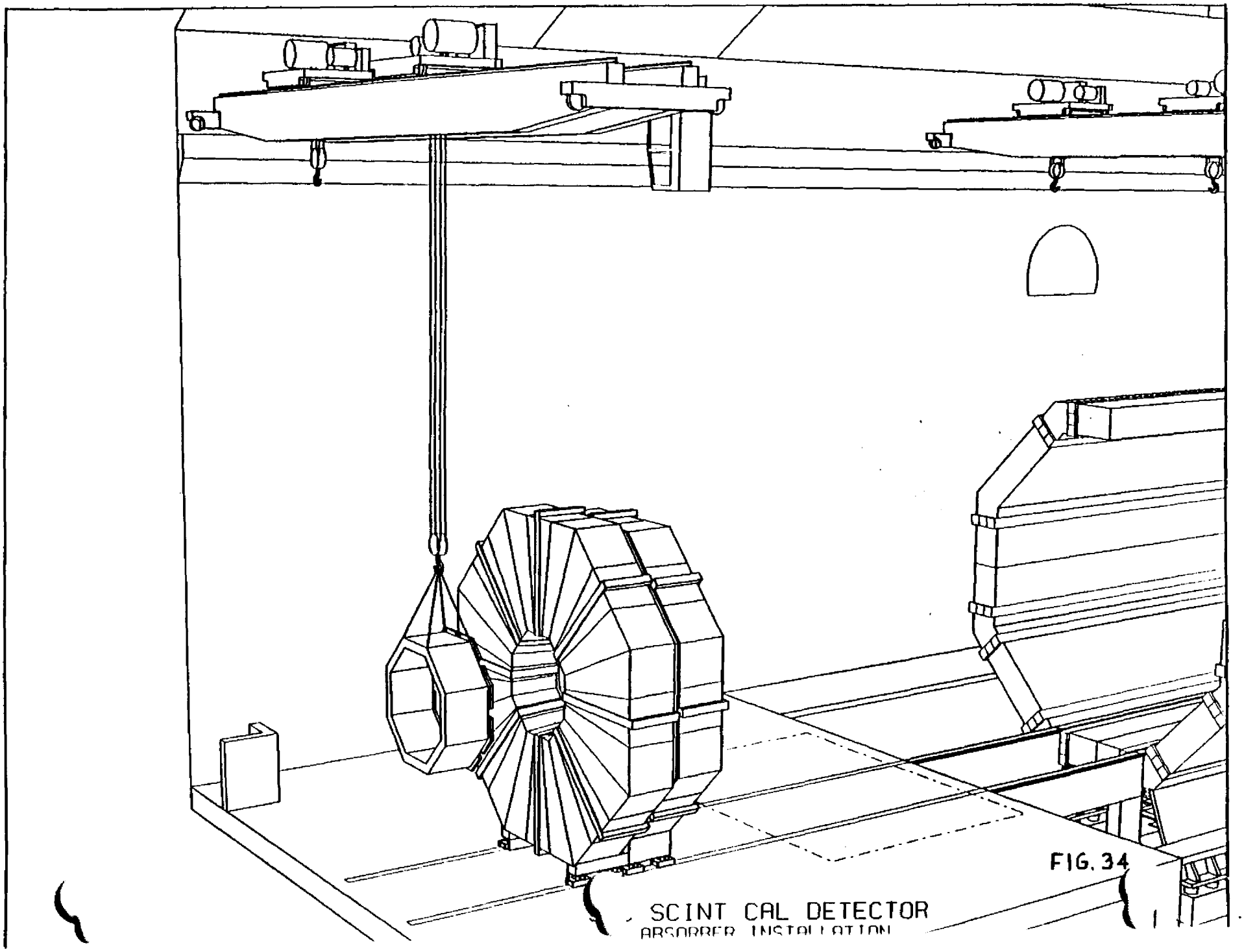

FIG. 34

SCINT CAL DETECTOR
ABSORBER INSTALLATION

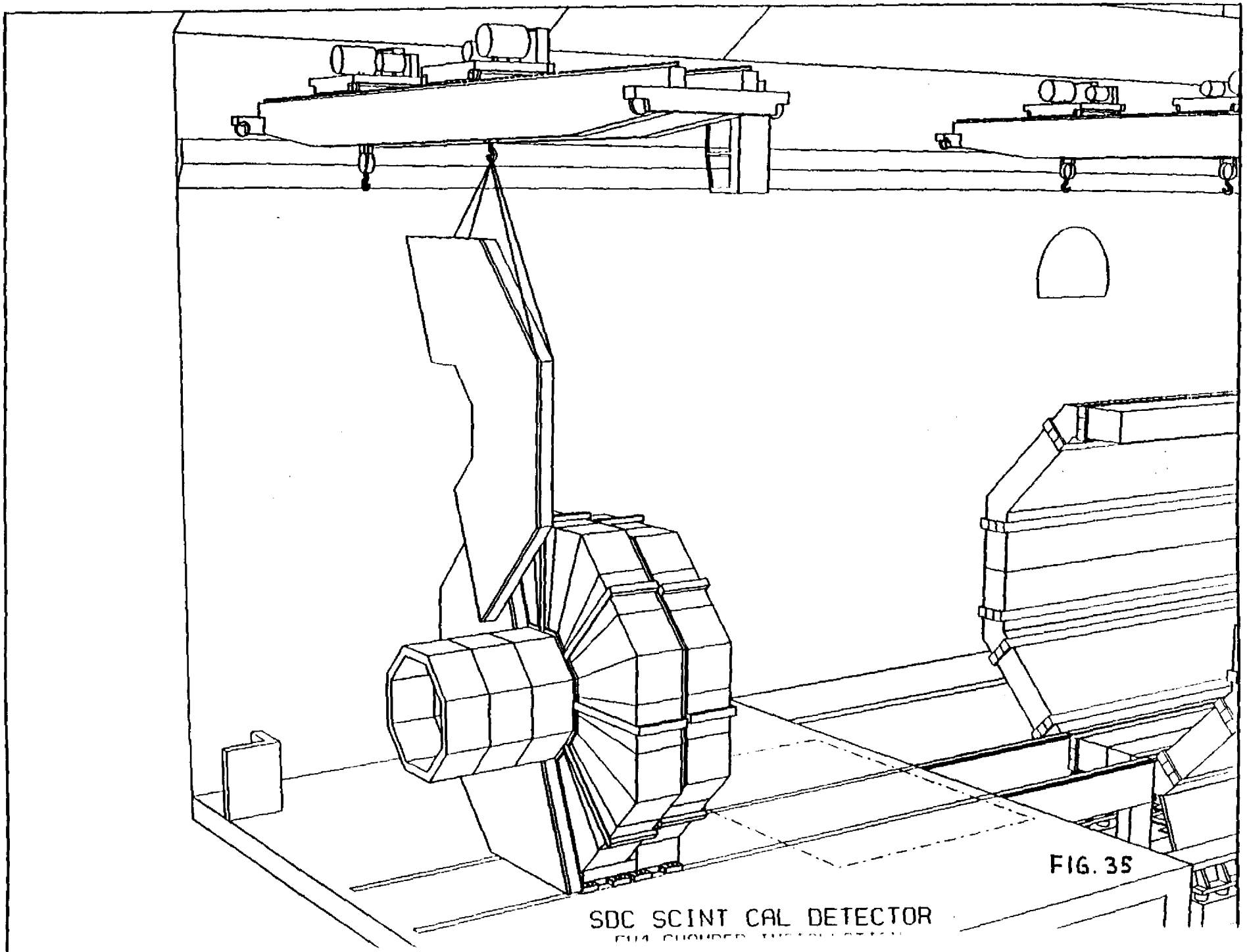

FIG. 35

SDC SCINT CAL DETECTOR

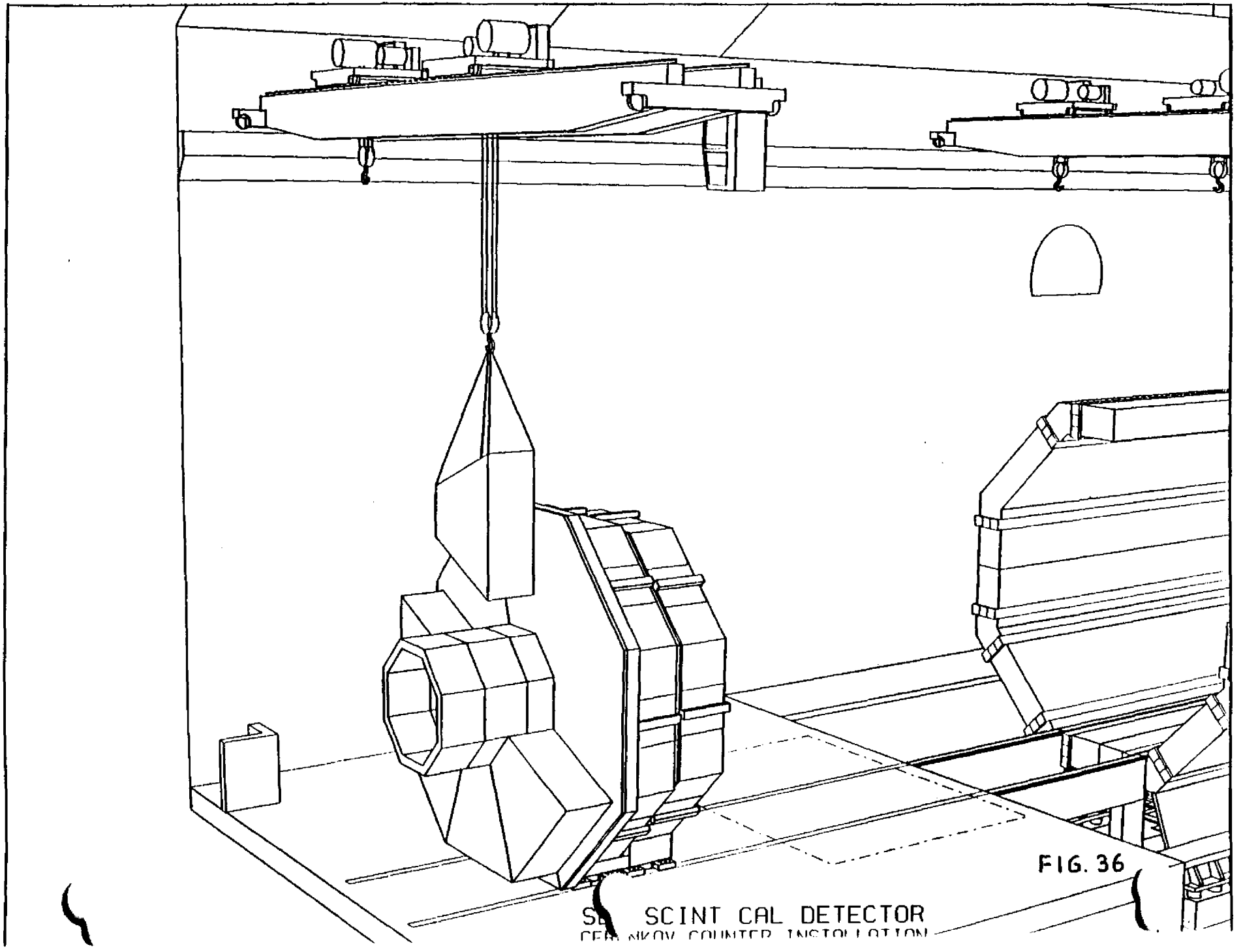

FIG. 36

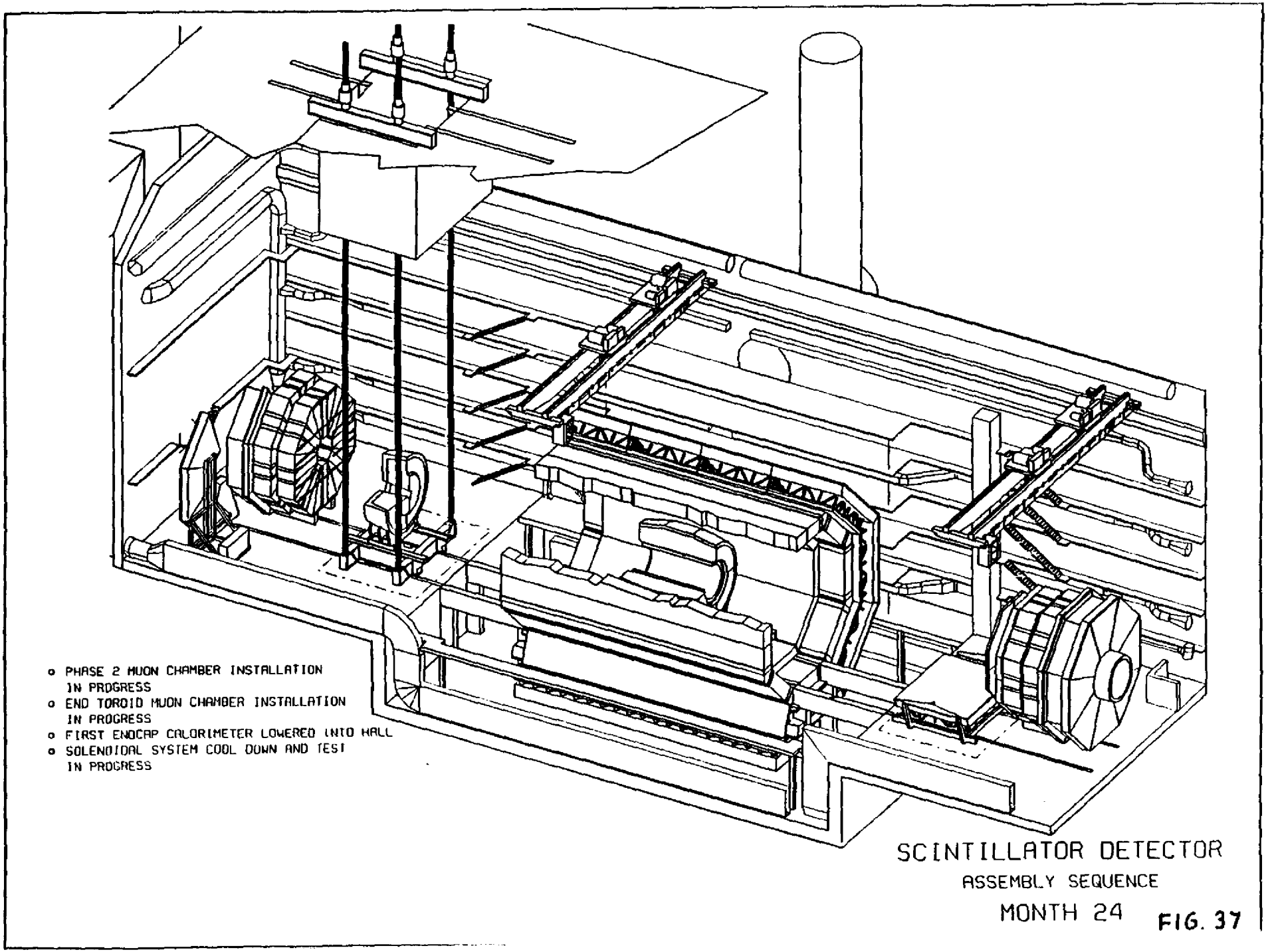
o PHASE 2 MUON CHAMBER INSTALLATION IN PROGRESS
o END TOROID MUON CHAMBER INSTALLATION IN PROGRESS
o FIRST ENDCAP CALORIMETER LOWERED INTO HALL
o SOLENOIDAL SYSTEM COOL DOWN AND TEST IN PROGRESS
SCINTILLATOR DETECTOR
ASSEMBLY SEQUENCE
MONTH 24

FIG. 37

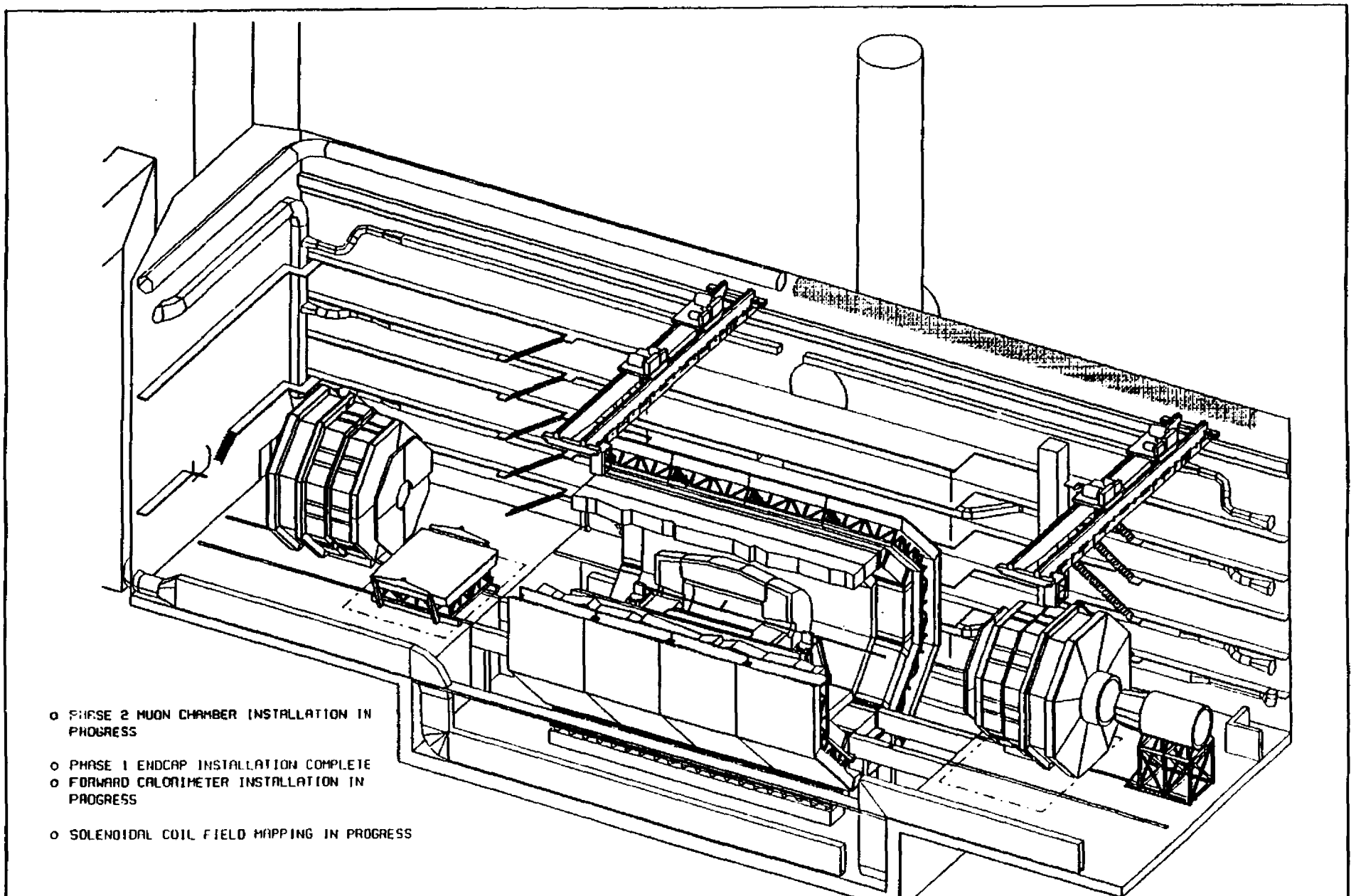

- PHASE 2 MUON CHAMBER INSTALLATION IN PROGRESS
- PHASE 1 ENDCAP INSTALLATION COMPLETE
- FORWARD CALORIMETER INSTALLATION IN PROGRESS
- SOLENOIDAL COIL FIELD MAPPING IN PROGRESS

SCINTILLATOR DETECTOR

ASSEMBLY SEQUENCE

MONTH 27

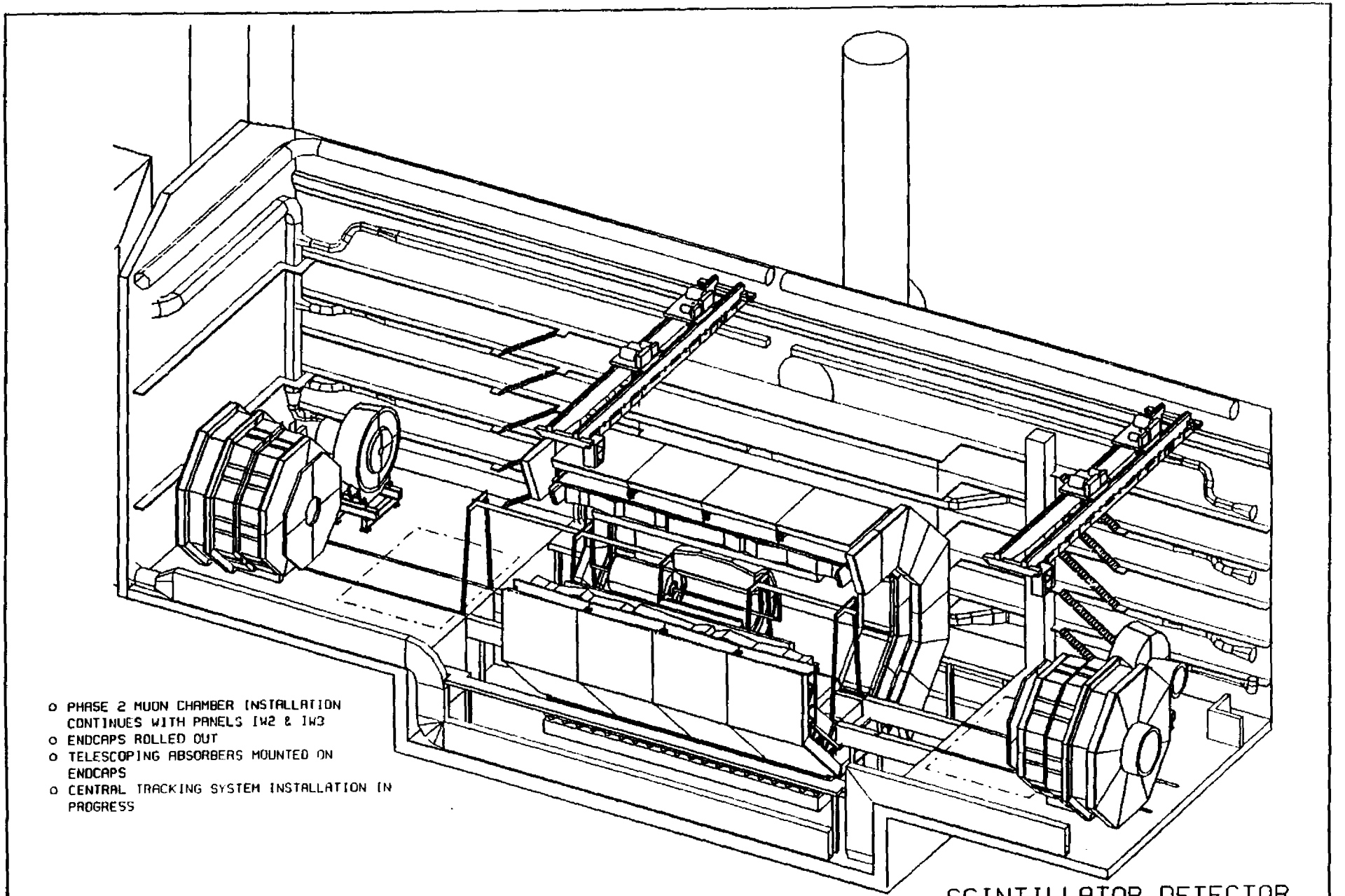

SCINTILLATOR DETECTOR

ASSEMBLY SEQUENCE

MONTH 30

FIG. 39

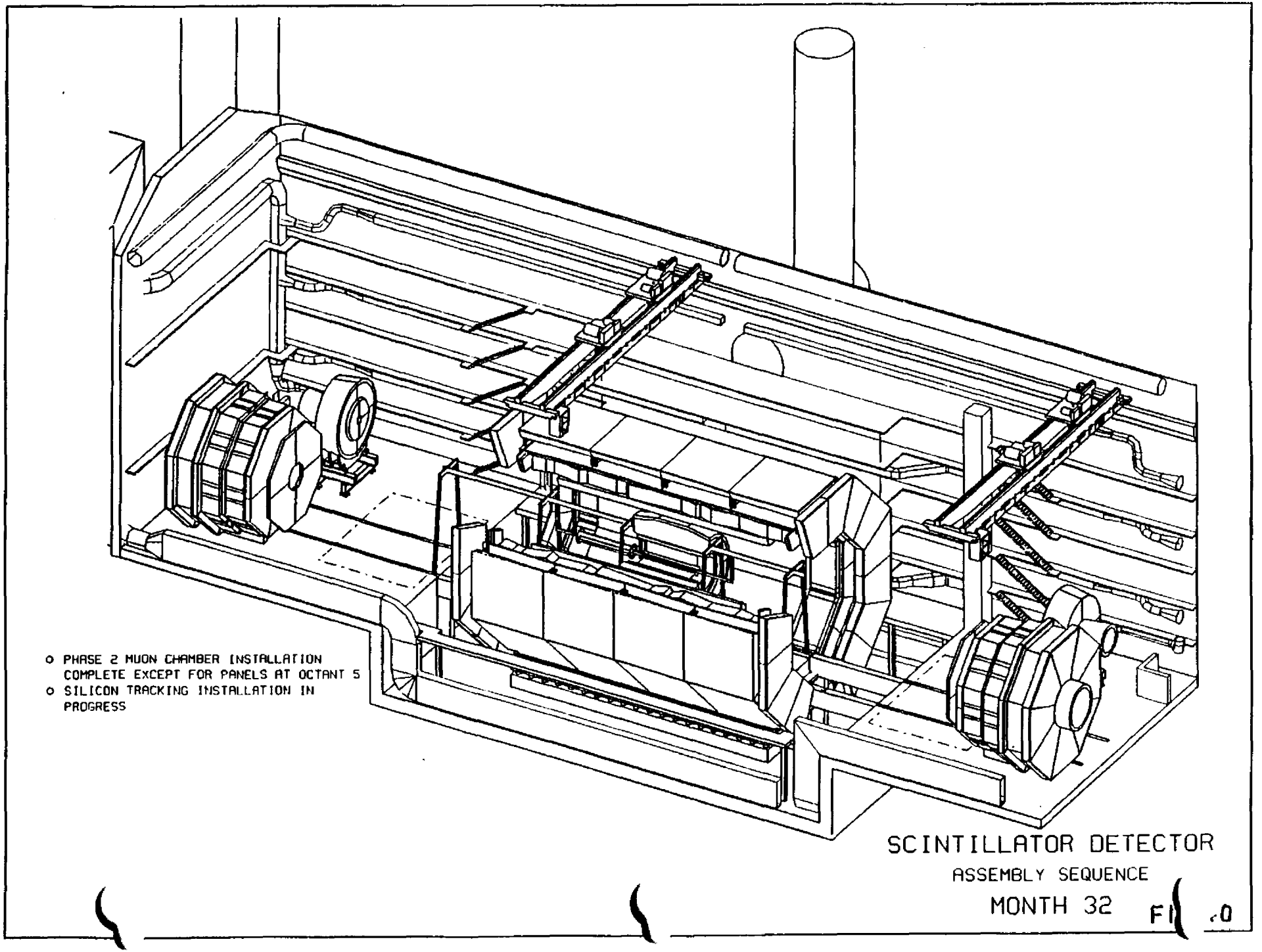
o PHASE 2 MUON CHAMBER INSTALLATION COMPLETE EXCEPT FOR PANELS AT OCTANT 5
o SILICON TRACKING INSTALLATION IN PROGRESS
SCINTILLATOR DETECTOR
ASSEMBLY SEQUENCE
MONTH 32

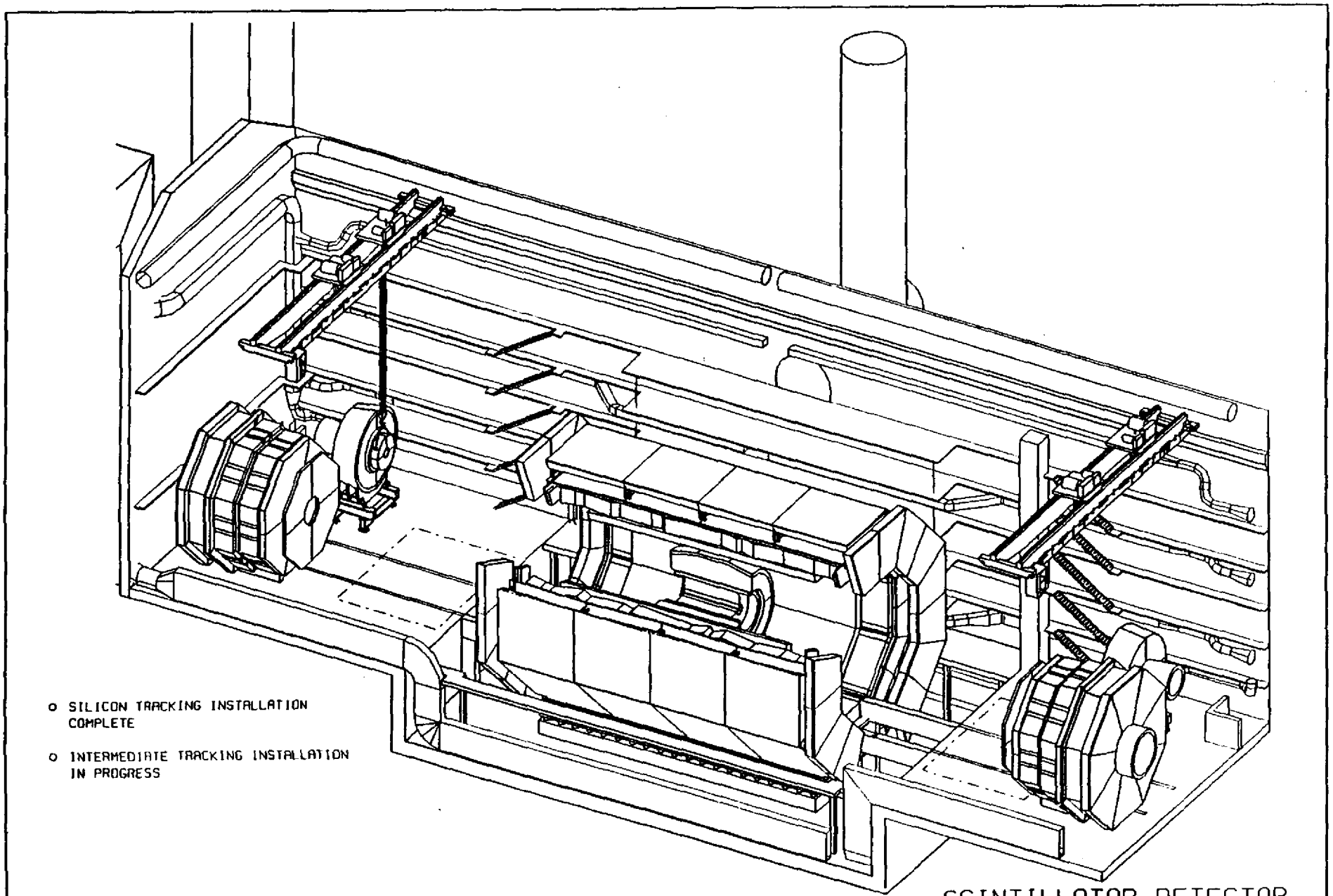

SCINTILLATOR DETECTOR

ASSEMBLY SEQUENCE

MONTH 35

FIG. 41

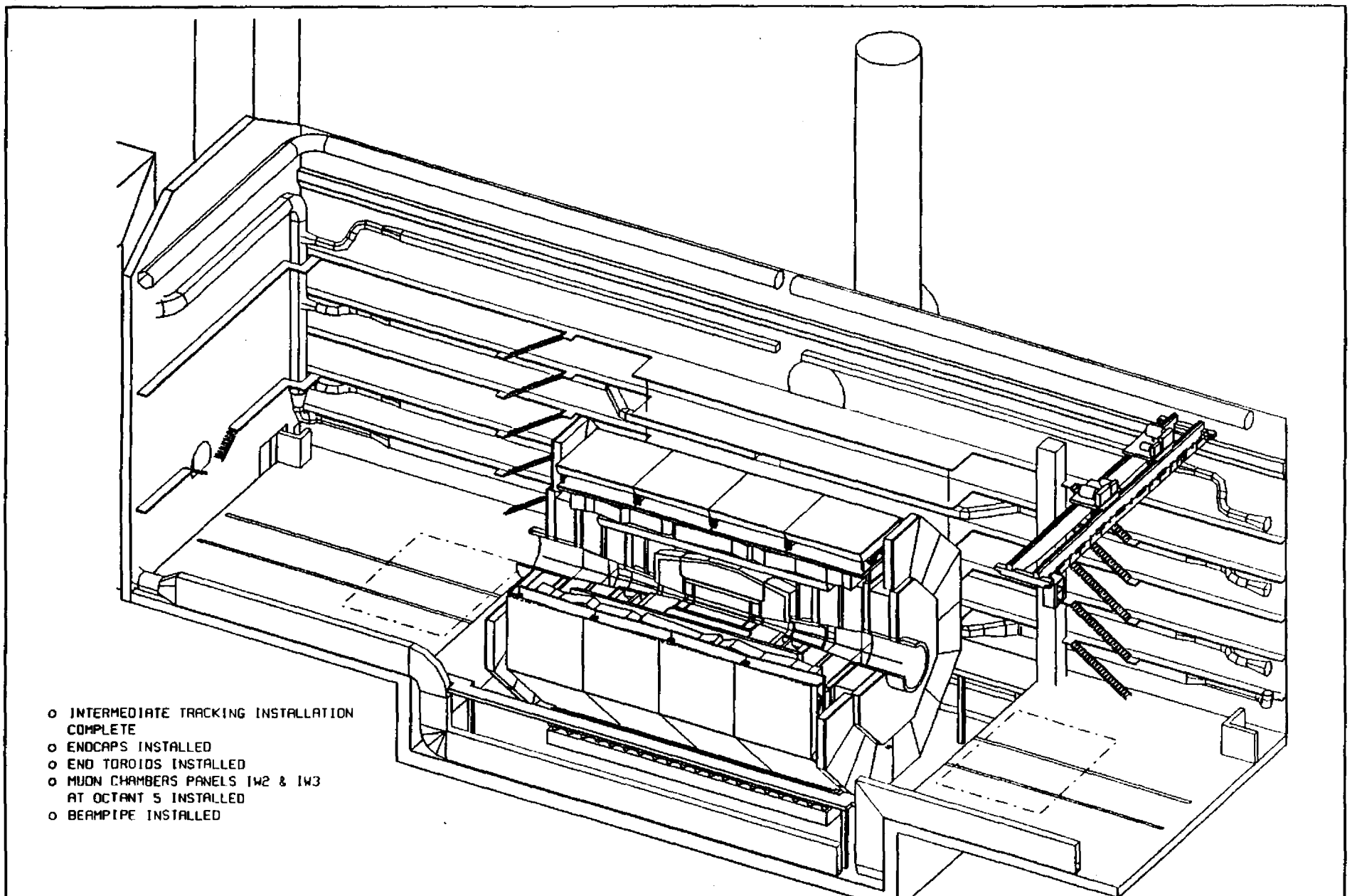

- o INTERMEDIATE TRACKING INSTALLATION COMPLETE
- o ENDCAPS INSTALLED
- o END TOROIDS INSTALLED
- o MUON CHAMBERS PANELS IW2 & IW3 AT OCTANT 5 INSTALLED
- o BEAMPIPE INSTALLED

SCINTILLATOR DETECTOR

ASSEMBLY SEQUENCE

MONTH 38

10. LAWRENCE BERKELEY LABORATORY (LBL)

Mechanical Integration

In response to the recently demonstrated need to descope the detector, a new detector cross section drawing (23D0145) was prepared and is shown in Figure 10-1. This Descope Option 1 includes a scintillation calorimeter with 0.2 m less steel shell thickness. The inner barrel muon chamber and all toroids have been reduced in thickness by 0.5 m. The 2D version of this drawing has been made available to all collaborators via E-mail. Drawing 23D0165, Figure 10-2, was prepared to show the integration of the Scintillator calorimeter and tracker electronics in this descoped detector. These drawings are in a continuous state of flux as additional input is received from the subsystem groups and particularly as the space requirements for their electronics evolves.

Drawing 23D0175, Figure 10-3, was prepared to show a descoped version of the Liquid Argon Calorimeter, Option 2. Drawing 23D0205, Figure 10-4, shows electronic crates integrated into this option. These drawings are evolving as various possible arrangements are investigated.

Technical note LBL SDC 0033 was extended to evaluate case D, the steel intercept versus theta through a vertex of the toroids, in the Descope option 1 version of the detector. A satisfactory pattern for the fall off of the intercept at the transition between the barrel and the forward toroids is maintained.

Layout drawing 23D0185, Figure 10-5, was prepared showing a conical warm liquid forward calorimeter installed in the forward muon assembly. Technical note LBL SDC 0040 was drafted to outline an installation scenario for this option. The proposed arrangement provides for withdrawing the endcap and forward calorimeters by 1m without moving the forward toroids. It also provides for the possibility of retracting the entire forward assembly by 3 to 4 meters without removing the quadrupole magnets. This layout includes a scheme for supporting the Cerenkov counter and forward muon chambers from the forward toroids.

SDC installation and service requirements which will affect the Accelerator were discussed at two Accelerator Interface workshops. The above drawing was employed to illustrate a possible geometry of the beam line in the region of the forward assembly. At the end of August, the accelerator group will provide some specific guidance and constraints for the SDC design.

A note describing an SDC global coordinate system and a code to identify major portions of the detector (LBL SDC 0035) was drafted and will be offered for comment at the next collaboration meeting.

LBL Mechanical Integration (MI) representatives participated in a LAC safety workshop on, July 8, to review a preliminary cryogenic hazards analysis. The result of the analysis will appear in a LAC report to the August SDC collaboration meeting.

LBL MI representatives participated in three workshops at which the SDC Experimental Facilities Requirements Report was being developed. Recommendations for modifications were made to the SSC to insure that mechanical services and utilities meet SDC need.

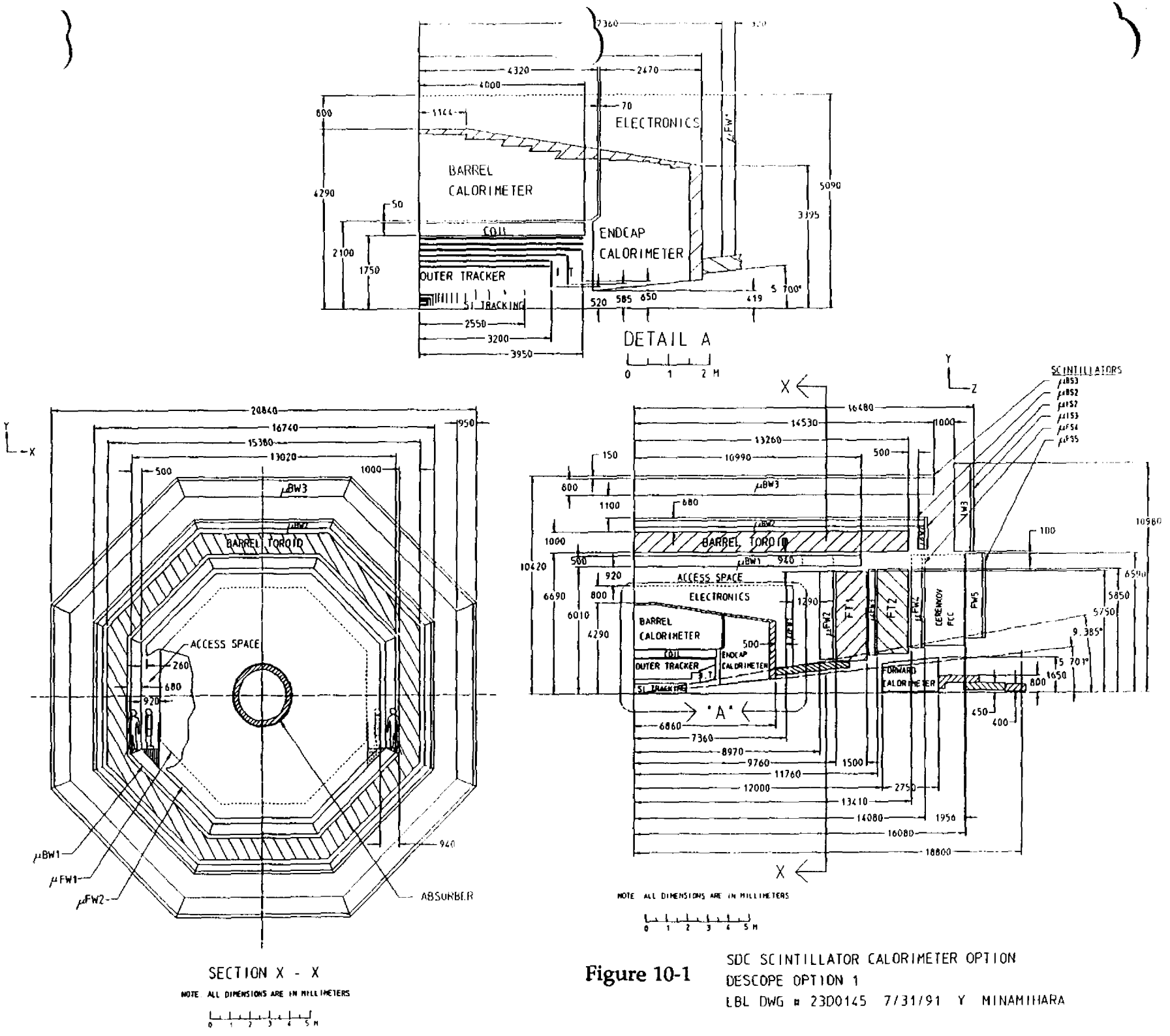

Figure 10-1

SDC SCINTILLATOR CALORIMETER OPTION
DESCOPE OPTION 1
LBL DWG # 23D0145 7/31/91 Y MINAMIHARA

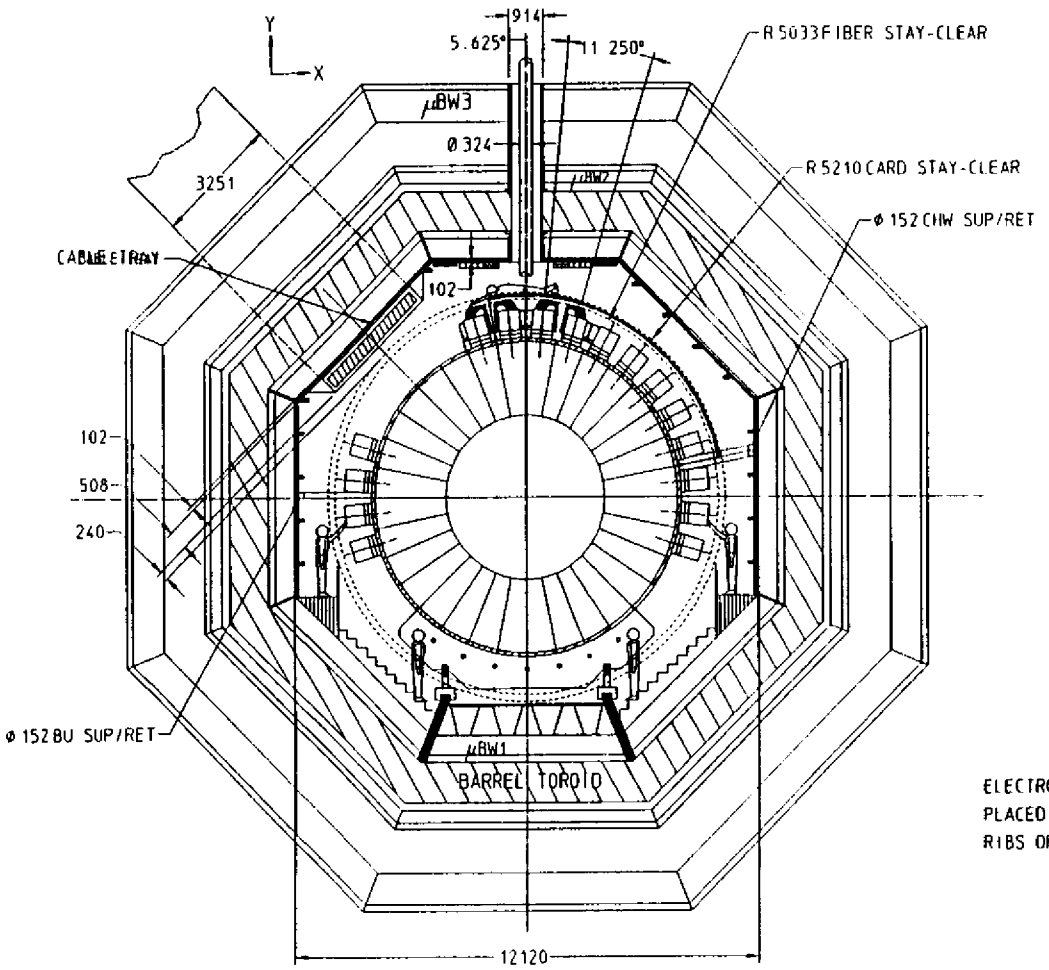

RING 1 X-SECTION

0 1 2 3 4 5 M

NOTE ALL DIMENSIONS ARE IN MILLIMETERS

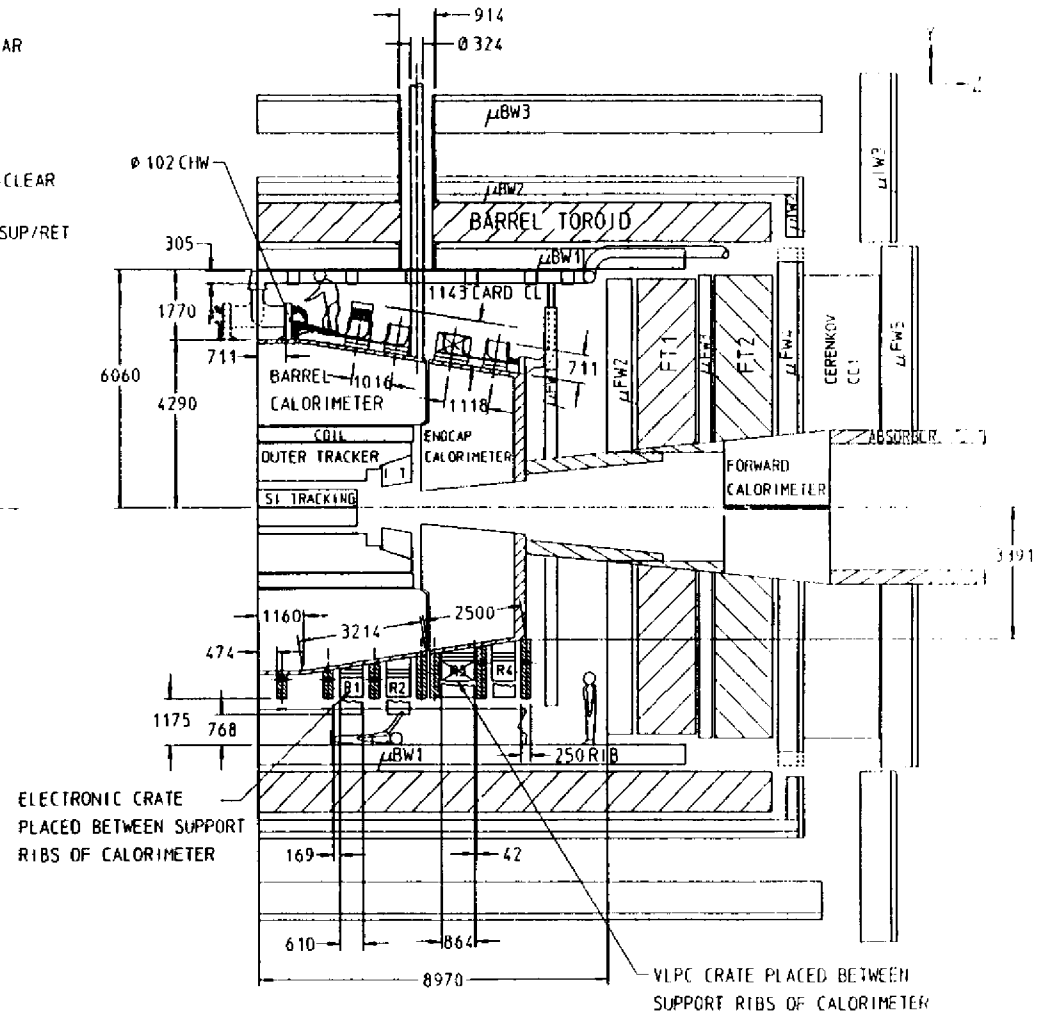

0 1 2 3 4 5 M

NOTE ALL DIMENSIONS ARE IN MILLIMETERS

UTILITY AND CRATE(192) LAYOUT
FOR DESCOPE OPTION 1 OF JUNE 29, 1991
FURTHER SUPPORT DETAILS
LBL DWG.# 23D0165 7/9/91 Y MINAMIHARA

Figure

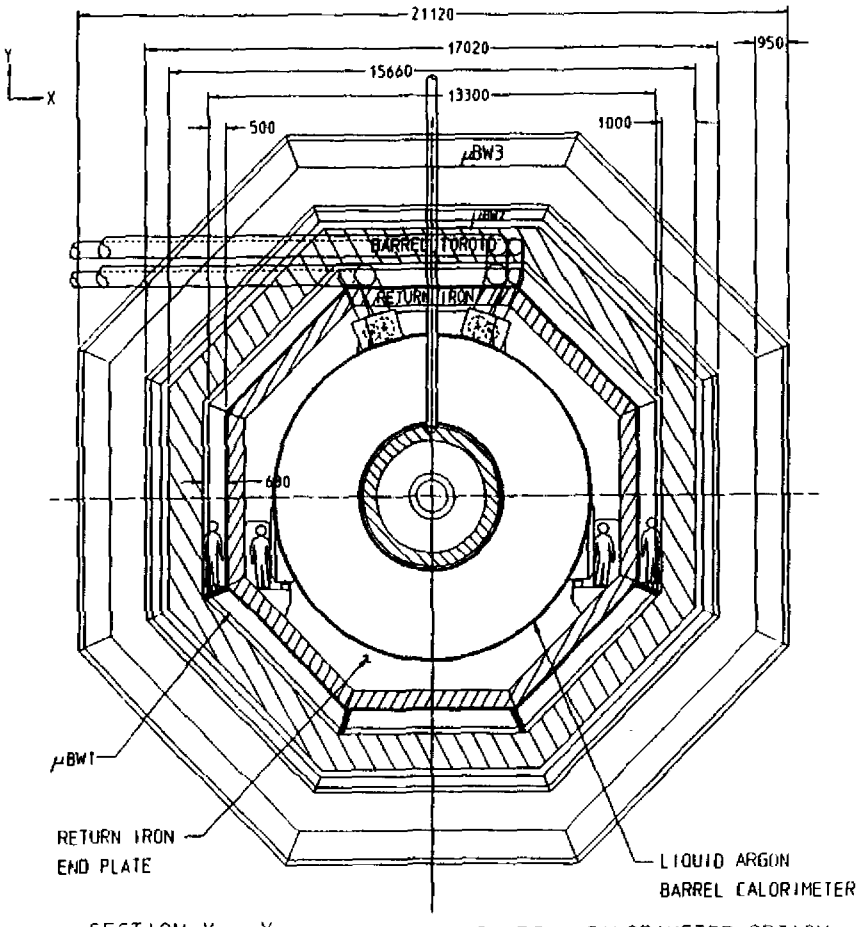

SECTION X - X

NOTE: ALL DIMENSIONS ARE IN MILLIMETERS

0 1 2 3 4 5 M

SDC LIQUID ARGON CALORIMETER OPTION

LAC DESCOPE OPTION 1

LBL DWG # 23D0175 8/1/91 Y. MINAMIHARA

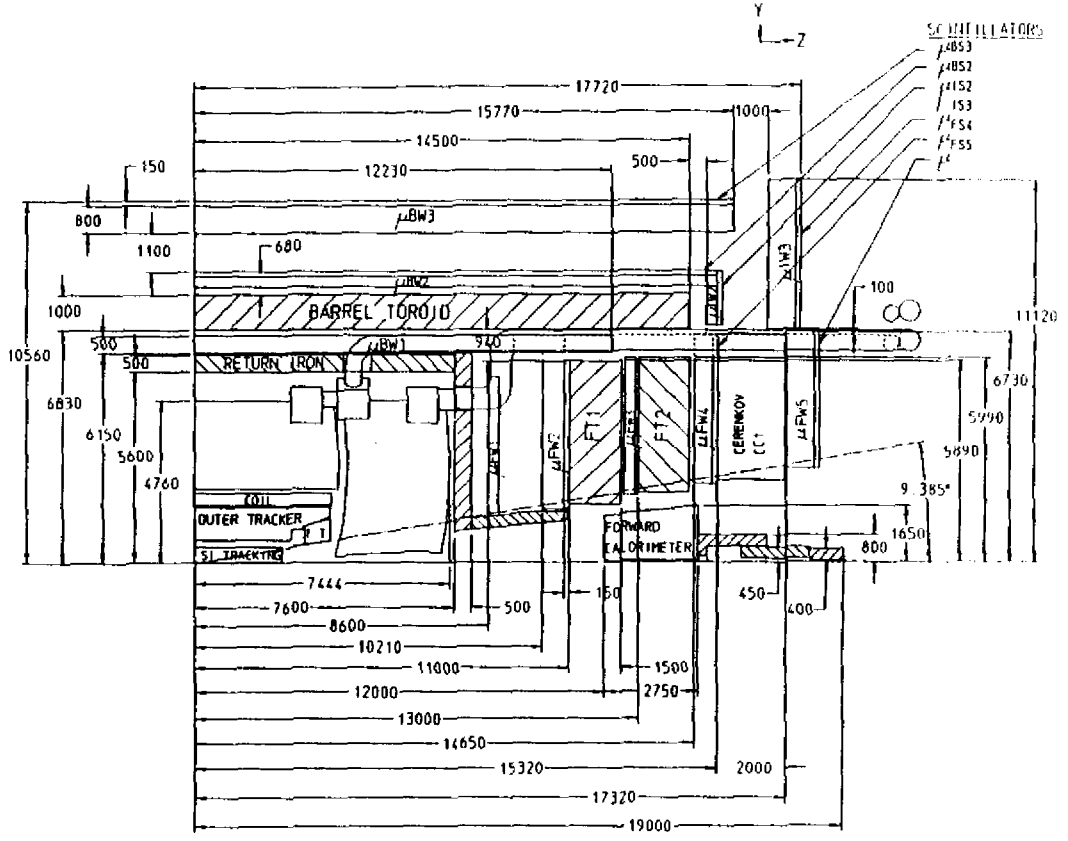

NOTE: ALL DIMENSIONS ARE IN MILLIMETERS

0 1 2 3 4 5 M

Figure 10-3

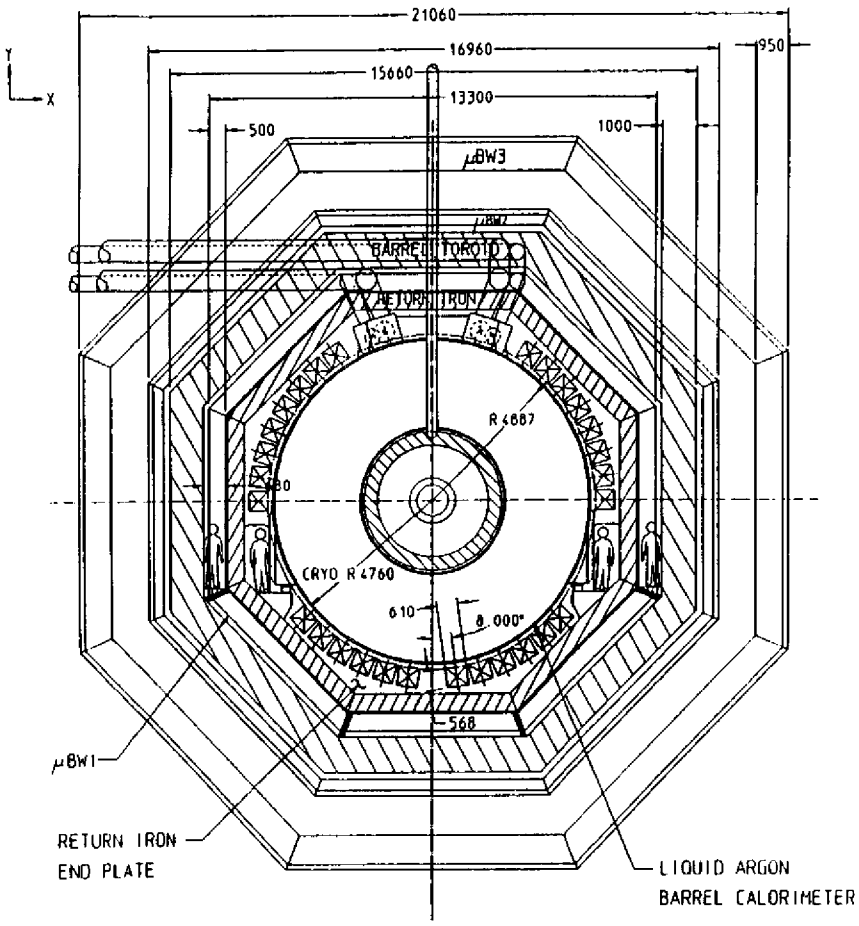

SECTION X - X

NOTE ALL DIMENSIONS ARE IN MILLIMETERS

0 1 2 3 4 5 M

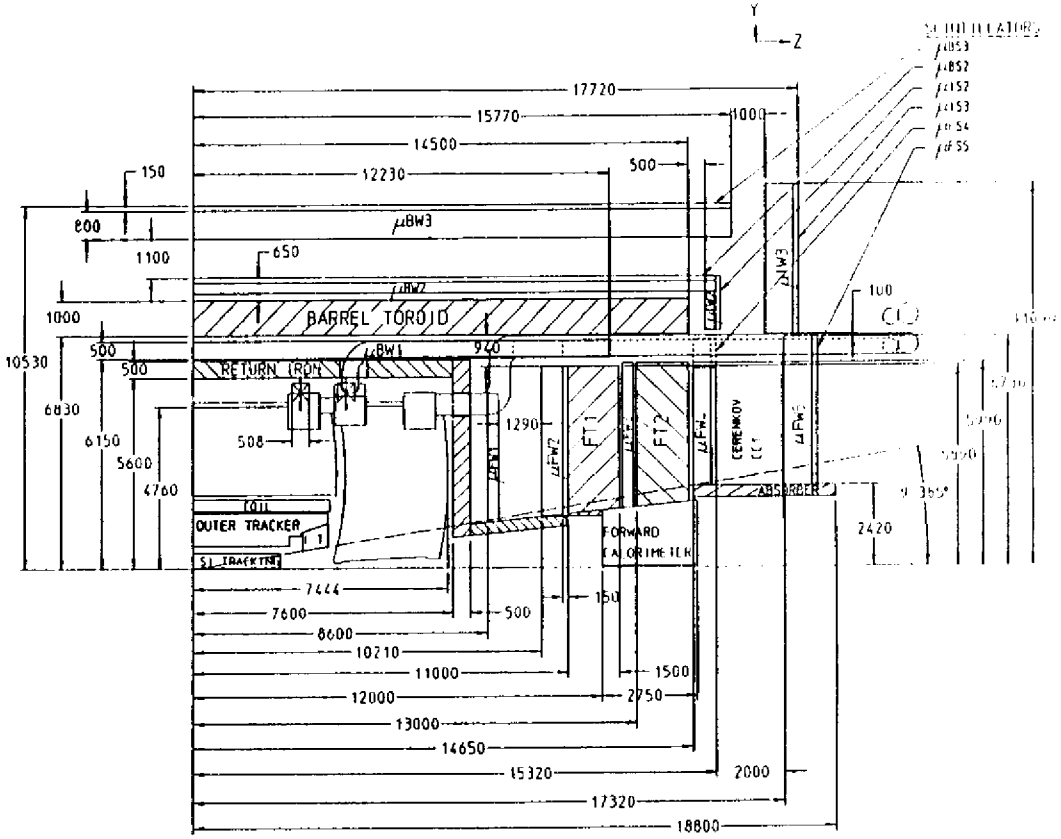

NOTE ALL DIMENSIONS ARE IN MILLIMETERS

0 1 2 3 4 5 M

SDC LIQUID ARGON CALORIMETER OPTION
LAC DESCOPE OPTION 1 CRATE LAYOUT
LBL DWG # 23D0205 7/31/91 Y MINAMIHARA

Figure 3-4

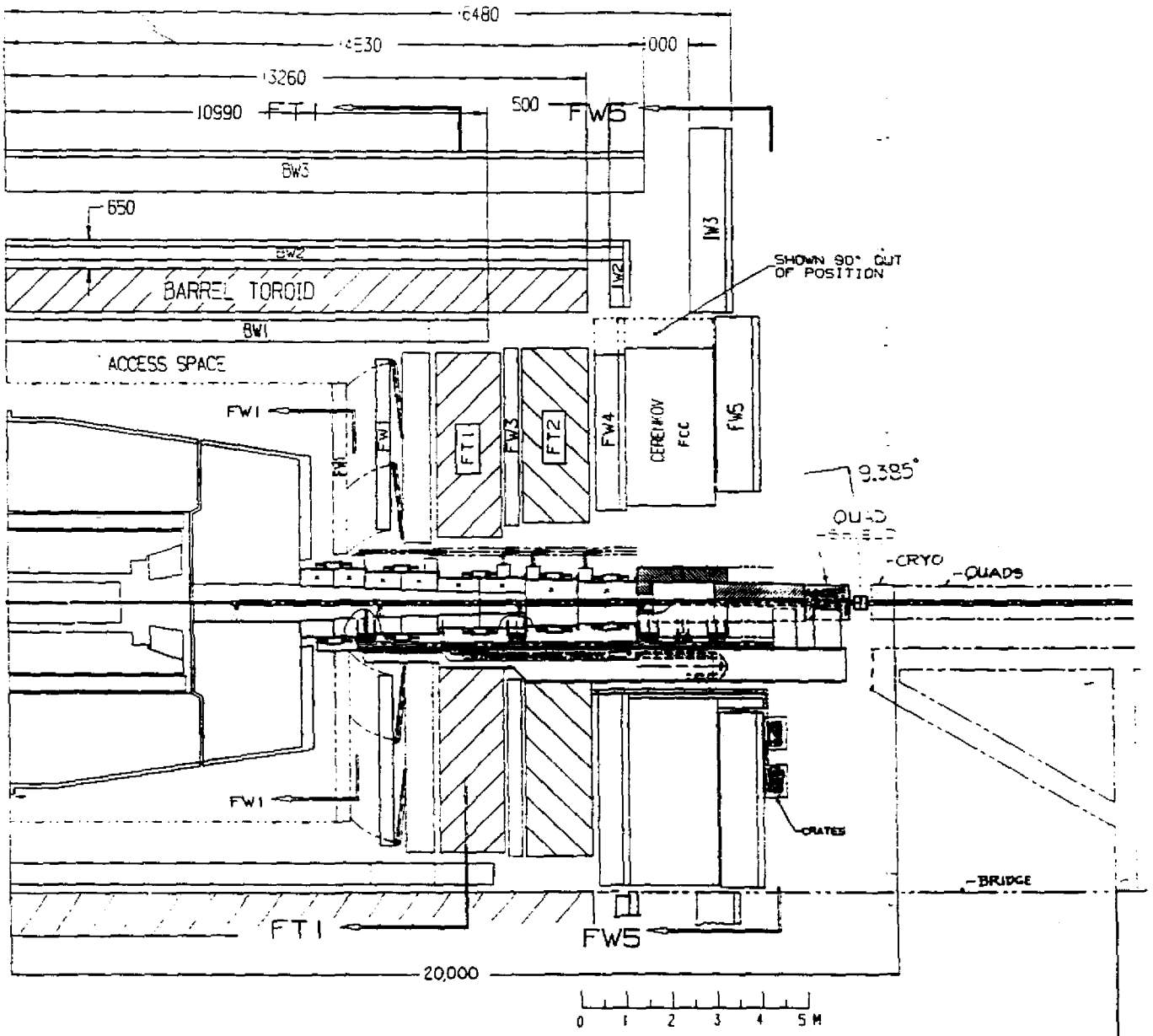
6480
3260
10990
500
FT1
FW5
BW3
650
BW2
BARREL TOROID
BW1
IW3
IW2
SHOWN 90° OUT OF POSITION
ACCESS SPACE
FW1
FW4
FT1
FW3
FT2
CERENKOV
FCC
FW5
9.385°
QUAD
CRYO
QUADS
CRATES
BRIDGE
FT1
FW5
20,000
0 1 2 3 4 5 M
2300185
CONICAL FORWARD CALORIMETER LAYOUT

Figure 10-5

Electrical Integration

The primary effort for the Electrical Systems Integration Group (ESIG) in July was to assist subsystem electronics groups in their cost/schedule activities. To that end, ESIG WBS assignments were made; Gene Oberst for WBS 5.1 & 5.5, Tom Moore for WBS 5.2, 5.3 and 5.4.

An ESIG representative called a meeting at Harvard of the muon and straw tracker subsystem contributors to determine if a self consistent, unified approach for the two, technologically similar, subsystems could be defined. The result is agreement that the subsystem technologies can be combined, taking advantage of common electronics component development activities and packaging. This will have future impact on the WBS organization as the combined developmental activities are defined.

ESIG representatives participated in a 3-day trigger coordination meeting held at the Univ. of Wisconsin, Madison. Configurations for several trigger scenarios were presented and discussed. ESIG members discussed with the other participants subjects pertaining to cost/schedule, decisions impacting civil construction requirements and the content of relevant design documents.

ESIG representatives participated in the review of electrical system requirements documents pertaining to SSC CCD direction at the SEFUR review meeting held at SSCL. Further work in defining these requirements, mostly formulating them into parameters consistent with those understood by the AE contractor, is needed before the documents will be ready to be passed to CCD.

Cost and Schedule

In early July, a review of the detector costs and contingencies had been completed to WBS level 5. The list of "holes" in the WBS, contingencies and EDIA percentages which had been flagged, etc. were then reviewed with the responsible C/S coordinators. It was planned in July to revise the "baseline" subsystem costs and to begin the process of checking the raw data. Late August now appears to be a more realistic completion date for the final baseline detector cost roll-up.

Efforts towards an integrated SDC project schedule continue. Some Subsystem schedules are underway and the conversion software is being finalized. OpenPlan - Mac is still being debugged. A fully integrated high level project schedule developed from subsystem information is still several months away.

Further planning towards shifting the C/S effort and responsibility to SSCL occurred throughout July. A preliminary budget for the FY '92 Cost and Schedule effort was discussed and agreed upon with Physics Division SDC staff.

Liquid Argon Calorimetry (LAC)

The month of July was full of exciting accomplishments for the LAC Detector option. The solution to the excess dead mass dilemma at eta 3 3 (a LAC issue), a new, credible

cost estimate from Martin Marrietta Astronautics (Tasks 1 & 2), which show that the LAC is indeed cost competitive, and sign-off by an SSCL directed Hazards Analysis review team on previously raised "LAC safety and access questions". The LAC design is summarized in the "Calorimeter Conceptual Design, Liquid Argon Option" which was completed on July 31.

Silicon Tracking

Cost & Schedule

Schedules for each of the silicon tracker sub-projects were submitted to the SDC C/S group. These included reduced effort, primarily in the later years. After the labor reduction and using unburdened LANL rates, the baseline is now at $57.4 M.

A descoped silicon tracker layout was received from tracker physicists and efforts are presently underway to determine the cost. A preliminary estimate for the proposed configuration is $40 M which was the goal set during the last SDC meeting.

Thermal & Structural Analysis

A simple analysis of heat transfer for a proposed "oreo" configuration was completed. The analysis was reported in technical note, LBL SDC 0038. The studied configuration and the results are shown by Figure 10-6. It was assumed that the power/channel was 1 mW and the readout length was 0.3 cm. No credit was taken for heat flow away from the cooling ring into the detector which will be cooled by natural convection. This will be studied next month. The results indicate that the detector material may be at about 10°C. This is higher than desired due to signal/noise considerations. Other configurations will be considered next month. The first will rotate the "top" oreo so that it is directly above the cooling. This should drop the detector temperature down to about 5°C.

A technical note, LBL SDC 0039, reporting the deflection and stress analysis results of the Design B option for the silicon tracker was distributed this month. Thermal analysis of the L-design pixel carrier is in progress with the ANSYS heat transfer model almost complete. The results of the first model runs will be compared with the temperatures predicted using hand calculations and worst case assumptions (discussed above). Convection considerations and more realistic assumptions will then be incorporated into the model. The model will also be used to evaluate other configurations.

Dummy silicon detector strips and pixels are ready for mechanical testing. Tests will include load-deflection measurements and thermal cycling.

Radiation Length Calculations

Work continued on the radiation length code. Runs have been completed for 6-, 12- and 18-cm detector layouts. The data is presently being plotted and the results will be reported next month. A new method of indicating material type on the drawings has been suggested. It would speed up the process of specifying which material occupies a

specific area. In addition, it would indicated where line errors had occurred. The ne algorithm uses cross hatching instead of colored line type for material specification.

Cabling

The contract with Engineering Solutions for cabling has been completed. A final document was submitted which compiled 15 progress reports. The highlights of this contract were the fabrication of aluminum transmission lines and the joining of two aluminum lines using an anisotropic conductive adhesive. A draft proposal for FY92 tasks has been received from Engineering Solutions.

Pixels

The first prototype of the pixel L carrier has been fabricated at LLNL and is presently being inspected. The final thickness of this part was 16 mils instead of the desired value of 12 mils. Another prototype is being fabricated at this time.

A layout of pixels on a carrier and two possible methods of carrier placement on support rings were completed. These are shown on Figure 10-7. The first layout provided 100% coverage, but needed additional material due to the layering in the radius direction. The second configuration is simpler, has less material, but has a gap that reduces the coverage by 0.4%. This configuration will be the baseline.

General

Members of the LBL tracker group attended two demonstrations this month to view equipment that can be used to accurately assemble detectors onto supports. It was decided to purchase one of the machines which can serve both as an assembly platform and an inspection device after module assembly.

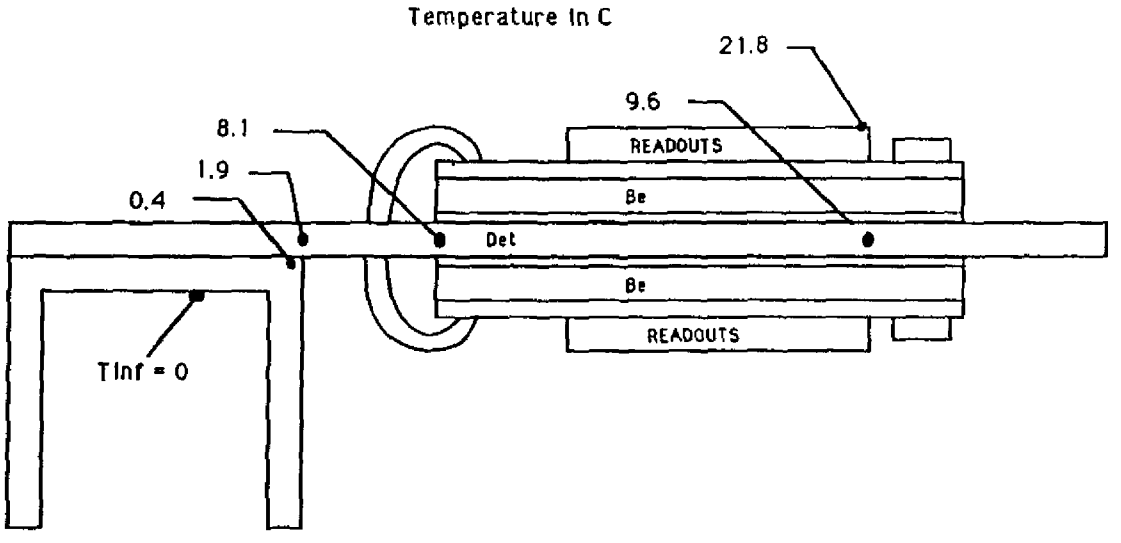

Figure 10-6 Oreo configuration and temperature at various locations.

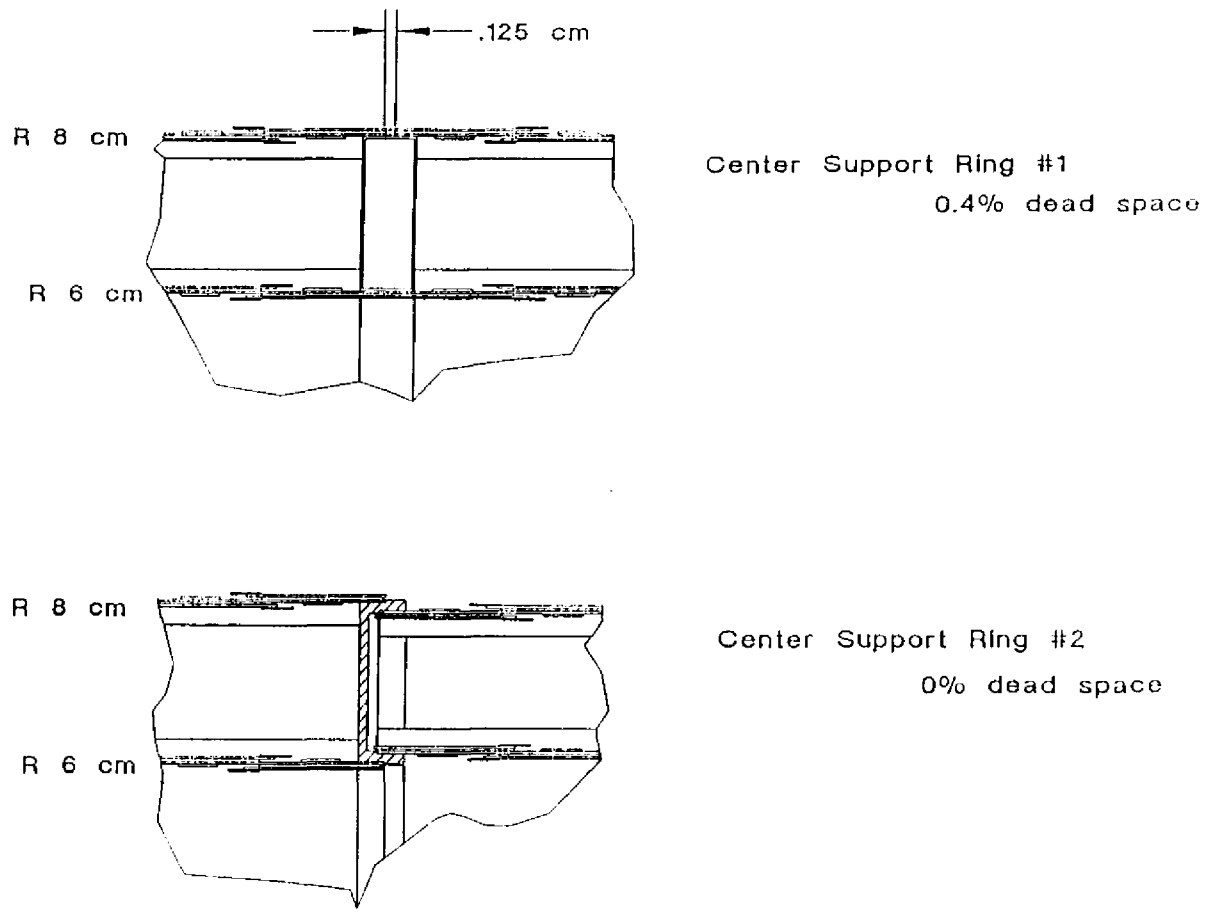

Figure 10-7 **Two layouts of carrier/support ring assemblies. The first has the pixels placed end-to-end and the second has them tiled in the radial direction.**

Computing Systems

Continuing the ObjectStore database work from June, several queries were coded to access the extremely simple database of dimuons in the U. of I. database. Derived quantities, in particular the dimuon mass, were calculated and events selected in a region bracketing the ψ mass. PV~Wave was used to histogram the masses and a clear ψ peak was found. See enclose plot (Figure 10-8).

At the SDC Computing Working Group Workshop in Dallas, 9-10 July, we discussed code management, data modeling, and top level system architecture. In particular it was agreed to work further with the Houston IBM team to make a first list of services to be provided by the basic system and to continue working towards a data model for SDC data.

Glenn Kubena and Kenneth Liao from IBM Houston came to LBL 16 July. The morning discussions established a preliminary list of services which should be provided for the SDC software and a list was made of standards and common industry interfaces which might be satisfactory providers. Further study is needed as to the interoperability of the items on the list.

Proceedings were initiated to obtain an OSF/1 Source licensee. LBL already has a source license for AT&T's version of Unix. The OSF/1 license will provide us with the ability to make detailed comparisons of the two major contenders for a widespread, common Unix Operating system.

Further discussions were held with LBL's local IBM representative. It appears likely that the LBL group can become IBM Software Developers for the RS/6000 system. This would provide 50% discounts on hardware and software from IBM. The RS/6000 is an attractive system because it can be used as a platform for IBM's RESQME, a very high quality resource queuing modeling system (should be used to model database performance, for example), and is a target platform for the OSF/1 operating system and the OSF/DCE Distributed Computing Environment. Getting working examples of the last two items would help enormously in addressing the interoperability questions raised by the list of software services made earlier in the month.

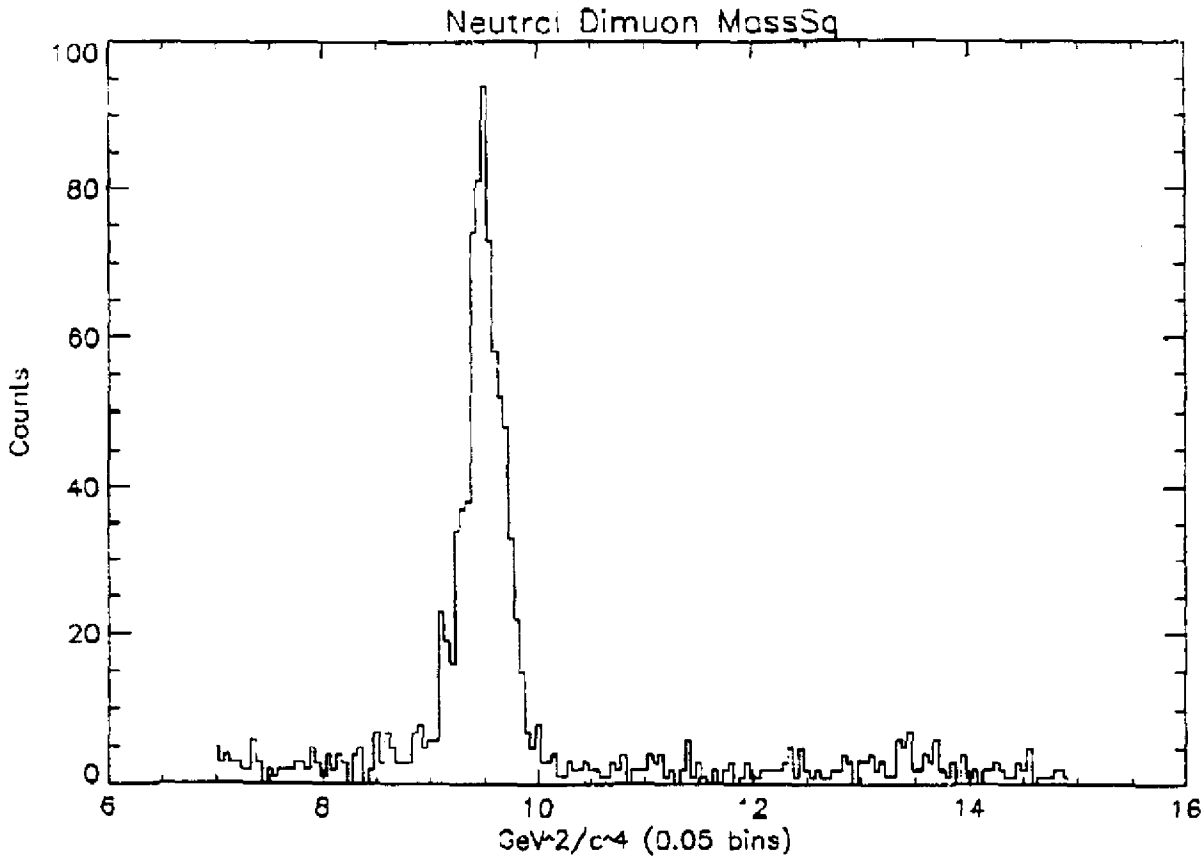
Neutral Dimuon MassSq
Counts
100
80
60
40
20
0
6
8
10
12
14
16
GeV^2/c^4 (0.05 bins)

Figure 10-8

B. PROGRAM COSTS

The budgets indicated below are for "post-LoI" funds allocated April 1991 and August 1991.

Institution	Budget	July Cost (Actual or Estimated)	Prior Months (actual cost) K$	Total Cost
1. ORNL	210	—	—	—
2. PSL - Muon	80			
3. *PSL-Trigger	75			
4. *FNAL				
A. SC Solenoid	390		120.4	
B. Calorimetry	190			
C. Data Acq. Sys.	50			
D. Muon	70			
E. Fiber Tracker Read-out	100			
5. ANL	230	33.6	77.6	111.2
6. WSTC	123	6.0	100.0	106.0
7. U. MICHIGAN	83			
8. LANL	150	40.0	35.0	75.0
9. KE	210	36.0	57.2	93.2
10. LBL				
A. Integration & Mgmt.	693	87.0	492.8	579.8
b. Liq. A Calorimetry	213	43.4	173.8	217.2
C. Silicon Tracker	72	24.0	1.0	25.0
D. Computing Systems	119	31.3	65.3	96.6
E. Calorimetry Electronics	25	—	10.4	10.4
F. Contract Costs	53	—	53.0	53.0
11. IBM	35	—	—	—
12. U. CHICAGO	47	—	—	—
13. HARVARD	47	—	—	—
14. U. PENNSYLVANIA	62	—	—	—
15. SANDIA	38	—	—	—

*Cost data was not submitted